INVESTIGATING SOURCES OF PERIPHERAL SEROTONIN SYNTHESIS: IMPLICATIONS FOR REGULATING METABOLISM

INVESTIGATING SOURCES OF PERIPHERAL SEROTONIN SYNTHESIS: IMPLICATIONS FOR REGULATING METABOLISM

By

JULIAN MERVYN PERRERAS YABUT, B.Sc.

A Thesis submitted to the School of Graduate Studies in partial fulfillment of the requirements for the Doctor of Philosophy Degree

McMaster University DOCTOR OF PHILOSOPHY (2020) Hamilton, Ontario (Medical Science – Nutrition & Metabolism)

TITLE: INVESTIGATING SOURCES OF PERIPHERAL SEROTONIN SYNTHESIS: IMPLICATIONS FOR REGULATING METABOLISM

AUTHOR: Julian M. P. Yabut, B.Sc.

SUPERVISOR: Professor Gregory R. Steinberg, Ph.D.

PAGE COUNT: xiii, 136

LAY ABSTRACT

Obesity, type 2 diabetes (T2D) and non-alcoholic fatty liver disease (NAFLD) can develop when caloric intake exceeds expenditure. In contrast to lipid-storing white fat, brown and beige fat burn calories. Serotonin is a hormone that reduces the burning of calories in fat, therefore finding ways to inhibit its effects on fat tissue without altering serotonin in the brain may lead to new therapies for obesity and other related diseases. In this thesis, we examined potential sources of serotonin that might inhibit the burning of calories in adipose tissue of mice. By reducing the synthesis of serotonin in a white blood cell called mast cells, but not fat cells, mice were protected from obesity, pre-diabetes and NAFLD due to increased activity of beige fat. Moreover, when we kept mice in a warm environment, thus reducing the need for mice to burn calories in brown and beige fat, this eliminated the effects of serotonin to promote obesity, but not pre-diabetes and NAFLD. These studies have identified how serotonin generated from mast cells inhibits the burning of calories in adipose tissue, a finding that may lead to new therapies for obesity, T2D and NAFLD.

ABSTRACT

Obesity is a major risk factor for type 2 diabetes (T2D) and non-alcoholic fatty liver disease (NAFLD), and is attributed to excess energy intake in comparison to energy expenditure. Therapeutics that reduce energy intake in obesity have limited efficacy, with weight loss typically reaching less than 10% of initial body mass, leading to efforts to uncover new therapies that may increase energy expenditure. Unlike lipid-storing white adipose tissue, brown and beige adipose tissues undergo futile cycling, oxidizing lipids and carbohydrates thereby increasing energy expenditure. With obesity, the metabolic activity of brown and beige adipose tissue is reduced, suggesting that restoring adipose tissue thermogenesis may represent a new means to enhance energy expenditure. Previous studies in mice have shown that peripheral serotonin synthesis by the enzyme tryptophan hydroxylase 1 (Tph1) inhibits adipose tissue thermogenesis and contributes to the development of obesity, insulin resistance and NAFLD. However, the primary Tph1 expressing tissue(s) inhibiting adipose tissue futile cycling is not known. In this thesis, we genetically removed Tph1 in mast cells of mice and discovered that this elevated beige adipose tissue activity protecting mice from developing high-fat diet induced obesity, insulin resistance and NAFLD. In contrast to these findings, genetic deletion of Tph1 in adipocytes did not result in protection from obesity, suggesting that mast cells are the primary source of serotonin that inhibits white adipose tissue thermogenesis. Lastly, to determine the importance of adipose tissue thermogenesis in mediating the beneficial metabolic

effects of reduced Tph1, mice were housed at thermoneutrality, blocking the requirement for adipose tissue thermogenesis. Under these conditions, mice lacking Tph1 had comparable brown and beige adipose tissue metabolic activity, energy expenditure and adiposity, however, surprisingly, were still protected from insulin resistance and NAFLD. The studies in this dissertation have discovered that mast cell Tph1 is critical for inhibiting adipose tissue thermogenesis and that serotonin plays an important role in promoting NAFLD, independently of its inhibitory effects on adipose tissue thermogenesis. Collectively, these findings further define the roles of serotonin in regulating whole-body energy metabolism, providing critical clues and mechanistic insights for potential therapies to mitigate metabolic diseases.

THESIS PUBLICATIONS

1. **Yabut, J. M.**, Crane, J. D., Green, A. E., Keating, D. J., Khan, W. I., & Steinberg, G. R. (2019). Emerging roles for serotonin in regulating metabolism: New implications for an ancient molecule. *Endocrine reviews*, *40*(4), 1092-1107.

2. **Yabut, J. M.**, Desjardins, E. M., Chan, E. J., Day, E. A., Leroux, J. M., Wang, B., Crane, E. D., Wong, W., Morrison, K. M., Crane, J. D., Khan, W. I. & Steinberg, G. R. (2020). Genetic Deletion of Mast Cell Serotonin Synthesis Prevents the Development of Obesity and Insulin Resistance. *Nature Communications*. 11.

3. **Yabut, J. M.**, Chan, E. J., Desjardins, E. M., Khan, W. I. & Steinberg, G. R. (2020). Reductions in Adipocyte Expressed Tph1 Do Not Attenuate Adipose Tissue Thermogenesis. *Prepared for submission in 2020.*

4. **Yabut, J. M.**, Chan, E. J., Desjardins, E. M., Khan, W. I. & Steinberg, G. R. Thermoneutrality promotes nonalcoholic fatty liver disease by increasing circulating serotonin. *Prepared for submission in 2020.*

OTHER PUBLICATIONS

1. Crane, J. D., Palanivel, R., Mottillo, E. P., Bujak, A. L., Wang, H., Ford, R. J., Collins, A., Blümer, R. M., Fullerton, M. D., **Yabut, J. M.**, Kim, J. J., Ghia, J., Hamza, S. M., Morrison, K. M., Schertzer, J. D., Dyck, J. R., Khan, W. I., Steinberg, G. R. (2015) Inhibiting peripheral serotonin synthesis reduces obesity and metabolic dysfunction by promoting brown adipose tissue thermogenesis. *Nature Medicine*, *21*(2), 166-172.

2. Mottillo, E. P., Desjardins, E. M., Fritzen, A.M., Zhou, V. Z., Crane, J. D., **Yabut, J. M.**, Kiens, B., Erion, D. M., Lanba, A., Granneman, J. G., Talukdar, S., Steinberg, G. R. (2017). FGF21 does not require adipocyte AMP-activated protein kinase (AMPK) or the phosphorylation of acetyl-CoA carboxylase (ACC) to mediate improvements in whole-body glucose homeostasis. *Molecular Metabolism*, *6*(6), 471-481.

3. Martin, A. M., **Yabut, J. M.**, Choo, J. M., Page, A. J., Sun, E.W., Jessup, C. F., Wesselingh, S. L., Khan, W. I., Rogers, G. B., Steinberg, G. R., Keating, D.J. (2019) The gut microbiome regulates host glucose homeostasis via peripheral serotonin. *Proceedings on the National Academy of Sciences*, *116*(40), 19802-19804.

ACKNOWLEDGEMENTS

To my supervisor and mentor, Dr. Gregory Steinberg, I am beyond thankful to have flown under your wing. You are at the forefront of tackling metabolic diseases and your vision to eradicate it is admirable and contagious. Your wisdom and ideologies have molded me to be the scientist that I am today and ultimately, the person that I will be in the real world. I can only hope to change the world as much as you have in such a short time, but I aspire to at the very least, match your positive impact. I am forever grateful to be a part of your journey and you to be a part of mine.

Dr. Waliul Khan, your insight and expertise in the field of serotonin was of utmost value, paving the way for a successful and seamless end to my doctoral studies. Dr. Katherine Morrison, your support and guidance was invaluable, propelling me through my doctoral milestones. You challenged me to think outside of the realm of mice to include the implications in man, which has shaped how I will solve the world's largest problems.

To my brother, Eric Desjardins, I am fortunate to have a great friend to sit beside at work every day, cultivating a comradery that will last a lifetime. You've taught me to be empathetic, to think about life in new ways and most importantly, the difference between all of the types of beers!

To Eric Chan, thank you for helping me be the teacher I am today. Without your hard work and dedication, the projects contained within this dissertation would not be the same.

To the Steinberg lab, we've forged friendships built to last. When I walk back into HSC 4N71, I want to be able to reminisce in all the great memories we shared and the moments of excitement after our discoveries. Your contribution to my training cannot be overstated and I only wish the best for those of you who continue to do great things in science and for those who will exert their ability to provide positive impact in the real world! Thanks to Emily, Marisa, Lindsay, Evelyn, Basma, Adam, Katarina, James, Justin and Emilio for the memories and scientific insights.

To my best friend, Joseph, thank you for your support through all the ups and downs during this rollercoaster ride called graduate school. Despite you not knowing what my research was completely about, the support and advice was always there.

To my sisters, Jessica and Jacklyn, and my mother, Marylou, thank you for supporting and trusting me on this journey for without you, I would not be in this position. Mom, your selflessness and sacrifice is forever imprinted onto me and only hope to do as much for you one day as you have for me.

TABLE OF CONTENTS

LIST OF ABBREVIATIONS AND SYMBOLS

ACC	Acetyl-CoA carboxylase
ADP	Adenosine diphosphate
Akt2	Protein kinase B
ATGL	Adipose triglyceride lipase
ATP	Adenosine triphosphate
ACLY	ATP citrate lyase
Ap2	Adipocyte protein 2
BAT	Brown adipose tissue
BMI	Body Mass Index
Ca^{2+}	Calcium
C/EBPβ	CCAAT/enhancer-binding protein β
cAMP	Cyclic adenosine monophosphate
CD36	Cluster of differentiation 36
CNS	Central Nervous System
CoA	Coenzyme A
Cpa3	Carboxypeptidase 3
Cre	Cre Recombinase
CREB	cAMP-responsive element-binding
$CreER^{T2}$	Cre recombinase under the control of estrogen receptor T2
CX	Cold Exposure
DAG	Diacylglycerol
Ebf2	Early B cell factor 2
FASN	Fatty Acid Synthase
FAT2/5	Fatty Acid Transporter 2/5
FOXO1	Forkhead box protein O1
G6P	Glucose 6 Phosphate
GLUT2/4	Glucose Transporter 2/4

GSK3β	glycogen synthase kinase 3β
gWAT	Gonadal white adipose tissue
HbA1c	Hemoglobin A1c
HFD	High fat diet
HSC	Hepatic Stellate Cells
HTR_X	Serotonin (type) Receptor
IgE	Immunoglobulin E
IL	Interleukin
IKKε	IkappaB Kinase ε
ILC2	Group 2 innate lymphoid cells
IRF4	Interferon regulatory factor 4
IRS1/2	Insulin Receptor Substrate 1/2
IRTK	Insulin receptor tyrosine kinase
iWAT	Inguinal white adipose tissue
KO	Knockout
LD	Lipid Droplet
Lrat	Lecithin-retinol acyltransferase
MRI	Magnetic Resonance Imaging
mRNA	Messenger ribonucleic acid
mTORC1	Mammalian target of rapamycin complex 1
Myf5	Myogenic factor 5
MYOD	Muscle-specific transcription factor myoblast determination protein
NE	Norepinephrine
NAFLD	Non-alcoholic fatty liver disease
NASH	Non-alcoholic steatohepatitis
PDGFRα	Platelet-derived growth factor receptor-α
PDK1	Pyruvate dehydrogenase kinase 1
PEPCK	Phosphoenolpyruvate carboxykinase
PET/CT	Positron emission tomography-computed tomography

PGC1α	PPARγ co-activator 1α
PKA	Protein kinase A
PKCε/θ	Protein Kinase C ε/θ
PPARγ	Proliferator activated receptor γ
PPP	Platelet Poor Plasma
PRDM16	PRDM16
RT	Room temperature
SREB1c	Sterol regulatory element-binding protein 1c
SRE	Sterol response element
T2D	Type 2 diabetes
TBK1	TANK-binding kinase 1
TG	Triglyceride
TLR4	Toll-like receptor 4
TN	Thermoneutrality/Thermoneutral
Tph1	Tryptophan hydroxylase 1
$Tph1^{-/-}$	Tph1 knockout
$Tph1^{+/+}$	Tph1 wildtype
$Tph1^{iAd\Delta/\Delta}$	Tph1 inducible adipocyte-specific knockout
$Tph1^{fl/fl}$	Tph1 double floxed
UCP1	Uncoupling protein 1
WAT	White adipose tissue

CHAPTER ONE

1. INTRODUCTION

1.1 BACKGROUND & RATIONALE

In humans, fatty acids and glucose are required to facilitate vital cellular processes such as respiration, proliferation and survival. Under conditions of normal physiological function, fatty acids and glucose are stored in adipose tissue, liver and muscle to prevent macronutrient (i.e. glucose and fatty acids) buildup and for use during a fast. Despite the necessity of these macromolecules in normal human physiology and function, the emergence of high calorie diets (i.e. Western diets, elevated simple sugar consumption and high fat diets) has been associated with dysregulation of human metabolism. Under states of chronic overnutrition, normal physiological processes involved in energy disposal and production are compromised and can manifest into a number of conditions including obesity, type 2 diabetes (T2D) and non-alcoholic fatty liver disease (NAFLD). These metabolic diseases are related to the aberrant disposal of fatty acids and glucose due to the lack of insulin action to its receptor on various metabolic tissues, termed insulin resistance. Despite the understanding that elevated plasma lipids and glucose are involved in metabolic pathologies, the secreted endocrine signals and the ensuing molecular mechanisms in insulin-sensitive tissues are currently under intensive investigation. These novel insights will be pivotal to the elucidation of potential drug candidates to mitigate the rise of metabolic diseases such as obesity.

The prevalence of global obesity and its comorbidities continue to rise, doubling in more than 70 countries since 1980 (The GBD 2015 Obesity

Collaborators, 2017) and increasing the proportion of obesity-related healthcare costs (Biener et al., 2018; Li et al., 2015). In 2015, it was estimated that 603.7 million adults and 107.7 million children world-wide were obese (The GBD 2015 Obesity Collaborators, 2017). A recent predictive analysis in the United States projects nearly 1 in 2 adults will have obesity by 2030 (Ward et al., 2019). There is a great need for therapies to cease the current obesity epidemic that is projected to get worst without new interventions.

NAFLD and T2D are associated metabolic pathologies that share obesity as a major risk factor (Marchesini et al., 2007). The global prevalence of NAFLD — a spectrum of liver diseases that ranges from simple steatosis to non- alcoholic steatohepatitis (NASH) — has been reported to be as high as 24% (Younossi et al., 2016), suggesting this disease to be of extreme clinical relevance. Hepatic insulin resistance is a hallmark of NAFLD and increases the risk of T2D diagnosis (Tilg et al., 2017), solidifying a strong connection between these ailments. T2D is characterized by elevated fasting blood sugar levels and whole-body insulin resistance, afflicting more than 420 million individuals worldwide in 2017 (Reusch and Manson, 2017) with extensive associated economic burden (Seuring et al., 2015). Despite the obvious parallels that exist between obesity, NAFLD and T2D, the underlying mechanisms that establish causality and temporality of these diseases is unclear.

The interplay between obesity, NAFLD and T2D is complex, involving the dysregulation of fatty acid and glucose storage. It is unlikely that one of these

metabolic disorders always precedes the others since individuals may only have one of the three conditions. However, obesity is a risk factor for T2D and NAFLD. Although the mechanisms underlying the pathogenesis of obesity, NAFLD and T2D are not completely understood, it is well known that insulin is a player in these metabolic diseases (Petersen and Shulman, 2018). Considering the role of insulin in postprandial macronutrient deposition, it is not surprising that metabolic diseases involving ectopic energy storage are related to this peptide.

1.2 HEPATIC INSULIN RESISTANCE

The liver is a key metabolic organ that orchestrates glucose and lipid metabolism. In addition to skeletal muscle, the liver uptakes a large proportion of glucose after a meal, which is necessary to prevent postprandial hyperglycemia (Shulman, 2014). Although glucose uptake is not directly regulated via insulin per se, indirect insulin-dependent regulation of glucose lowering enzymes is imperative to normoglycemia. Postprandial insulin signaling reduces downstream hepatic glucose-generating processes — such as gluconeogenesis and glycogenolysis — and increases glycogen synthesis (Perry et al., 2014). Inhibition of glycogenolysis also occurs independent of insulin mediated by the import of glucose via glucose transporter 2 (GLUT2). The liver reduces postprandial blood glucose via insulin-dependent and independent regulation on hepatic enzymes involved in glucose metabolism.

Hepatic insulin action involves a cascade of intracellular signals initiated by insulin receptor tyrosine kinase (IRTK) activation. Upon insulin binding, autophosphorylation of tyrosine residues occurs, resulting in the phosphorylation and subsequent activation of insulin receptor substrate 2 (IRS2). IRS2 activation increases 3-phosphoinositide-dependent kinase-1 (PDK1) and results in elevated activity of Akt2 via PDK1 phosphorylation. Activated Akt2 suppresses hepatic glucose production by 1) reducing the expression of gluconeogenic enzymes via nuclear exclusion of Forkhead box protein O1 (FOXO1) and 2) inactivating glycogen synthase kinase 3β (GSK3β), which results in glycogen synthase activity. Collectively, hepatic insulin signalling suppresses glucose production.

Insulin is a potent stimulator of processes that promote glucose storage, but its activity is compromised due to hepatic insulin resistance. During fed conditions, lack of insulin action results in 1. reductions in glycogen synthase activity due to less phosphorylation of GSK3β and 2. elevations of transcription of gluconeogenic enzymes (i.e. PEPCK and G6P) due to increased phosphorylated FOXO1 (Shulman, 2014). The inability of insulin to activate glycogen synthesis and reduce gluconeogenesis in the insulin resistant state results in elevated hepatic glucose output, contributing to hyperglycemia. Increased glucose in the bloodstream and within hepatocytes promotes the synthesis of fatty acids and hepatic lipid accumulation.

Liver insulin resistance is closely linked to NAFLD (Loomba et al., 2012). The inability of insulin to act on its receptor in hepatocytes is deemed hepatic

insulin resistance, resulting in glucose and fatty acid storage abnormalities. The lack of insulin action is attributed to the activation of Protein Kinase Cε (PKCε). PKCε activity has been shown in mouse studies to directly phosphorylate T1150 IRTK activity (Samuel et al., 2007), preventing the phosphorylation of IRS2 and ultimately, blunting hepatic insulin signalling. This process is initiated due to the combination of increased fatty acid flux and reduced mitochondria fat oxidation in hepatocytes, collectively increasing long-chain CoAs and diacylglycerol (DAG). DAGs have been shown to increase PKCε activity and subsequent IRTK inhibition (Samuel et al., 2007), resulting in processes that increase glucose production and *de novo* lipogenesis. This role of PKCε is supported by studies in whole-body *Prkce* knockout mice (Raddatz et al., 2011) and rats treated with hepatic-specific PKCε antisense oligonucleotides (Samuel et al., 2007) that are protected from lipid-induced insulin resistance.

In concert with the hyperglycemia characteristics of hepatic insulin resistance, hepatic lipid accumulation is exacerbated due to insulin inaction in adipose tissue and skeletal muscle (Shulman, 2014). Approximately 60% of liver lipid accretion in obese humans are attributed to adipose tissue lipolysis (Ferré and Foufelle, 2010). Since insulin robustly blunts adipocyte lipolysis, insulin-dependent inhibition of lipolysis is impaired in insulin resistant individuals. Lipolysis continues in the presence of insulin, providing fatty acids for hepatic lipid accumulation. This is supported by studies using PPARγ activators (i.e. TZDs) that can reduce adipocyte lipolysis, resulting in reduced liver lipids (Mayerson et al.,

2002). Further, PPARγ knockout mice that are lipoatrophic have hepatic steatosis and insulin resistance (Wang et al., 2013a). Lastly, genetic knockout mice with reduced adipocyte lipolysis (ATGL and PPARγ KO mice) are protected from HFD-induced insulin resistance due to reductions in hepatic acetyl-CoA (Perry et al., 2015). Hepatic lipid accumulation is heavily influenced by adipocyte lipolysis to provide substrate in insulin resistance.

In addition to suppressing hepatic glucose production, insulin signaling has robust effects on fatty acid metabolism. Insulin-dependent phosphorylation of Akt2 activates the nuclear transcription factor sterol regulatory element-binding protein 1c (SREB1c) by upregulating mRNA transcription and cleavage of SREBP1c precursor proteins into its active form (Brown and Goldstein, 2008). Insulin also upregulates mammalian target of rapamycin complex 1 (mTORC1), which increases mRNA and processing of SREBP1c (Samuel and Shulman, 2018). Active SREBP1c enters the nucleus and binds to sterol response element (SRE) on enhancer/promoter regions of target genes including fatty acid synthase (FASN), Acetyl-CoA carboxylase (ACC) and ATP citrate lyase (ACLY), which are all genes involved in fatty acid synthesis (Ferré and Foufelle, 2010; Horton et al., 2002; Pinkosky et al., 2017).

Hepatic lipid levels are elevated via uptake of fatty acids from adipose tissue lipolysis and chylomicrons from the diet (Perry et al., 2014). Lipid and chylomicrons from the bloodstream are broken down by lipases and enter hepatocytes via CD36 (Wilson et al., 2016) or FAT2/5 proteins (Doege et al., 2008).

The fatty acids that enter the hepatocytes can be used as substrates for triacylglycerol (TAG) synthesis.

Muscle insulin resistance also increases hepatic lipid accumulation. Synonymous to hepatic insulin resistance, PKCθ inhibits the phosphorylation of IRS1 to increase GLUT4 translocation to the membrane, negating glucose import into myocytes. Since hepatocytes do not require insulin for glucose uptake, much of the glucose not taken up is a substrate for hepatic lipogenesis. This notion is supported by the presence of NAFLD in mice with 1. a muscle-specific deletion of GLUT4 (Kim et al., 2001) or 2. deletion of AS160 - a protein required for GLUT4 translocation in muscle and adipose (Wang et al., 2013b). Thus, muscle insulin resistance can change the fate of glucose to become intrahepatic lipid.

1.3 ADIPOSE TISSUE FUTILE CYCLING

Adipose tissue is a complex network of immune cells, progenitors and adipocytes that work in concert to facilitate fatty acid and glucose homeostasis (Kajimura, 2017). White adipose tissue (WAT) stores fatty acids in the form of triglycerides and also mobilizes energy from fatty acids under periods of fasting (Lee et al., 2014b). Compartmentalization of lipids and triglycerides into white adipocytes is required for energy homeostasis considering fatless mice and lipodystrophic patients are susceptible to a slew of metabolic abnormalities (Gandotra et al., 2011). In contrast to the parenchymal storage functions of white adipocytes, brown and beige adipocytes employ a mitochondrial futile cycling

system and can effectively expend lipid for the purposes of thermogenesis under conditions of cold stress or β_3-adrenergic receptor agonism (Chouchani and Kajimura, 2019). Recent work has been conducted to understand how thermogenic fat cells function with hopes in identifying therapies that can effectively increase energy expenditure.

Compared to lean adipose tissue, obese white adipose is characterized by adipocyte hyperplasia, hypertrophy and excessive lipid deposition (Chouchani and Kajimura, 2019). White adipocytes are responsible for buffering large amounts of lipid after a meal. In response to an obesogenic diet, white adipocytes expand and increase in number, preventing ectopic lipid accumulation. Over long durations of excessive caloric intake (i.e. obesity), lipid accumulates in other metabolic tissues such as liver and muscle, interfering with regular function. Thus, obesity-related insulin resistance can be attributed to multiple factors that include reductions in adipose tissue insulin sensitivity and ectopic lipid accumulation. The morphological changes in obesity involve the complex interplay between alterations in transcriptional regulation of adipocytes and various immune cell messengers.

1.3.1 THERMOGENIC ADIPOSE TISSUE

Brown adipose tissue (BAT) utilizes lipids in order to maintain body temperature in response to cold stress or β_3-adrenergic stimulation and its activation can increase energy expenditure. Much of the seminal research on the energy-

expending properties of BAT was conducted in rodents (Cannon and Nedergaard, 2004). It was known that infants have a devoted BAT pad in a similar anatomical location to rodents to generate heat (Aherne and Hull, 1966), that was thought to recede to non-existent levels as the individual ages (Cannon and Nedergaard, 2004). The lack of BAT in adult humans has since been challenged since active BAT was identified in the supraclavicular, paracervical and anterior neck of adult humans by multiple independent groups (Cypess et al., 2009; van Marken Lichtenbelt et al., 2009; Virtanen et al., 2009) a decade ago using imaging techniques such as positron emission tomography-computed tomography (PET/CT) with ^{18}F-fluoro-thiaheptadecanoic acid or ^{18}F-fluorodeoxyglucose tracers. These studies indicate that adult BAT is a metabolic sink that can sequester large amounts of glucose and fatty acids suggesting it may be a clinically-relevant therapeutic target that can increase whole-body energy expenditure.

Brown adipocytes are the functional units in BAT that perform thermogenesis, characterized as polygonal shaped cells that contain multilocular lipid droplets (LD) and spherical shaped mitochondria (Ravussin and Galgani, 2011). Unlike the energy storing function of WAT, BAT is a highly oxidative tissue that oxidizes glucose and fatty acids to generate heat. This ability to undergo thermogenesis is dependent on the expression of uncoupling protein 1 (UCP1), the protein responsible for mitochondrial proton gradient dissipation and heat generation (Chouchani et al., 2019). This results in the loss of mitochondrial membrane potential that cannot be used for ATP synthesis, thereby reducing the

inhibition of respiration attributed to high ATP:ADP ratios (Chouchani and Kajimura, 2019). Collectively, mitochondrial uncoupling in brown and beige adipose tissue results in elevated rates of respiration, substrate oxidation and energy expenditure.

Brown adipocytes are regulated by norepinephrine (NE) and are highly innervated with noradrenergic fibres (Cannon and Nedergaard, 2004). In rodents NE-dependent stimulation of β_3-adrenergic pathways are found exclusively in adipose tissue and is responsible for stimulating lipolysis of triglyceride into fatty acids and glycerol, providing substrate for brown adipocyte thermogenesis (Mottillo et al., 2014). β_3-adrenergic receptors can also be activated pharmacologically using a β_3-specific adrenergic agonist, CL-316,243 (Largis et al., 1994). In contrast to rodents, human BAT is characterized by high expression of the β_1-adrenergic receptor.

In addition to induction of BAT thermogenesis, chronic activation of this pathway pharmacologically or through cold exposure induces adaptive alterations in WAT morphology and function (Lee et al., 2014b). In response to adrenergic activation, UCP1$^+$ multilocular lipid clusters coined beige (also known as "brite") adipocytes form amongst unilocular white adipocytes in WAT. Akin to brown adipocytes, beige adipocytes are capable of Ucp1-dependent thermogenesis and harness the same energy-expending capabilities (Shabalina et al., 2013). Chronic high-dose CL-316,243 administration or cold exposure can induce the emergence of this cell type (Chouchani and Kajimura, 2019). Although beige adipocytes are

only expressed in rodent WAT, rodent beige adipocytes possess a gene expression profile that is reminiscent of human BAT (Sharp et al., 2012), suggesting studies focused on the induction of rodent "browning" — the process of increasing $UCP1^{+}$ mitochondrial biogenesis in WAT — are of clinical importance.

1.3.2 TRANSCRIPTIONAL REGULATION

Development of thermogenic adipocytes is dependent on a two-part process consisting of lineage commitment and differentiation, both of which are governed by transcriptional regulation. Classical brown adipocytes arise from myogenic factor 5 positive ($Myf5^{+}$) dermomyotomes, precursors to skeletal muscle (Wang and Seale, 2016). Determination of myoblast or pre-brown adipocyte lineage commitment is dependent on early B cell factor 2 (Ebf2), which potently reduces the expression of the muscle-specific transcription factors myoblast determination protein (MYOD) and myogenin (Rajakumari et al., 2013; Wang et al., 2014) in rodents. In humans, EBF2 is expressed in brown pre-adipocytes, which may suggest its importance in brown pre-adipocyte determination (Inagaki et al., 2016). Ebf2 is a transcription factor that plays a key role in brown adipocyte lineage commitment.

Differentiation into mature brown adipocytes is highly reliant on four transcriptional regulators: peroxisome proliferator activated receptor gamma (PPARγ), CCAAT/enhancer-binding protein β (C/EBPβ), PR domain containing 16 (PRDM16) and PPARγ co-activator 1α (PGC1α). PPARγ and C/EBPβ are transcription factors that bind directly to DNA and dictate adipocyte cell fate by

promoting adipocyte-lineage specific genes (Wang and Seale, 2016). PRDM16 is a transcriptional co-regulator that promotes brown adipocyte formation adipogenesis by creating a transcriptional complex with PPARγ (Harms et al., 2014; Seale et al., 2007) and C/EBPβ (Kajimura et al., 2009). And similar to Ebf2, PRDM16 blunts myogenesis in pre-brown adipocytes (Seale et al., 2008), suggesting two distinct ways PRDM16 induces brown adipocyte cell lineage commitment and differentiation.

Beige adipocytes arise from $Myf5^-$ precursors, suggesting brown adipocytes developing from a distinct developmental lineage. Indeed, beige adipocytes emerge from bipotent stem cells positive for platelet-derived growth factor receptor-α ($PDGFR\alpha^+$) (Lee et al., 2012). Despite distinct lineages, the transcriptional control of beige adipocyte cell fate and differentiation is similar to that of brown adipocyte development. Ebf2 promotes beige adipocyte formation in rodent WAT (Stine et al., 2016; Wang et al., 2014) and is also highly expressed in $PDGFR\alpha^+$ precursor cells (Wang et al., 2014). PRDM16 activates beige-selective genes to induce beige adipogenesis, while deletion severely hinders this process (Cohen et al., 2014; Ohno et al., 2012; Seale et al., 2011).

Thermogenic adipose tissue function is highly dependent on the presence of the mitochondrial protein, UCP1 and the mechanisms are briefly described here (Cannon and Nedergaard, 2004). Canonically, Ucp1 expression is initiated after sympathetic nervous system (SNS) dependent stimulation of β-adrenergic receptor agonism on adipocytes. This induces the activation of G_s-linked adenylyl cyclase

to increase intracellular cAMP, which increases PKA activity. PKA phosphorylates cAMP-responsive element-binding (CREB) and ATF2 transcription factors leading to expression of *Ucp1* and *Pgc1a*. PGC1α is a transcriptional co-activator and a regulator of the thermogenic program in both brown and beige adipocytes. It can form complexes with PRDM16 and interferon regulatory factor 4 (IRF4) to regulate two distinct pathways of *Ucp1* transcription.

1.3.3 TEMPERATURE REGULATION

Shivering is an acute means of thermoregulation that involves the recruitment of muscle to undergo futile cycling. From an etiological perspective, rodents and human infants with small surface area to volume ratios require responses beyond shivering to regulate adequate heat production. Thus, non-shivering thermogenesis via thermogenic adipose tissues are required to defend against external environmental stresses (i.e. cold exposure) to maintain consistent internal body temperatures.

Cold exposure (4-10ºC) potently activates UCP1-dependent thermogenesis. The importance of Ucp1 in mouse thermoregulation is highlighted by the findings that Ucp1 ablation results in defective BAT thermogenesis (Enerbäck et al., 1997). Brown adipocytes are highly innervated with sympathetic nerve fibres that release norepinephrine in response to cold exposure. Through the β-adrenergic pathway described previously, cold exposure directly promotes the transcription of *Ucp1* and *Pgc1a* in brown adipocytes (Barbatelli et al., 2010; Bartelt et al., 2011; Sanchez-

Gurmaches et al., 2018) and subsequently plays a role in BAT thermogenesis (Crane et al., 2014). Similar β_3-adrenergic receptor-dependent mechanisms are employed in WAT since β_3-adrenenoreceptor knockout mice have a reduced ability to recruit brown adipocyte-like cells in WAT (Barbatelli et al., 2010; Guerra et al., 1998).

Mice housed in human room temperature (22-23ºC) are under chronic mild cold stress, resulting in the recruitment of adipose tissue-dependent thermogenesis. In contrast, temperatures that are thermoneutral (28-30ºC) for mice reduce the need for *Ucp1* expression, protein and thermogenic function in both BAT and subcutaneous WAT of mice (Cui et al., 2016; Feldmann et al., 2009; Roh et al., 2018). Recently, the characteristics of thermoneutral rodent BAT was shown to be similar to that of human BAT, suggesting translational studies aimed at human BAT recruitment should utilize rodents in thermoneutrality (de Jong et al., 2019). Studying mice in thermoneutrality and comparing to lower temperatures is a useful experimental methodology to study thermogenic adipose tissue-dependent regulation on systemic metabolism (Nedergaard and Cannon, 2010) with potential clinical relevance.

Obesity and insulin resistance are associated with reductions in adipose tissue futile cycling. The loss of adipose tissue thermogenesis is partially attributed to adipose tissue mitochondrial dysfunction. Further, obesity (Xiao et al., 2014) and type 2 diabetes (Choo et al., 2006) is related to losses in adipose tissue mitochondrial oxidative phosphorylation. Since the discovery of active BAT in

adult humans, significant research efforts have been devoted to finding regulators — intracellular proteins, extracellular messengers and receptors — of adipose tissue thermogenesis. As alluded to previously, the ability of thermogenic adipocytes to expend energy via mitochondrial uncoupling carries attractive therapeutic potential since it results in the total dissipation of glucose and fatty acids. Individuals with obesity, type 2 diabetes and old age have reductions in BAT function (Cypess et al., 2009; van Marken Lichtenbelt et al., 2009). Thus, therapies aimed at increasing BAT-dependent energy expenditure may hold merit to mitigate metabolic disease (Carey and Kingwell, 2013; Loh et al., 2017).

1.3.4 IMMUNE CELL REGULATION

The immune system is a complex network of cells, tissues and organs that work in concert to protect the body from foreign pathogen infection. Additionally, it regulates homeostasis of metabolic tissues such as brown, beige and white adipose tissues (Gregor and Hotamisligil, 2011; Man et al., 2017; Mraz and Haluzik, 2014). Macrophages are functionally and numerically dominant and can influence the state of adipose tissue inflammation (Nguyen et al., 2011). Adipose tissue is populated by macrophages, immune cells that can adopt an alternatively-activated, anti-inflammatory (M2 macrophages) or classically-activated, pro-inflammatory (M1 macrophages) phenotype when exposed to cytokines from other resident immune cells or adipocytes (Lumeng et al., 2007).

Lean WAT function is reliant on a complex network of resident anti-inflammatory immune cells, such as M2 macrophages, and their respective secretory cytokines. In lean adipose tissue, type 2 immune cells such as eosinophils, group 2 innate lymphoid cells (ILC2s), T_H2 and T_{reg} cells secrete anti-inflammatory cytokines that polarize resident macrophages to the alternatively activated (M2) phenotype, a non-inflammatory macrophage state. IL-4 and IL-13, cytokines secreted by eosinophils and ILC2s, respectively, are required for the biogenesis of beige adipose tissue (Lee et al., 2014a; Qiu et al., 2014). This is done in two ways: (1) they stimulate proliferation and commitment of PDGFRα^+ progenitors in WAT to become beige adipocytes (Lee et al., 2014a; Wang and Seale, 2016) and (2) they support M2 macrophage polarization to increase adrenergic tone of adipose tissues (Nguyen et al., 2011; Qiu et al., 2014). Furthermore, T_{reg} and T_H2 lymphocytes secrete type 2 cytokines (i.e. IL-4, IL-5 and IL-13) that inhibit macrophage migration and induce M2 macrophage polarization (Man et al., 2017). And while M2 macrophages were thought to be essential for adaptations to cold stress through thermogenic regulation of BAT function and "browning" of WAT (Nguyen et al., 2011), this has not been observed in all studies (Fischer et al., 2017). Thus, the role of M2 macrophages in regulating adipose tissue thermogenesis is equivocal. The role of other immune cells such as mast cells in regulating adipose tissue thermogenesis is largely unknown.

Obese adipose tissue is associated with the infiltration of pro-inflammatory immune cells. Most notably, M1 macrophages and mast cells increase in mouse and

human obese WAT (Altintas et al., 2011; Liu et al., 2009). The number of pro-inflammatory M1 macrophages is vastly increased in obese humans (Aron-Wisnewsky et al., 2009) and HFD-induced rodents (Lumeng et al., 2007; Weisberg et al., 2003), impairing anti-inflammatory macrophage-dependent adipose tissue insulin sensitivity and adipocyte differentiation. These alterations in adipose tissue function are partially attributed to M1 macrophage-dependent secretion of cytokines such as TNF and IL-6.

Despite their main function in regulating asthma and allergy, mast cells have been associated with obesity and insulin resistance in rodents and humans. The seminal work by Liu and colleagues in 2009 showed that genetic deletion or pharmacological stabilization of mast cell degranulation was associated with improvements in insulin sensitivity and weight gain in HFD-fed mice (Liu et al., 2009). Soon after, mast cells were shown to be associated with obese adipose tissue inflammation (Divoux et al., 2012) and fibrosis (Gurung et al., 2019; Hirai et al., 2014). Further, the absence of mast cell-derived leptin or reconstitution of leptin-deficient mast cells has been associated with higher M2 macrophage polarization in obese rodents (Zhou et al., 2015).

1.4 SEROTONERGIC REGULATION OF METABOLISM

EMERGING ROLES FOR SEROTONIN IN REGULATING METABOLISM: NEW IMPLICATIONS FOR AN ANCIENT MOLECULE

Published in *Endocrine Reviews*. Volume 40. Issue 4. Pages 1092-1107.
August 2019

Julian M. Yabut, Justin D. Crane, Alexander E. Green, Damien J. Keating, Waliul I. Khan & Gregory R. Steinberg

In this review of the literature, we aimed to summarize the existing literature on the ancient bioamine, serotonin and how it regulates whole-body metabolism. Specifically, we looked into the etiology of serotonin and discovered that it plays a highly conserved role in energy balance across different phyla, ranging from primitive photosynthetic organisms to humans. Although serotonin is primarily synthesized in the raphe nuclei and the gastrointestinal system, it can be synthesized in many other peripheral tissues such as pancreatic β-cells, adipocytes, and mast cells. We also discussed the primary serotonin receptors regulating serotonin signalling in different tissues. Further, we collated the literature and came to the novel conclusion that serotonin plays a key role in promoting energy storage by enhancing insulin secretion and *de novo* lipogenesis in the liver and white adipose tissue, while reducing the activity of thermogenic adipose tissues. Since serotonin plays a pivotal role in lipid storage, we suggest that inhibition of serotonin synthesis or signaling may be a potential therapeutic target to treat obesity, type 2 diabetes and non-alcoholic fatty liver disease (NAFLD).

J.M.Y. and G.R.S. wrote the manuscript. J.D.C., A.E.G., D.J.K.,W.I.K. edited the manuscript and provided comments and additional references. J.M.Y. was the lead author.

J.M.Y. wrote entire manuscript and conceptualized all figures.

REVIEW

Emerging Roles for Serotonin in Regulating Metabolism: New Implications for an Ancient Molecule

Julian M. Yabut,[1,2] Justin D. Crane,[3] Alexander E. Green,[1,2] Damien J. Keating,[4] Waliul I. Khan,[2,5,6] and Gregory R. Steinberg[1,2,7]

[1]Division of Endocrinology and Metabolism, Department of Medicine, McMaster University, Hamilton, Ontario L8N 3Z5, Canada; [2]Centre for Metabolism, Obesity and Diabetes Research, McMaster University, Hamilton, Ontario L8N 3Z5, Canada; [3]Department of Biology, Northeastern University, Boston, Massachusetts 02115; [4]College of Medicine and Public Health, Flinders University, Bedford Park, South Australia 5042, Australia; [5]Farncombe Family Digestive Health Research Institute, McMaster University, Hamilton, Ontario L8N 3Z5, Canada; [6]Department of Pathology and Molecular Medicine, McMaster University, Hamilton, Ontario L8N 3Z5, Canada; and [7]Department of Biochemistry and Biomedical Sciences, McMaster University, Hamilton, Ontario L8N 3Z5, Canada

ORCiD numbers: 0000-0001-5425-8275 (G. R. Steinberg).

ABSTRACT Serotonin is a phylogenetically ancient biogenic amine that has played an integral role in maintaining energy homeostasis for billions of years. In mammals, serotonin produced within the central nervous system regulates behavior, suppresses appetite, and promotes energy expenditure by increasing sympathetic drive to brown adipose tissue. In addition to these central circuits, emerging evidence also suggests an important role for peripheral serotonin as a factor that enhances nutrient absorption and storage. Specifically, glucose and fatty acids stimulate the release of serotonin from the duodenum, promoting gut peristalsis and nutrient absorption. Serotonin also enters the bloodstream and interacts with multiple organs, priming the body for energy storage by promoting insulin secretion and *de novo* lipogenesis in the liver and white adipose tissue, while reducing lipolysis and the metabolic activity of brown and beige adipose tissue. Collectively, peripheral serotonin acts as an endocrine factor to promote the efficient storage of energy by upregulating lipid anabolism. Pharmacological inhibition of serotonin synthesis or signaling in key metabolic tissues are potential drug targets for obesity, type 2 diabetes, and nonalcoholic fatty liver disease (NAFLD). ***(Endocrine Reviews 40: 1092 – 1107, 2019)***

ISSN Print: 0163-769X
ISSN Online: 1945-7189
Printed: in USA

Received: 24 December 2018
Accepted: 18 March 2019
First Published Online: 22 March 2019

Serotonin, also known as 5-hydroxytryptamine (5-HT), is a key messenger that mediates a range of central and peripheral functions in the human body. As a neurotransmitter in the central nervous system (CNS), it is required for several brain functions and is associated with anxiety and behavior. Furthermore, central serotonin contributes to neuronal control of motility and intestinal fluid secretions in the gut (1). However, the actions of serotonin extend beyond neuronal communication in the CNS and enteric nervous system (ENS) to peripheral tissues. Serotonin mediates numerous nonneuronal processes such as bladder function, respiratory drive, hemostasis, vascular tone, immune function, and intestinal inflammation (2–6).

Serotonin is also a major regulator of both inputs of energy balance, energy intake, and energy expenditure. CNS serotonin is intricately involved in appetite and subsequent nutrient intake, a complex process that has been extensively reviewed (7). Serotonin's inhibitory effect on appetite has led to the approval of receptor agonists for the treatment of obesity (8–11). Furthermore, aspects of digestion (12), insulin production (13, 14), and liver repair (15) are dependent on peripheral serotonin-mediated signaling. Other studies demonstrate that reducing peripheral serotonin synthesis (16) and signaling in adipose tissue (17) can prevent obesity, insulin resistance, and nonalcoholic fatty liver disease (NAFLD) due to enhanced energy expenditure of brown and beige adipose tissues. Consistent with these roles in regulating energy balance and insulin production, genetic polymorphisms associated with serotonin synthesis and signaling have been linked to the development of obesity and type 2

 doi: 10.1210/er.2018-00283

ESSENTIAL POINTS

- Serotonin is a bioamine that has been involved in regulating metabolism across different phyla for billions of years
- Serotonin synthesis in the periphery (*e.g.*, outside the central and enteric nervous system) is dependent on the enzyme tryptophan hydroxylase 1
- Peripheral serotonin exerts effects in multiple metabolic tissues through distinct serotonin receptors to promote nutrient absorption and storage while inhibiting futile cycling/thermogenesis
- Inhibiting peripheral serotonin synthesis or signaling may be effective for treating obesity, type 2 diabetes, and nonalcoholic fatty liver disease

diabetes (18–20). In this review, we discuss the role of serotonin in regulating metabolism, how tissue disequilibrium of serotonergic signaling can manifest as metabolic disease, and how emerging evidence implicates serotonin as a critical sensor of nutrient balance that promotes whole-body lipid anabolism.

Primitive Origins of Serotonin

Serotonin is a highly conserved biogenic amine within the phylogenetic tree. Chemically, serotonin is a bioactive monoamine that can capture light via its indole ring—a key aromatic structure present in both serotonin and its precursor, tryptophan (21). Because of this property, the tryptophan present within primitive unicellular organisms (*i.e.*, cyanobacteria and green algae) became oxidized by high-energy solar photons to produce the important energy metabolite reduced nicotinamide adenine dinucleotide (NADH) via the electron transport chain (22). This process represented an early method of acquiring energy from the environment for conversion into useable, biochemical energy. The rising atmospheric oxygen in the Archean Eon due to anaerobic metabolism shifted cellular carboxylases to acquire their hydroxylase function (23), which is the enzyme class responsible for the rate-limiting step in serotonin synthesis [tryptophan hydroxylase (Tph)]. Although it is still unclear why serotonin was specifically selected to play a key role in energy balance, its conservation across modern phyla and its actions on numerous tissues underscores its importance in metabolism.

As evolutionarily-driven selective pressure conserved serotonergic signaling across species, there is considerable overlap among vertebrates and invertebrates with regard to its regulation of energy balance. *Drosophila melanogaster* is a well-studied arthropod whose fat body serves as a highly diverse organ with analogous functions to human adipose, liver, vascular, and immune tissues and similar tissue metabolic regulation (24). In accordance with serotonergic underpinnings to appetite in invertebrates, Vargas *et al.* (25) observed increased food intake when *D. melanogaster* is fed the serotonin precursor 5-hydroxytryptophan (5-HTP). In contrast, in arthropods, the injection of serotonin into the brain of honeybees and blowflies reduces sucrose and amino acid consumption (26, 27). In addition to directly regulating appetite, serotonin signaling is also required for blood-sucking organisms such as *Rhodnius prolixus* (the "kissing bug") and the medicinal leech (various *Hirudo* species) to extend the abdominal wall and increase crop contraction frequency after feeding, a process that enables these organisms to consume meals up to 15 times their original size (28–31). *Caenorhabditis elegans*, a model organism often used to study energy balance and lipid metabolism, employs a central serotonergic system that reduces fat content by increasing fat oxidation (32) and promotes food intake behaviors such as pharyngeal pumping (33, 34). Many other invertebrates such as gastropods, annelids, and various other arthropods also rely on serotonergic processes to mediate feeding behaviors (28, 35–37). Thus, diverse arrays of primitive invertebrate phyla regulate energy balance via serotonin-dependent mechanisms.

Serotonin Synthesis, Metabolism, and Signaling in Mammals

Synthesis

In mammals, serotonin is synthesized from tryptophan (Fig. 1). The synthesis of serotonin is tightly linked to tryptophan availability, kynurenine synthesis (discussed below), and the rate-limiting enzyme Tph. Tph produces the precursor 5-HTP, which is then rapidly converted to serotonin by aromatic amino acid decarboxylase (Fig. 1). Tph exists in two isoforms: Tph1 is mainly present in the periphery, whereas Tph2 predominates in the raphe nuclei of the brainstem (38–40), with the exception of the ENS, which also predominantly expresses Tph2 (Fig. 2). Because serotonin does not readily pass the blood–brain barrier, its central and peripheral pools (with the exception of the ENS) are largely functionally distinct and regulate serotonin-dependent processes in the brain and periphery, respectively.

REVIEW

In the periphery, circulating serotonin is primarily synthesized by Tph1 within enterochromaffin (EC) cells of the gastrointestinal tract (38, 40–44) (Fig. 2). The expression and activity of Tph1 in EC cells is regulated by the action of surrounding cells and nutrients (Fig. 2). For example, in response to enteric parasitic infection, EC cell serotonin synthesis is enhanced by $CD4^+$ T cells and IL-13 (45). Carbohydrates (*i.e.*, glucose, fructose, and sucrose) also increase serotonin secretion of colonic and duodenal EC cells (46), thus directly linking nutrient availability to serotonin production (47). In rodents, this response to

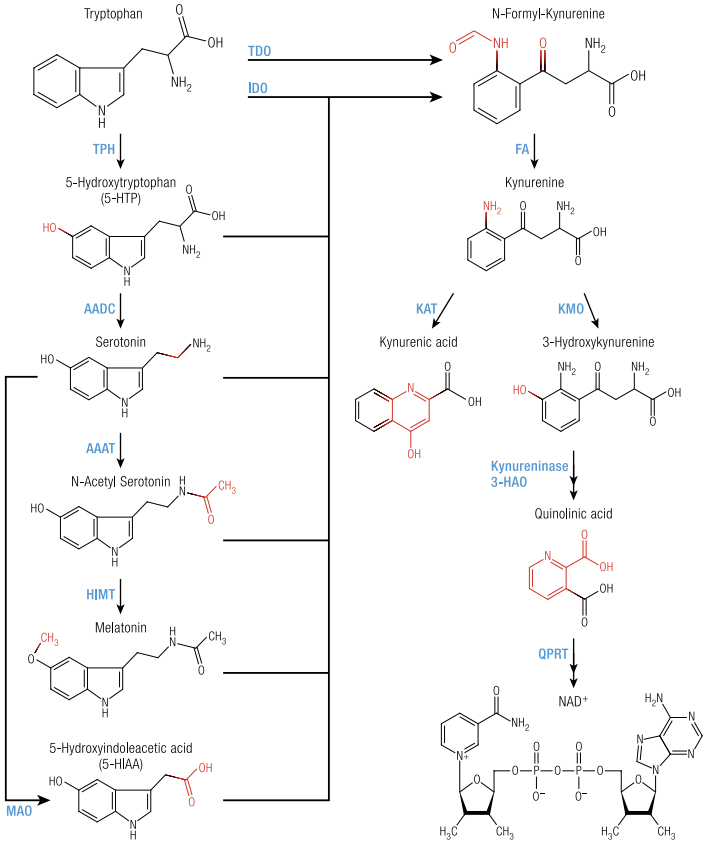

Figure 1. Key enzymes regulating tryptophan metabolism. Left panel: Tryptophan is metabolized by Tph to 5-HTP and subsequently metabolized to serotonin by amino acid decarboxylase (AADC). Serotonin can be metabolized into either 5-HIAA by MAO or *N*-acetyl-serotonin by arylalkylamine *N*-acetyltransferase (AAAT). *N*-acetyl-serotonin is subsequently metabolized into melatonin by hydroxyindole-*O*-methyl transferase (HIMT). Right panel: Tryptophan is also a substrate for TDO to produce *N*-formyl kynurenine, which can be made into kynurenine by formamidase (FA). IDO can also metabolize tryptophan into *N*-formyl-kynurenine alongside any other molecules that contain an indole moiety. Kynurenine aminotransferase (KAT) and kynurenine 3-monooxygenase (KMO) form kynurenic acid and 3-hydroxykynurenine, respectively, from kynurenine. Kynurenine is broken down by kynureninase and 3-hydroxyanthranilic acid dioxygenase (3-HAO) to form quinolinic acid, which can be further metabolized by quinolinic acid phosphoribosyltransferase (QPRT) to form precursors for NAD^+. Atoms in red are the structural changes of the previous enzymatic reaction. MarvinSketch (from ChemAxon) was used for drawing and displaying chemical structures in this figure.

Figure 2. Tissue-specific regulation of tryptophan, serotonin, and kynurenine metabolism. Left panel: EC cell Tph1 activity is regulated by microbiota-derived short-chain fatty acids (SCFAs), glucose, and secretory products of $CD4^+$ T cells in the gut lumen. Middle panel: Tryptophan (white circle) is converted into 5-HTP in the CNS or in EC cells by Tph2 and Tph1, respectively, and is then quickly metabolized to serotonin (5-HT) by amino acid decarboxylase (AADC). Central (orange circle) and peripheral (blue circle) pools of serotonin are distinct, as they cannot pass the blood–brain barrier (BBB). Centrally synthesized serotonin can affect various areas of the brain such as POMC neurons, ventral tegmental area (VTA), and nucleus of the solitary tract (NST). Serotonin synthesis in the ENS is dependent on Tph2 and innervates neurons in the submucosal plexus (Smp) and myenteric plexus (MyP) to induce motility. Serotonin produced by Tph1 in EC cells is imported into enterocytes by SERT (orange transporter) and subsequently degraded by enterocyte MAO into 5-HIAA (gray circle). Tryptophan is also metabolized into kynurenine (Kyn; green circle) in the liver by TDO. Serotonin, 5-HIAA, and Kyn can be excreted into the circulation. Serotonin is sequestered by SERT of blood platelets, transported to the circulation, and effects systemic metabolism upon release into the plasma (double arrow).

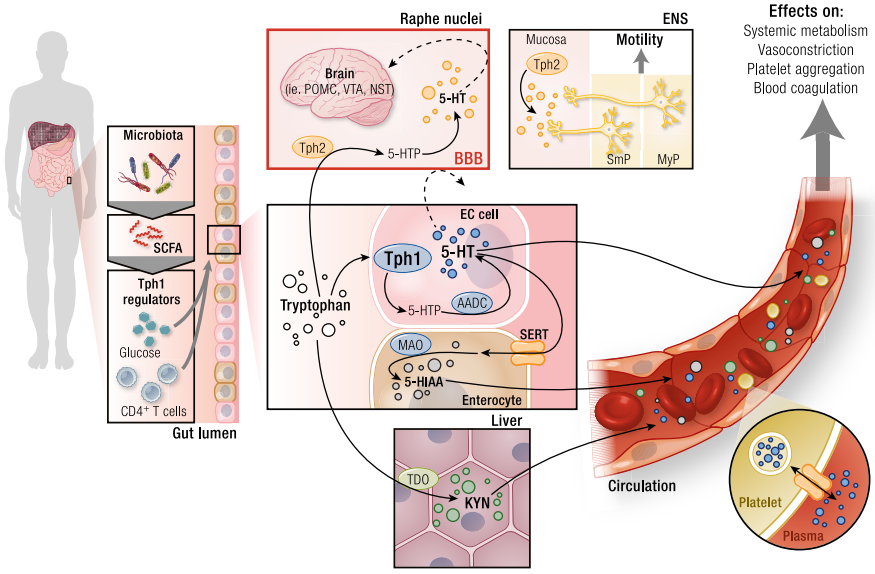

nutrients has been shown to be modulated by the gut microbiome production of short-chain fatty acids (*i.e.*, acetate and butyrate), which increase Tph1 expression and serotonin synthesis in EC cells, resulting in elevated circulating serotonin concentrations in the bloodstream (48, 49). However, this axis has recently been challenged because exposure of EC cells to acetate or butyrate on EC cells does not acutely elevate serotonin secretion from duodenal or colonic EC cells (46). Further studies investigating factors regulating Tph1 expression, activity, and subsequent serotonin synthesis in humans are warranted.

In addition to serotonin synthesis, a large majority of dietary tryptophan is directed toward kynurenine (Figs. 1 and 2) (50). The conversion of tryptophan to kynurenine requires the rate-limiting enzymes indoleamine 2,3-dioxygenase (IDO), found ubiquitously except in the liver, or tryptophan 2,3-dioxygenase (TDO), which is found in hepatic tissues (51, 52). IDO has a broader substrate specificity than TDO (51), reacting with the indole moiety of a variety of serotonergic pathway constituents (*i.e.*, tryptophan, 5-HTP, serotonin, melatonin). IDO activation by proinflammatory cytokines such as IFNγ and TNFα reduces serotonin and enhances kynurenine levels (51, 53). IDO activation is linked to increases in kynurenine and reductions in serotonin associated with depression (54). In neurons, subsequent metabolism of kynurenine to picolinic acid instead of quinolinic acid, which is metabolized to NAD^+ (55, 56), is protective against neurotoxicity (57). Thus, in addition to Tph, the kynurenine pathway is also important for dictating serotonin synthesis and availability.

Excretion and transportation

EC cell stimulation triggers the release of serotonin into the interstitial space of surrounding cells (Fig. 2). EC cells act as sensory transducers that respond to postprandial disruptions in the lumen of the gut such

REVIEW

as pH changes or the presence of nutrients and toxins. Owing to the absence of direct contact between the lumen and the ENS, EC cells act as a mediator between the two by secreting serotonin, stimulating nearby enteric neurons and increasing gut motility and peristalsis. EC cells possess serotonin that can be released basolaterally to stimulate ENS afferent neurons (41) or apically to the mucosal surface of the gut lumen in response to luminal stimuli (58). It has been shown that serotonin release is regulated in part through a population of gut epithelial EC cells that are mechanosensitive to luminal forces, and this process requires Piezo2 (59). Released serotonin activates receptors to induce transient gut peristalsis. However, it must be removed from the interstitial space to cease signaling when it is no longer required.

The high levels of serotonin generated by EC cells necessitates a well-regulated control system to remove serotonin from the interstitial space of the gut to terminate serotonergic signaling and prevent serotonin toxicity (Fig. 2). Clearance of interstitial serotonin occurs by either sequestration of serotonin into enterocytes or transport into the circulatory system. Enterocytes of the intestinal mucosa take up serotonin via the serotonin transporter (SERT), and it is then degraded by monoamine oxidase (MAO). The remaining serotonin enters the circulation through capillary beds in the submucosa of the intestinal wall. Once in the bloodstream, most serotonin is sequestered by SERT-mediated transport within platelets (60). Because platelets lack Tph, there is no ability to synthesize serotonin, and thus they act solely as a carrier (61). Once within platelets, vesicular monoamine transporters compartmentalize serotonin into dense granules (62). As in many cell types, platelets can also degrade granular serotonin by MAO (63). Significant quantities, but not all, of serotonin packaged in platelets can then be efficiently transported throughout the circulation. Circulating platelets then release serotonin in response to stimuli, where it can induce vasoconstriction (4), enhance platelet aggregation and thus blood coagulation (64).

The serotonin found outside platelets is freely soluble in plasma and is thought to be the active metabolite available for import and signaling in peripheral tissues. However, the analysis and biological relevance of this platelet-free fraction are not completely understood. This is due to numerous factors, including sample contamination by platelets, pathophysiological-induced changes in platelet fragility, or anticoagulation methods to isolate plasma, which can all impact quantification of free serotonin in the blood. Thus, a clear relationship between free, unbound circulating serotonin and pathology is not clearly established (65). Given the challenges of assessing platelet-free serotonin in blood, the assessment of more stable downstream metabolites (discussed in detail below) such as 5-hydroxyindoleacetic acid (5-HIAA) in urine is frequently used as a more reliable proxy of circulating serotonin levels (66).

Metabolism

Most serotonin is broken down by MAO (Figs. 1 and 2). MAO has two isoforms, MAO-A and MAO-B, with the former having a much higher affinity for serotonin (67). The product of MAO-dependent catabolism of serotonin is 5-hydroxyindole aldehyde, which is further metabolized into 5-HIAA by aldehyde dehydrogenase (68). Serotonin can also be metabolized to *N*-acetyl-serotonin by arylalkylamine *N*-acetyltransferase and, subsequently, into melatonin by hydroxyindole *O*-methyltransferase (69). As discussed above, serotonin can also be metabolized by IDO to enter the kynurenine pathway (68). Thus, the abundance of serotonin is dependent on not only tryptophan availability and the expression and activity of Tph but also the activity of enzymes involved with serotonin metabolism such as MAO, IDO, and TDO.

Signaling

Serotonin can signal by receptor transduction and may also signal posttranslationally via a concept termed "serotonylation." Serotonylation was first described by Walther and *et al.* (13) as a transamidation of serotonin to small GTPases by the enzyme transglutaminase in platelets. This process blocks GTP hydrolysis and results in constitutive activity of the respective GTPase, in the outcome, which is platelet degranulation. This process has also been observed in pancreatic β-cells, where serotonylation of small GTPases facilitates insulin secretion (14).

Although serotonylation of target proteins may be important in some contexts, the vast majority of serotonin's functions are thought to occur through binding to one of 14 cell surface 5-HT receptors (HTRs), categorized into seven families based on their functional, structural, and signal transduction properties (70) (Fig. 3). With the exception of HTR_3, which is a ligand-gated ion channel, the other six families are G-protein–coupled receptors. Thus, serotonin can initiate two intracellular mechanisms: plasma membrane depolarization or G-protein–mediated modification of intracellular messenger (cAMP, inositol triphosphate, diacylglycerol) levels upon the binding of serotonin (71). Briefly, the HTR_1 and HTR_5 families initiate a G_i/G_o-protein–coupled transduction that subsequently decreases cAMP levels. Conversely, the HTR_4, HTR_6, and HTR_7 receptor families are coupled to the G_s-protein and increase cellular cAMP levels. Lastly, the HTR_2 family is coupled to the G_q/G_{11}-protein and increases levels of inositol triphosphate and diacylglycerol. The initial receptor actions and receptor localization are summarized in Fig. 3. Thus, multiple facets of regulation and signaling can occur simultaneously upon serotonin binding to multiple receptors. Additionally, the expression of the seven

Figure 3. Serotonin receptor expression and signaling pathways. The seven distinct serotonin receptors (HTR_x) families have unique tissue-specific distributions and can be grouped into four distinct downstream signaling pathways. The HTR_2 pathway employs the G-protein $\alpha_{q/11}$ subunit (G_q/G_{11}), which induces phospholipase C (PLC), leading to the upregulation of inositol triphosphate (IP_3), calcium, and diacylglycerol (DAG), which activates protein kinase C (PKC). HTR_1/HTR_5 use the G-protein α_i subunit (G_i/G_o) that inhibits adenylate cyclase (AC), thereby reducing the production of cAMP from ATP. HTR_4/HTR_6/HTR_7 use the G-protein α_s subunit (G_s) that activates AC, which increases cAMP and induces the phosphorylation of protein kinase A (PKA). HTR_3 is a serotonin-gated ion channel that increases intracellular concentrations of cations, which can cause cell depolarization.

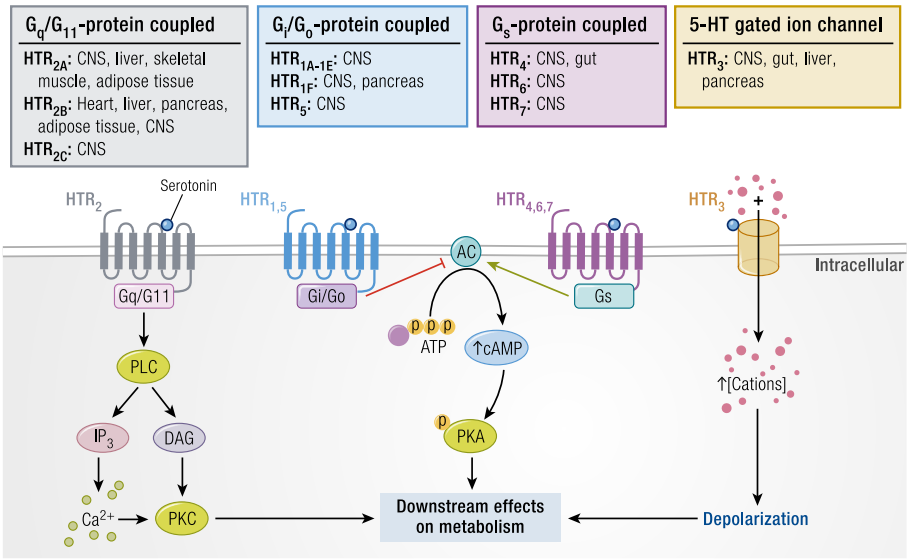

families and 14 individual HTRs vary across tissues in the central and peripheral systems, which further allows serotonin to exert differential effects.

Central Serotonin Regulation of Energy Balance

The role of central serotonin in suppressing appetite in mammals is well established, and several recent reviews have detailed the mechanisms mediating these effects (72, 73). Therefore, this review only provides a general overview. Broadly, central serotonergic systems suppress feeding behaviors in vertebrate species, and depletion of central serotonin induces hyperphagia and body weight gain in rodents (74). Appetite is primarily regulated by processes innervated in the hypothalamus, where proopiomelanocortin (POMC) is expressed in neurons of the hypothalamic arcuate nucleus (ARC) and brainstem. POMC is posttranscriptionally modified to form α- and β-melanocyte–stimulating hormones and activate melanocortin-4 receptors to reduce food intake and appetite. Moreover, agouti-related protein exists exclusively in agouti-related peptide (AgRP)/neuropeptide Y (NPY) neurons in the ARC, which functions as a direct inhibitor of melanocortin-4 receptor activation to increase appetite and food intake. Activation of AgRP/NPY neurons release γ-aminobutyric acid, which inhibits POMC neurons and decreases food intake. ARC POMC neurons are stimulated and AgRP/NPY neurons are inhibited by hypothalamic serotonin (75, 76), which is synonymous to the actions of leptin on these neurons (77, 78).

The suppressive effects of serotonin on appetite appear to be primarily driven by HTR_{2C}. Specifically, Tecott and colleagues (79) observed that mice lacking HTR_{2C} had increased appetite and were prone to obesity. It was later found that HTR_{2C} mutant mice also displayed decreased food intake and body weight after acute leptin administration (78). Subsequent studies demonstrated that these suppressive effects on appetite were dependent on HTR_{2C} within POMC neurons (80, 81). With the advent of new genetic approaches, recent reports have demonstrated that HTR_{2C} also suppresses appetite through dopaminergic neurons (82), the ventral

REVIEW

tegmental area (83), and the nucleus of the solitary tract (84). Note that in some instances activation of HTR_4 (85) and HTR_{1B} (86, 87) may also suppress appetite, but under most physiological conditions HTR_{2C} appears to be predominant. Highlighting the importance of HTR_{2C}, therapeutic agonists such as lorcaserin suppress appetite and have been approved in some countries to treat obesity (8–11).

Serotonin regulation of appetite might also potentially be involved with weight gain associated with the use of some antidepressants. For example, selective serotonin reuptake inhibitors (SSRIs), which inhibit SERT function and prolong serotonin neurotransmission, have been linked to modest increases in weight gain and the incidence of type 2 diabetes (88–90). Mechanistically, these observations are consistent with increased obesity, glucose intolerance, and insulin resistance in mice lacking SERT (91, 92). However, many SSRIs also alter the activity of other neurotransmitter pathways (89, 93–96) and, as a result, weight gain is not consistently observed (88, 97, 98). Further randomized controlled trials are needed to evaluate whether SSRIs regulate appetite, weight gain, and possibly energy expenditure (detailed below) and the potential importance of serotonin in mediating these side effects.

In addition to the regulation of appetite and energy intake, central serotonin is also implicated in increasing energy expenditure. As recently reviewed (99), serotonin increases energy expenditure by enhancing sympathetic drive to brown adipose tissue (BAT). This increase in energy expenditure by serotonin may be mediated through activation of HTR_{1A} and HTR_7 within the intermediolateral nucleus of the spinal cord (100, 101). Importantly, alleviation of central serotonin signaling in the brain results in a loss of thermoregulation due to reduced uncoupling protein 1 (Ucp1) content in both BAT and inguinal white adipose tissue (WAT) (102). Despite the described roles of central serotonin to stimulate energy expenditure, mice lacking central serotonin synthesis due to reductions in Tph2 are lean and have increased energy expenditure (103, 104). This is surprising, as a lack of central serotonin would be expected to lower energy expenditure if it were critical for modulating sympathetic tone. Future studies investigating the role of central

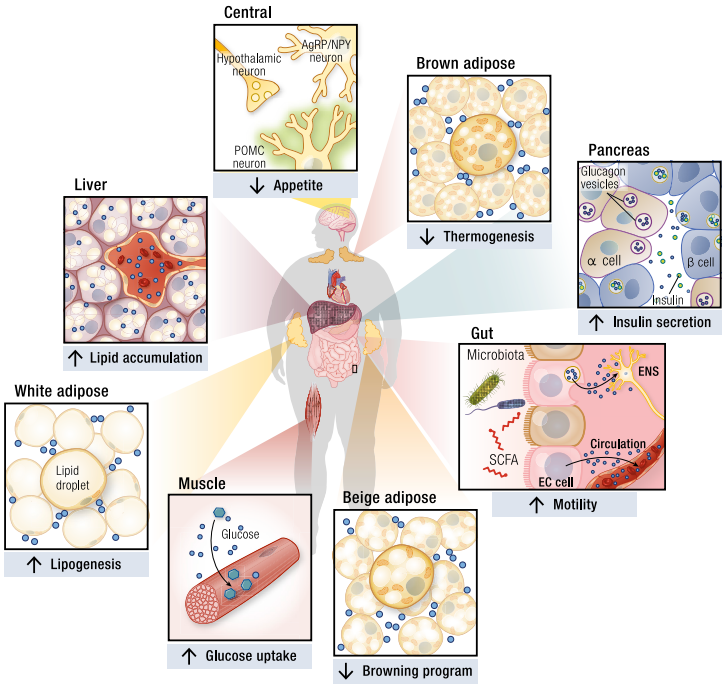

Figure 4. Metabolic functions of serotonin in different tissues. Central serotonin suppresses appetite, reducing nutrient intake. In the periphery, serotonin promotes nutrient storage by increasing gut motility to facilitate absorption after feeding. Serotonin enhances insulin secretion from pancreatic islets, which enhances nutrient storage in different tissues. The effects of insulin to promote nutrient storage are further enhanced through direct actions of serotonin to promote *de novo* lipogenesis in WAT and liver and to stimulate glucose uptake in skeletal muscle while at the same time inhibiting futile cycling/thermogenesis within BAT and beige adipose tissue.

serotonin in regulating nonshivering thermogenesis will be important.

Peripheral Serotonin Regulation of Energy Balance

More than 95% of the body's serotonin is found outside of the CNS. Although it has been recognized for more than half of a century that serotonin can regulate actions in the periphery, such as vasodilation (105) and blood pressure control (106), only in recent years has the role of serotonin in regulating the function of key metabolic organs and energy homeostasis emerged.

Gastrointestinal tract

An important role for serotonin in regulating energy balance involves its control of gut motility (Fig. 4). Serotonin induces and regulates muscular peristaltic activity in the gastrointestinal tract by modulating motor and sensory functions in the gut via serotonin receptor transduction in enteric neurons. For example, it influences the activation and inhibition of submucosal and myenteric neurons involved in intestinal peristalsis, secretion, and sensation via HTR_3 and HTR_4 (107). Additionally, HTR_4 accelerates propulsive motility (108) and mediates postnatal ENS growth and neurogenesis (109). Tph1 expression and EC cell density can be upregulated by certain spore-forming bacteria to increase gastrointestinal motility (48). Removal of Tph1 depletes serotonin from mucosal cells in the murine gut, but it does not affect serotonin content in enteric neurons (6). Removal of EC cells or Tph1 expression and EC cell serotonin synthesis does not result in loss of gut motility, but it acts to reduce the frequency of contractile events underlying peristalsis such as colonic migrating motor complexes (110–112). The lack of *in vivo* changes to gut transit time in the Tph1 knockout mouse model is likely attributable to developmental changes occurring in the gut such as enlarged bowel width and length (110) and increased villus height and crypt depth (6). Tph2-dependent serotonin synthesis is required for proper development of the ENS, with loss of ENS serotonin synthesis resulting in improper development and survival of enteric dopaminergic neurons (6). The creation of inducible models of Tph1 and Tph2 ablation may be a suitable approach that circumvents such developmental issues in these existing knockout models. Furthermore, a recent report suggests that mucosal serotonin can rectify the abnormal colonic motor activity in germ-free mice, which further emphasizes the role of EC-derived serotonin in gut motility (113). Highlighting the importance of serotonin in regulating gut motility, pan-Tph1/2 inhibitors have recently been approved owing to their pronounced effect on reducing gut motility (diarrhea) in patients with carcinoid syndrome (benign tumors that synthesize excessive serotonin) (114, 115).

In addition to its role in gut motility, serotonin from the gastrointestinal tract has been implicated in gut inflammation. The pathogenesis of colitis, that is, inflammation of the inner lining of the colon, has been attributed to serotonin (5). Serotonin has also been implicated in various gastrointestinal diseases, such as inflammatory bowel disease, irritable bowel syndrome, and celiac disease (116). Therefore, understanding the role of serotonin in gut peristalsis and inflammation has important implications for nutrient absorption, nutrient intake, and for illnesses that affect the gut.

Pancreas

The pancreas plays a pivotal role in controlling blood glucose through the secretion of insulin and glucagon from β-cells and α-cells, respectively. Pancreatic islets increase their serotonin production when treated with 5-HTP (117), indicating an inherent capacity for serotonin synthesis. Serotonin and insulin are colocalized in secretory β-granules (118) and are cosecreted when stimulated by glucose (119). Indeed, recent studies have shown common expression profiles of genes and transcription factors between serotonergic neurons and β-cells (120).

Local effects of serotonin in the pancreas are regulated by a complex network of receptor signaling. High glucose-stimulated β-cell secretion of serotonin (coreleased with insulin) activates α-cell HTR_{1F} and inhibits glucagon secretion in a paracrine manner (121). Recent *in vitro* work in INS-1 cells has found that activation of HTR_{2B} stimulates insulin secretion in response to glucose (122); however, the opposite effect appears to be observed in some species for reasons that are not clear (123–126). Importantly, *in vivo* Tph1 deletion in β-cells causes glucose intolerance, impaired insulin release, and decreased serum insulin in mice fed a high-fat diet (127). Furthermore, Kim *et al.* (127) observed that high-fat diet–fed HTR_3 knockout mice also have impaired insulin secretion and display glucose intolerance. Consistent with the role of serotonin in stimulating insulin release in pregnancy, Tph1 and Tph2 gene expression is increased during pregnancy, and serotonin acts on the HTR_{2B} to increase β-cell expansion, with a subsequent increase in glucose responsiveness (128). In addition to receptor-mediated signaling mechanisms, higher ratios of intracellular to extracellular serotonin within pancreatic islets causes serotonylation of GTPases (Rab3a and Rab27a), which in turn promotes glucose-mediated insulin secretion (14). Collectively, these data suggest that serotonin acts in the pancreas to promote insulin secretion (Fig. 4).

Adipose tissue

WAT is an important storage depot for glucose and lipids. Aside from the gut EC cells and microbiome,

serotonin may also be synthesized by WAT (17, 129) (Fig. 4). Importantly, however, note that in contrast to the EC cells, serotonin synthesis does not appear to contribute to total circulating serotonin levels. Early literature suggested the presence of serotonin in interscapular and epididymal adipose tissue (130), but its synthesis by adipocytes was unclear. Recent evidence demonstrates elevated *Tph1* gene expression and serotonin content in the WAT of obese mice (17, 129). However, it is not known whether mature adipocytes or other cell types (*i.e.*, stromovascular or immune cells) contribute to these changes. Serotonin promotes adipogenesis in white adipocytes (129, 131), effects that have been suggested to be mediated through HTR_{2A} signaling (17). Lipid uptake has also been shown to be promoted by serotonin in white adipocytes via HTR_{2A} signaling (17). Consistent with the concept of enhancing adipose tissue storage, activation of HTR_{2A} has also been shown to suppress isoprenaline-induced lipolysis (132). However, basally (in the absence of β-adrenergic signaling) serotonin may have a modest effect on reducing lipolysis through HTR_{2B} (133). Overall, serotonin appears to favor an energy storage phenotype (*i.e.*, enhanced adipogenesis, lipid uptake, and suppressed lipolysis) under fed conditions (Fig. 4).

BAT is a highly oxidative form of adipose tissue that appears to be dysfunctional in obesity and type 2 diabetes (134). BAT contains numerous mitochondria enriched with Ucp1 that can dissipate the inner membrane proton gradient, resulting in futile oxidation of substrates and the generation of heat. A decrease in BAT activity is observed in individuals with obesity and type 2 diabetes, which is thought to exacerbate weight gain and metabolic disease by lowering energy expenditure (135–138). It has been known for some time that serotonin is present within rodent BAT (139). In lean mice, a reduction in peripheral serotonin (due to *Tph1* deletion) has minor effects on fat mass and weight gain (16). However, when Tph1 is genetically or pharmacologically inhibited during high-fat diet–induced obesity, BAT-dependent thermogenesis and energy expenditure are elevated (16, 17), protecting mice from weight gain, insulin resistance, glucose intolerance, and NAFLD (16) (Fig. 4). Importantly, the effects of serotonin on BAT occur in a cell-autonomous manner by inhibiting both differentiation (140) and β-adrenergic–induced activation of brown adipocytes *in vitro* (16), inferring a direct deleterious effect on brown adipocytes. Interestingly, similar to Tph1 deletion, germline deletion of HTR_3 in mice also results in a lean phenotype (17). However, it is likely this is due to HTR_3 expression in the CNS where this receptor is highly expressed. Future studies identifying the primary HTR mediating the effects of serotonin on BAT energy expenditure are required.

Under periods of cold or β-adrenergic stimulation, WAT undergoes "browning," a process of converting WAT to beige/brite adipose tissue, which exhibits a thermogenic phenotype resembling some aspects of BAT (134). This has important implications because the browning of WAT is associated with reductions in adiposity and insulin resistance in rodents due to increased Ucp1-dependent and -independent thermogenesis, and rodent beige adipose tissue also has a molecular signature similar to BAT in humans (141–143). In parallel to its effects on BAT, genetic or pharmacological inhibition of Tph1 in mice increases the abundance of beige adipose tissue (16, 17). Furthermore, direct exposure of beige adipocytes to serotonin reduces *Ucp1* mRNA, indicating direct inhibitory effects of serotonin (Fig. 4). Importantly, hormone-sensitive lipase phosphorylation in adipocytes does not change when cells are exposed to other serotonin metabolites such as 5-HTP or 5-HIAA (16). Collectively, these studies indicate multiple roles for serotonin to promote energy storage by increasing adipogenesis in WAT and suppressing brown and beige adipose activity and energy expenditure.

Consistent with a role for serotonin in inhibiting adipose tissue energy expenditure and promoting adipogenesis, a recent study has indicated that kynurenic acid, a metabolite of kynurenine that is produced in skeletal muscle in response to exercise and cannot pass the blood–brain barrier, promotes adipocyte-derived energy expenditure through the browning of WAT (144). These effects on WAT browning were attributed to activation of adipose tissue G-protein–coupled receptor 35, the induction of peroxisome proliferator–activated receptor γ coactivator 1-α (PGC1α), and the suppression of inflammation (144). Surprisingly, despite these prominent effects of kynurenic acid to promote adipose tissue browning *in vivo*, when delivered acutely *in vitro*, kynurenic acid treatment dampened the effects of isoproterenol to stimulate cAMP levels in isolated adipocytes (144), analogous to observations with serotonin (16). These contradictory observations *in vitro* and *in vivo* may potentially be the result of kynurenine metabolism to NAD^+ (55, 56), which increases the activity of sirtuins and PGC1α to enhance mitochondrial function in adipose tissue (145) and potentially other tissues (146) *in vivo*. Thus, it is interesting to speculate that kynurenic acid increases adipose tissue NAD^+, and this may be important for increasing adipose tissue energy expenditure.

Liver

The liver is an important regulator of circulating glucose and lipids. During periods of fasting, the liver increases glycogenolysis and gluconeogenesis to maintain plasma glucose levels. Conversely, the liver sequesters large quantities of glucose and fatty acids after feeding to form glycogen and triglycerides. Because the hepatic portal circulation receives a significant proportion of postprandial nutrients from the gut, researchers have hypothesized that serotonin may

be an important gut-to-liver signal of nutrient status. Sumara *et al.* (133) found that HTR_{2B} activation by serotonin promotes liver gluconeogenesis and inhibits glucose uptake, increasing blood glucose levels during periods of fasting. Additionally, they showed that blockade of gut-derived Tph1 serotonin synthesis protects mice from diet-induced insulin resistance. Thus, they posited that under conditions of elevated serotonin observed in high-fat diet–induced obesity, the greater plasma glucose can be partially attributed to serotonergic activation of hepatocytes and the subsequent increase in systemic glucose production. Based on these observations, serotonergic signaling in hepatocytes appears to regulate glucose production.

Serotonin has also been shown to regulate hepatic lipid balance (Fig. 4). Primary hepatocytes incubated with fatty acids and serotonin were shown to accumulate more triglycerides compared with controls (147). Furthermore, treatment of *ob/ob* mice with an HTR_3 antagonist reduces liver fat deposition (148), suggesting a role of peripheral serotonin in increasing lipid accumulation *in vivo*. A recent report described that administration of Tph inhibitors (*i.e.*, *para*-chlorophenylalanine and LP533401) reduce liver lipid accumulation by suppressing lipid uptake (149). This group subsequently confirmed gut-derived serotonin to be the source regulating high-fat diet–induced hepatic steatosis and established that these effects on liver lipid metabolism are mediated specifically through hepatocyte-specific expression of HTR_{2A} (150). This protection from NAFLD could also be recapitulated in mice treated daily with the peripherally restrained HTR_{2A} antagonist sarpogrelate. These effects on NAFLD were also reported to be independent of changes in brown/beige adipose tissue morphology, Ucp1 content, or energy expenditure, a known negative regulator of liver lipid deposition (16, 17). These data suggest that inhibition of liver HTR_{2A} may be an effective target for reducing NAFLD.

Hepatic steatosis associated with NAFLD is the initiating cause of nonalcoholic steatohepatitis and liver cirrhosis. As recently reviewed, hepatic stellate cells (HSCs) are implicated in regulating liver fibrosis and steatohepatitis, and serotonin appears to play a direct role in activating this cell type (151). Pan-HTR_2 antagonists reduce proliferation and elevate rates of apoptosis induced by serotonin (152). In congruence with previous studies, HSC activation has been shown to be regulated by HTR_{2A} and HTR_{2B}. Administration of HTR_{2A} antagonists sarpogrelate and ketanserin inhibit *in vitro* HSC activation and is associated with reductions in liver inflammation and fibrosis in a rat model of cirrhosis (153). HTR_{2B} signaling also reduces hepatocyte regeneration by producing TGF-β1, as shown through increased liver growth in a genetic HTR_{2B} knockout mouse or following receptor blockade (154). This group also observed reductions in fibrogenesis and improvements in liver function due to HTR_{2B} antagonism. Consistent with these findings indicating a role for $HTR_{2A/2B}$ signaling in HSCs, these receptors are also important for promoting liver regeneration following transplantation (15). Collectively, these data suggest that inhibiting HTR_{2A} and HTR_{2B} signaling in hepatocytes and HSCs, respectively, may be effective for reducing liver fibrosis and steatosis. Future studies examining whether nonalcoholic steatohepatitis and fibrosis can be reversed in advanced models of disease using specific pharmacological antagonists to HTR_{2A} will be important.

Cardiac muscle, skeletal muscle, and exercise

Serotonin has metabolic and developmental effects in skeletal and cardiac muscle, respectively (Fig. 4). In cultured myotubes and rat soleus muscle, serotonin increases glucose uptake (155), potentially through the activation of HTR_{2A} (156). The physiological importance of serotonin regulation of skeletal muscle glucose uptake is currently unclear, as Tph1-null mice appear to have normal rates of basal and insulin-stimulated skeletal muscle glucose disposal (16, 17).

During exercise, serotonin metabolism in skeletal muscle may be influenced by the conversion of kynurenine into kynurenic acid by kynurenine aminotransferase (157, 158). This conversion of kynurenine (which can cross the blood–brain barrier) into kynurenic acid (which cannot cross the blood–brain barrier) is dependent on PGC1α in skeletal muscle and may contribute to reductions in depression with endurance exercise (157, 158).

"...when Tph1 is genetically or pharmacologically inhibited during high-fat diet–induced obesity, BAT-dependent thermogenesis and energy expenditure are elevated."

With respect to cardiac function, germline deletion of Tph1 leads to cardiac function abnormalities that can progress to heart failure (40). These effects of serotonin may involve HTR_{2B}, as mice lacking this receptor from birth have enlarged hearts and pericardial leakage (159). Pharmacological blockage of HTR_{2B} in spontaneous hypertensive rats (using RS-127445 at 1 mg/kg/d) does not affect left ventricular hypertrophy, fibrosis, or diastolic dysfunction but does amplify subendocardial fibrosis and left ventricular dilatation (160). These data suggest some role for serotonin in cardiac muscle; however, whether this is of therapeutic importance remains to be established.

Immunity

The immune system and tissue parenchymal cells form a complex network required to maintain metabolic homeostasis. With the main purpose of negating the advance of pathogenic intruders or removal of infectious organisms, the immune system employs various innate and adaptive cell types to defend the body from harm. In response to damaged endothelium, serotonin is released by blood platelets, promoting immune cell infiltration (107). Additionally, serotonin has been shown to be a chemotactic molecule for various immune cells such as eosinophils, dendritic cells, and mast cells (MCs) (116), suggesting a

role for serotonin in initiating and potentiating the immune response. Furthermore, type 2 immune cells have been implicated in regulating adipose tissue homeostasis via eosinophils (161, 162) and type 2 innate lymphoid cells (163, 164), suggesting that constituents of the immune system play an integral role in energy homeostasis.

In addition to the storage of serotonin in platelets, MCs are capable of synthesizing, storing, and secreting serotonin. MCs accumulate in target tissues in response to allergic or inflammatory stimuli and secrete various substances such as cytokines, proteases, and bioamines (*i.e.*, serotonin and histamine) (165). Of these various substances released by MCs, serotonin has been shown to be released in significant amounts by both human and rodent MCs (166–168). Additionally, MCs have the greatest (~1000-fold) Tph1 mRNA expression compared with other immune cell types such as macrophages and lymphocytes (169). MCs have been linked to obesity because they accumulate in obese adipose tissue in humans (170) and mice (171). However, whether MC-derived serotonin is sufficient to signal in adipose tissue is not clear. In addition to MCs, it is possible that other immune cells such as basophils and monocytes may also be recruited to sites of inflammation and can secrete serotonin in response to injury or pathogens (107), but similar to MCs, the quantity of serotonin would be expected to be very low compared with platelet-derived serotonin.

Associations Between Serotonin and Obesity

Various single-nucleotide polymorphisms of serotonergic genes, including some serotonin receptors, have been linked to greater adiposity or metabolic disease (172, 173). Variants in HTR_{2A} are associated with higher body mass index (BMI) (174), waist circumference (18, 19), and components of the metabolic syndrome (19, 20). Variants in HTR_{2C} have also been associated with obesity (20, 175, 176), weight gain (177), and BMI (178). Additionally, a *Tph1* gene variant is associated with BMI and waist circumference (179). Single-nucleotide polymorphisms in *SLC6A4* and *SLC6A14*, transporters for serotonin and tryptophan, respectively, have also been associated with obesity (180, 181), impairments in fat oxidation (182), and BMI (183). Thus, there appears to be genetic evidence supporting a correlation between obesity and genes controlling serotonin synthesis and signaling. Future studies are needed to understand the function of these polymorphic variants and their primary site of action (*i.e.*, central vs peripheral and in what specific tissues).

In addition to these links between obesity and genetic variants, there is also emerging evidence linking obesity with alterations in peripheral serotonin levels. For example, Kim *et al.* (184) have observed higher serum levels of serotonin in high-fat diet–fed mice in comparison with lean mice. Similarly, humans who are

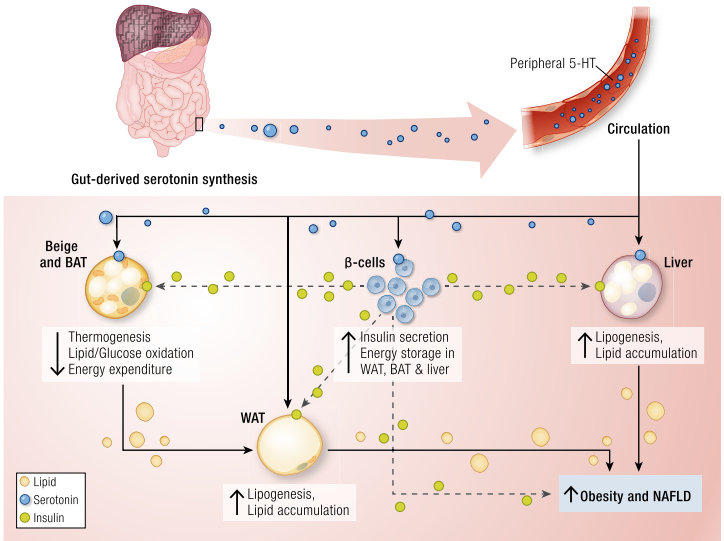

Figure 5. Multifaceted effects of peripheral serotonin to promote obesity and NAFLD. Peripheral serotonin promotes obesity and NAFLD by promoting insulin secretion, inhibiting the thermogenesis in beige adipose tissue and BAT, and increasing *de novo* lipogenesis in both WAT and liver. Collectively, these actions may promote the development of obesity and NAFLD.

obese have elevated platelet-poor plasma serotonin compared with lean controls (185). Changes in peripheral serotonin metabolites have also been connected to alterations in energy balance and glucose metabolism. Specifically, elevated levels of 5-HIAA, the major downstream metabolite of serotonin, has been observed in plasma (66) and urine (186) of humans with obesity. Additionally, these studies found fasting blood glucose and HbA1c to be positively correlated with 5-HIAA. Consistent with elevations in plasma serotonin with obesity, rats fed a high-fat, high-cholesterol diet have greater Tph1 expression and elevated secretion of serotonin from the small intestine (58). Similarly, in humans who are obese, the intraduodenal infusion of glucose leads to greater release of serotonin from the duodenum compared with lean controls and is tightly linked with Tph1 expression (185). Furthermore, Tph1 expression is higher in individuals with obesity in the duodenum due to an increased density of EC cells (185). Obesity also disrupts the circadian rhythm and meal-induced release of circulating serotonin (187). These data collectively suggest that release of serotonin from EC cells of the gastrointestinal tract into the circulation increases with obesity and possibly type 2 diabetes.

Conclusions and Future Directions

Considering the high amounts of serotonin synthesized by EC cells in response to the presence of luminal nutrients (both glucose and fatty acids), it is interesting to speculate that increases in peripheral serotonin may be a key marker and effector of nutrient status that promotes lipid absorption and storage. For example, the gut relies on Tph1-derived serotonin to induce motility and vasodilation for efficient absorption of lipid along the entire length of the gut apical membrane (188). In the liver, serotonin promotes fat deposition and lipogenesis (148, 150). In the pancreas, serotonin promotes the release of insulin, which further promotes the effects of serotonin on increasing adipogenesis (129, 131) and lipogenesis (17) while also suppressing lipolysis (132). Lastly, serotonin directly inhibits BAT thermogenesis and browning of WAT (16, 17), which use fatty acids as the primary substrate (134). Collectively, these actions of serotonin promote efficient lipid storage consistent with its evolutionarily conserved role as a key modulator of energy balance.

As the role of peripheral serotonin in modulating nutrient absorption, storage, and utilization continues to expand, a key challenge will be to isolate how tissues are individually affected to understand the role of peripheral serotonin in the pathogenesis of various diseases (Fig. 5). With the development of tissue-selective Tph1 and HTR knockout mice, it should be possible to shed light on the complex serotonergic network in peripheral organ systems to isolate key signaling nodes. The elucidation of this complex signaling network in peripheral tissues may lead to the development of new pharmacological strategies designed to alleviate the burden of metabolic diseases such as obesity, type 2 diabetes, and NAFLD.

References and Notes

1. Shajib MS, Baranov A, Khan WI. Diverse effects of gut-derived serotonin in intestinal inflammation. *ACS Chem Neurosci*. 2017;**8**(5):920–931.
2. Ramage AG. The role of central 5-hydroxytryptamine (5-HT, serotonin) receptors in the control of micturition. *Br J Pharmacol*. 2006;**147**(Suppl 2):S120–S131.
3. Eilers H, Schumacher MA. Opioid-induced respiratory depression: are 5-HT4a receptor agonists the cure? *Mol Interv*. 2004;**4**(4):197–199.
4. Kaumann AJ, Levy FO. 5-Hydroxytryptamine receptors in the human cardiovascular system. *Pharmacol Ther*. 2006;**111**(3):674–706.
5. Ghia JE, Li N, Wang H, Collins M, Deng Y, El-Sharkawy RT, Côté F, Mallet J, Khan WI. Serotonin has a key role in pathogenesis of experimental colitis. *Gastroenterology*. 2009;**137**(5):1649–1660.
6. Li Z, Chalazonitis A, Huang YY, Mann JJ, Margolis KG, Yang QM, Kim DO, Côté F, Mallet J, Gershon MD. Essential roles of enteric neuronal serotonin in gastrointestinal motility and the development/survival of enteric dopaminergic neurons. *J Neurosci*. 2011;**31**(24):8998–9009.
7. Tecott LH. Serotonin and the orchestration of energy balance. *Cell Metab*. 2007;**6**(5):352–361.
8. Smith SR, Weissman NJ, Anderson CM, Sanchez M, Chuang E, Stubbe S, Bays H, Shanahan WR; Behavioral Modification and Lorcaserin for Overweight and Obesity Management (BLOOM) Study Group. Multicenter, placebo-controlled trial of lorcaserin for weight management. *N Engl J Med*. 2010;**363**(3):245–256.
9. Fidler MC, Sanchez M, Raether B, Weissman NJ, Smith SR, Shanahan WR, Anderson CM; BLOSSOM Clinical Trial Group. A one-year randomized trial of lorcaserin for weight loss in obese and overweight adults: the BLOSSOM trial. *J Clin Endocrinol Metab*. 2011;**96**(10):3067–3077.
10. O'Neil PM, Smith SR, Weissman NJ, Fidler MC, Sanchez M, Zhang J, Raether B, Anderson CM, Shanahan WR. Randomized placebo-controlled clinical trial of lorcaserin for weight loss in type 2 diabetes mellitus: the BLOOM-DM study. *Obesity (Silver Spring)*. 2012;**20**(7):1426–1436.
11. Bohula EA, Wiviott SD, McGuire DK, Inzucchi SE, Kuder J, Im K, Fanola CL, Qamar A, Brown C, Budaj A, Garcia-Castillo A, Gupta M, Leiter LA, Weissman NJ, White HD, Patel T, Francis B, Miao W, Perdomo C, Dhadda S, Bonaca MP, Ruff CT, Keech AC, Smith SR, Sabatine MS, Scirica BM; CAMELLIA–TIMI 61 Steering Committee and Investigators. Cardiovascular safety of lorcaserin in overweight or obese patients. *N Engl J Med*. 2018;**379**(12):1107–1117.
12. Bülbring E, Crema A. 5-Hydroxytryptamine on the peristaltic reflex. *Br J Pharmacol*. 1958;**13**:444–457.
13. Walther DJ, Peter JU, Winter S, Höltje M, Paulmann N, Grohmann M, Vowinckel J, Alamo-Bethencourt V, Wilhelm CS, Ahnert-Hilger G, Bader M. Serotonylation of small GTPases is a signal transduction pathway that triggers platelet α-granule release. *Cell*. 2003;**115**(7):851–862.
14. Paulmann N, Grohmann M, Voigt JP, Bert B, Vowinckel J, Bader M, Skelin M, Jevsek M, Fink H, Rupnik M, Walther DJ. Intracellular serotonin modulates insulin secretion from pancreatic beta-cells by protein serotonylation. *PLoS Biol*. 2009;**7**(10):e1000229.
15. Lesurtel M, Graf R, Aleil B, Walther DJ, Tian Y, Jochum W, Gachet C, Bader M, Clavien PA. Platelet-derived serotonin mediates liver regeneration. *Science*. 2006;**312**(5770):104–107.
16. Crane JD, Palanivel R, Mottillo EP, Bujak AL, Wang H, Ford RJ, Collins A, Blümer RM, Fullerton MD, Yabut JM, Kim JJ, Ghia JE, Hamza SM, Morrison KM, Schertzer JD, Dyck JR, Khan WI, Steinberg GR. Inhibiting peripheral serotonin synthesis reduces obesity and metabolic dysfunction by promoting brown adipose tissue thermogenesis. *Nat Med*. 2015;**21**(2):166–172.
17. Oh CM, Namkung J, Go Y, Shong KE, Kim K, Kim H, Park BY, Lee HW, Jeon YH, Song J, Shong M, Yadav VK, Karsenty G, Kajimura S, Lee IK, Park S, Kim H.

Regulation of systemic energy homeostasis by serotonin in adipose tissues. *Nat Commun*. 2015;**6**(1):6794.
18. Rosmond R, Bouchard C, Björntorp P. Increased abdominal obesity in subjects with a mutation in the 5-HT$_{2A}$ receptor gene promoter. *Ann N Y Acad Sci*. 2002;**967**(1):571–575.
19. Halder I, Muldoon MF, Ferrell RE, Manuck SB. Serotonin receptor 2A (*HTR2A*) gene polymorphisms are associated with blood pressure, central adiposity, and the metabolic syndrome. *Metab Syndr Relat Disord*. 2007;**5**(4):323–330.
20. Kring SII, Werge T, Holst C, Toubro S, Astrup A, Hansen T, Pedersen O, Sørensen TI. Polymorphisms of serotonin receptor 2A and 2C genes and *COMT* in relation to obesity and type 2 diabetes. *PLoS One*. 2009;**4**(8):e6696.
21. Azmitia EC. Serotonin and brain: evolution, neuroplasticity, and homeostasis. *Int Rev Neurobiol*. 2007;**77**(06):31–56.
22. Azmitia EC. Evolution of serotonin: sunlight to suicide. In: Müller CR, Jacobs B, eds. Handbook of the Behavioral Neurobiology of Serotonin. London, UK: Academic Press; 2010:3–22.
23. Smith BN. Evolution of C4 photosynthesis in response to changes in carbon and oxygen concentrations in the atmosphere through time. *Biosystems*. 1976;**8**(1):24–32.
24. Hotamisligil GS. Inflammation and metabolic disorders. *Nature*. 2006;**444**(7121):860–867.
25. Vargas MA, Luo N, Yamaguchi A, Kapahi P. A role for S6 kinase and serotonin in postmating dietary switch and balance of nutrients in *D. melanogaster*. *Curr Biol*. 2010;**20**(11):1006–1011.
26. French AS, Simcock KL, Rolke D, Gartside SE, Blenau W, Wright GA. The role of serotonin in feeding and gut contractions in the honeybee. *J Insect Physiol*. 2014;**61**(1):8–15.
27. Haselton AT, Downer KE, Zylstra J, Stoffolano JG. Serotonin inhibits protein feeding in the blow fly, *Phormia regina* (Meigen). *J Insect Behav*. 2009;**22**(6):452–463.
28. Lent CM. Serotonergic modulation of the feeding behavior of the medicinal leech. *Brain Res Bull*. 1985;**14**(6):643–655.
29. Lent CM, Fliegner KH, Freedman E, Dickinson MH. Ingestive behaviour and physiology of the medicinal leech. *J Exp Biol*. 1988;**137**:513–527.
30. Orchard I, Lange AB, Barret FM. Serotonergic supply to the epidermis of Rhodnius prolixus: evidence for serotonin as the plasticising factor. *J Insect Physiol*. 1988;**34**(9):873–879.
31. Orchard I. Serotonin: a coordinator of feeding-related physiological events in the blood-gorging bug, *Rhodnius prolixus*. *Comp Biochem Physiol A Mol Integr Physiol*. 2006;**144**(3):316–324.
32. Srinivasan S, Sadegh L, Elle IC, Christensen AG, Faergeman NJ, Ashrafi K. Serotonin regulates *C. elegans* fat and feeding through independent molecular mechanisms. *Cell Metab*. 2008;**7**(6):533–544.
33. Sze JY, Victor M, Loer C, Shi Y, Ruvkun G. Food and metabolic signalling defects in a *Caenorhabditis elegans* serotonin-synthesis mutant. *Nature*. 2000;**403**(6769):560–564.
34. Cunningham KA, Hua Z, Srinivasan S, Liu J, Lee BH, Edwards RH, Ashrafi K. AMP-activated kinase links serotonergic signaling to glutamate release for regulation of feeding behavior in *C. elegans*. *Cell Metab*. 2012;**16**(1):113–121.
35. Kabotyanski EA, Baxter DA, Cushman SJ, Byrne JH. Modulation of fictive feeding by dopamine and serotonin in *Aplysia*. *J Neurophysiol*. 2000;**83**(1):374–392.
36. Zhang Y, Lu H, Bargmann CI. Pathogenic bacteria induce aversive olfactory learning in *Caenorhabditis elegans*. *Nature*. 2005;**438**(7065):179–184.
37. Liscia A, Solari P, Gibbons ST, Gelperin A, Stoffolano JG, Jr. Effect of serotonin and calcium on the supercontractile muscles of the adult blowfly crop. *J Insect Physiol*. 2012;**58**(3):356–366.
38. Walther DJ, Peter JU, Bashammakh S, Hörtnagl H, Voits M, Fink H, Bader M. Synthesis of serotonin by a second tryptophan hydroxylase isoform. *Science*. 2003;**299**(5603):76.
39. Zhang X, Beaulieu JM, Sotnikova TD, Gainetdinov RR, Caron MG. Tryptophan hydroxylase-2 controls brain serotonin synthesis. *Science*. 2004;**305**(5681):217.
40. Côté F, Thévenot E, Fligny C, Fromes Y, Darmon M, Ripoche MA, Bayard E, Hanoun N, Saurini F, Lechat P, Dandolo L, Hamon M, Mallet J, Vodjdani G. Disruption of the nonneuronal tph1 gene demonstrates the importance of peripheral serotonin in cardiac function. *Proc Natl Acad Sci USA*. 2003;**100**(23):13525–13530.
41. Gershon MD. Nerves, reflexes, and the enteric nervous system: pathogenesis of the irritable bowel syndrome. *J Clin Gastroenterol*. 2005;**39**(5 Suppl 3):S184–S193.
42. Mawe GM, Hoffman JM. Serotonin signalling in the gut—functions, dysfunctions and therapeutic targets (published correction appears in *Nat Rev Gastroenterol Hepatol*. 2013;**10**(10):564). *Nat Rev Gastroenterol Hepatol*. 2013;**10**(8):473–486.
43. Legay C, Faudon M, Héry F, Ternaux JP. 5-HT metabolism in the intestinal wall of the rat—I. The mucosa. *Neurochem Int*. 1983;**5**(6):721–727.
44. Yadav VK, Ryu JH, Suda N, Tanaka KF, Gingrich JA, Schütz G, Glorieux FH, Chiang CY, Zajac JD, Insogna KL, Mann JJ, Hen R, Ducy P, Karsenty G. Lrp5 controls bone formation by inhibiting serotonin synthesis in the duodenum. *Cell*. 2008;**135**(5):825–837.
45. Wang H, Steeds J, Motomura Y, Deng Y, Verma-Gandhu M, El-Sharkawy RT, McLaughlin JT, Grencis RK, Khan WI. CD4$^+$ T cell-mediated immunological control of enterochromaffin cell hyperplasia and 5-hydroxytryptamine production in enteric infection. *Gut*. 2007;**56**(7):949–957.
46. Martin AM, Lumsden AL, Young RL, Jessup CF, Spencer NJ, Keating DJ. Regional differences in nutrient-induced secretion of gut serotonin. *Physiol Rep*. 2017;**5**(6):e13199.
47. Bertrand RL, Senadheera S, Markus I, Liu L, Howitt L, Chen H, Murphy TV, Sandow SL, Bertrand PP. A Western diet increases serotonin availability in rat small intestine. *Endocrinology*. 2011;**152**(1):36–47.
48. Yano JM, Yu K, Donaldson GP, Shastri GG, Ann P, Ma L, Nagler CR, Ismagilov RF, Mazmanian SK, Hsiao EY. Indigenous bacteria from the gut microbiota regulate host serotonin biosynthesis (published correction appears in *Cell*. 2015;**163**:258). *Cell*. 2015;**161**(2):264–276.
49. Reigstad CS, Salmonson CE, Rainey JF III, Szurszewski JH, Linden DR, Sonnenburg JL, Farrugia G, Kashyap PC. Gut microbes promote colonic serotonin production through an effect of short-chain fatty acids on enterochromaffin cells. *FASEB J*. 2015;**29**(4):1395–1403.
50. Gál EM, Sherman AD. L-Kynurenine: its synthesis and possible regulatory function in brain. *Neurochem Res*. 1980;**5**(3):223–239.
51. Oxenkrug GF. Metabolic syndrome, age-associated neuroendocrine disorders, and dysregulation of tryptophan-kynurenine metabolism. *Ann N Y Acad Sci*. 2010;**1199**(1):1–14.
52. Cervenka I, Agudelo LZ, Ruas JL. Kynurenines: tryptophan's metabolites in exercise, inflammation, and mental health. *Science*. 2017;**357**(6349):eaaf9794.
53. Grohmann U, Fallarino F, Puccetti P. Tolerance, DCs and tryptophan: much ado about IDO. *Trends Immunol*. 2003;**24**(5):242–248.
54. Miura H, Ozaki N, Sawada M, Isobe K, Ohta T, Nagatsu T. A link between stress and depression: shifts in the balance between the kynurenine and serotonin pathways of tryptophan metabolism and the etiology and pathophysiology of depression. *Stress*. 2008;**11**(3):198–209.
55. Bender DA. Biochemistry of tryptophan in health and disease. *Mol Aspects Med*. 1983;**6**(2):101–197.
56. Bender DA, McCreanor GM. Kynurenine hydroxylase: a potential rate-limiting enzyme in tryptophan metabolism. *Biochem Soc Trans*. 1985;**13**(2):441–443.
57. Guillemin GJ, Cullen KM, Lim CK, Smythe GA, Garner B, Kapoor V, Takikawa O, Brew BJ. Characterization of the kynurenine pathway in human neurons. *J Neurosci*. 2007;**27**(47):12884–12892.
58. Bertrand PP, Bertrand RL. Serotonin release and uptake in the gastrointestinal tract. *Auton Neurosci*. 2010;**153**(1–2):47–57.
59. Alcaino C, Knutson KR, Treichel AJ, Yildiz G, Strege PR, Linden DR, Li JH, Leiter AB, Szurszewski JH, Farrugia G, Beyder A. A population of gut epithelial enterochromaffin cells is mechanosensitive and requires Piezo2 to convert force into serotonin release. *Proc Natl Acad Sci USA*. 2018;**115**(32):E7632–E7641.
60. Mercado CP, Kilic F. Molecular mechanisms of SERT in platelets: regulation of plasma serotonin levels. *Mol Interv*. 2010;**10**(4):231–241.
61. Morrissey JJ, Walker MN, Lovenberg W. The absence of tryptophan hydroxylase activity in blood platelets. *Proc Soc Exp Biol Med*. 1977;**154**(4):496–499.
62. Holmsen H. Physiological functions of platelets. *Ann Med*. 1989;**21**(1):23–30.
63. Sandler M, Reveley MA, Glover V. Human platelet monoamine oxidase activity in health and disease: a review. *J Clin Pathol*. 1981;**34**(3):292–302.
64. Lopez-Vilchez I, Diaz-Ricart M, White JG, Escolar G, Galan AM. Serotonin enhances platelet procoagulant properties and their activation induced during platelet tissue factor uptake. *Cardiovasc Res*. 2009;**84**(2):309–316.
65. Brand T, Anderson GM. The measurement of platelet-poor plasma serotonin: a systematic review of prior reports and recommendations for improved analysis. *Clin Chem*. 2011;**57**(10):1376–1386.
66. Fukui M, Tanaka M, Toda H, Asano M, Yamazaki M, Hasegawa G, Imai S, Nakamura N. High plasma 5-hydroxyindole-3-acetic acid concentrations in subjects with metabolic syndrome. *Diabetes Care*. 2012;**35**(1):163–167.
67. Billett EE. Monoamine oxidase (MAO) in human peripheral tissues. *Neurotoxicology*. 2004;**25**(1-2):139–148.
68. Keszthelyi D, Troost FJ, Masclee AAM. Understanding the role of tryptophan and serotonin metabolism in gastrointestinal function. *Neurogastroenterol Motil*. 2009;**21**(12):1239–1249.
69. Ganguly S, Coon SL, Klein DC. Control of melatonin synthesis in the mammalian pineal gland: the critical role of serotonin acetylation. *Cell Tissue Res*. 2002;**309**(1):127–137.
70. Hoyer D, Clarke DE, Fozard JR, Hartig PR, Martin GR, Mylecharane EJ, Saxena PR, Humphrey PP. International Union of Pharmacology classification of

receptors for 5-hydroxytryptamine (serotonin). *Am. Soc. Pharmacol. Exp. Ther.* 1994;**46**(2):157–203.
71. Nichols DE, Nichols CD. Serotonin receptors. *Chem Rev*. 2008;**108**(5):1614–1641.
72. Williams KW, Elmquist JK. From neuroanatomy to behavior: central integration of peripheral signals regulating feeding behavior. *Nat Neurosci*. 2012; **15**(10):1350–1355.
73. Yeo GS, Heisler LK. Unraveling the brain regulation of appetite: lessons from genetics. *Nat Neurosci*. 2012;**15**(10):1343–1349.
74. Breisch ST, Zemlan FP, Hoebel BG. Hyperphagia and obesity following serotonin depletion by intraventricular p-chlorophenylalanine. *Science*. 1976; **192**(4237):382–385.
75. Heisler LK, Cowley MA, Tecott LH, Fan W, Low MJ, Smart JL, Rubinstein M, Tatro JB, Marcus JN, Holstege H, Lee CE, Cone RD, Elmquist JK. Activation of central melanocortin pathways by fenfluramine. *Science*. 2002;**297**(5581):609–611.
76. Heisler LK, Jobst EE, Sutton GM, Zhou L, Borok E, Thornton-Jones Z, Liu HY, Zigman JM, Balthasar N, Kishi T, Lee CE, Aschkenasi CJ, Zhang CY, Yu J, Boss O, Mountjoy KG, Clifton PG, Lowell BB, Friedman JM, Horvath T, Butler AA, Elmquist JK, Cowley MA. Serotonin reciprocally regulates melanocortin neurons to modulate food intake. *Neuron*. 2006;**51**(2): 239–249.
77. Cowley MA, Smart JL, Rubinstein M, Cerdán MG, Diano S, Horvath TL, Cone RD, Low MJ. Leptin activates anorexigenic POMC neurons through a neural network in the arcuate nucleus. *Nature*. 2001; **411**(6836):480–484.
78. Sohn JW, Xu Y, Jones JE, Wickman K, Williams KW, Elmquist JK. Serotonin 2C receptor activates a distinct population of arcuate pro-opiomelanocortin neurons via TRPC channels. *Neuron*. 2011;**71**(3): 488–497.
79. Tecott LH, Sun LM, Akana SF, Strack AM, Lowenstein DH, Dallman MF, Julius D. Eating disorder and epilepsy in mice lacking 5-HT^{2C} serotonin receptors. *Nature*. 1995;**374**(6522):542–546.
80. Xu Y, Jones JE, Kohno D, Williams KW, Lee CE, Choi MJ, Anderson JG, Heisler LK, Zigman JM, Lowell BB, Elmquist JK. 5-HT$_{2C}$Rs expressed by pro-opiomelanocortin neurons regulate energy homeostasis. *Neuron*. 2008; **60**(4):582–589.
81. Berglund ED, Liu C, Sohn JW, Liu T, Kim MH, Lee CE, Vianna CR, Williams KW, Xu Y, Elmquist JK. Serotonin 2C receptors in pro-opiomelanocortin neurons regulate energy and glucose homeostasis (published correction appears in *J Clin Invest*. 2014; **124**(4):1868). *J Clin Invest*. 2013;**123**(12):5061–5070.
82. Xu P, He Y, Cao X, Valencia-Torres L, Yan X, Saito K, Wang C, Yang Y, Hinton A Jr, Zhu L, Shu G, Myers MG Jr, Wu Q, Tong Q, Heisler LK, Xu Y. Activation of serotonin 2C receptors in dopamine neurons inhibits binge-like eating in mice. *Biol Psychiatry*. 2017;**81**(9):737–747.
83. Valencia-Torres L, Olarte-Sánchez CM, Lyons DJ, Georgescu T, Greenwald-Yarnell M, Myers MG Jr, Bradshaw CM, Heisler LK. Activation of ventral tegmental area 5-HT$_{2C}$ receptors reduces incentive motivation. *Neuropsychopharmacology*. 2017;**42**(7): 1511–1521.
84. D'Agostino G, Lyons D, Cristiano C, Lettieri M, Olarte-Sanchez C, Burke LK, Greenwald-Yarnell M, Cansell C, Doslikova B, Georgescu T, Martinez de Morentin PB, Myers MG Jr, Rochford JJ, Heisler LK. Nucleus of the solitary tract serotonin 5-HT$_{2C}$ receptors modulate food intake. *Cell Metab*. 2018; **28**(4):619–630.e5.
85. Jean A, Laurent L, Delaunay S, Doly S, Dusticier N, Linden D, Neve R, Maroteaux L, Nieoullon A, Compan V. Adaptive control of dorsal raphe by 5-HT4 in the prefrontal cortex prevents persistent hypophagia following stress. *Cell Reports*. 2017; **21**(4):901–909.
86. Bovetto S, Richard D. Functional assessment of the 5-HT 1A-, 1B-, 2A/2C-, and 3-receptor subtypes on food intake and metabolic rate in rats. *Am J Physiol*. 1995;**268**(1 Pt 2):R14–R20.
87. Lucas JJ, Yamamoto A, Scearce-Levie K, Saudou F, Hen R. Absence of fenfluramine-induced anorexia and reduced c-Fos induction in the hypothalamus and central amygdaloid complex of serotonin 1B receptor knock-out mice. *J Neurosci*. 1998;**18**(14): 5537–5544.
88. Schwartz TL, Nihalani N, Jindal S, Virk S, Jones N. Psychiatric medication-induced obesity: a review. *Obes Rev*. 2004;**5**(2):115–121.
89. Raeder MB, Bjelland I, Emil Vollset S, Steen VM. Obesity, dyslipidemia, and diabetes with selective serotonin reuptake inhibitors: the Hordaland Health Study. *J Clin Psychiatry*. 2006;**67**(12):1974–1982.
90. Kivimäki M, Hamer M, Batty GD, Geddes JR, Tabak AG, Pentti J, Virtanen M, Vahtera J. Antidepressant medication use, weight gain, and risk of type 2 diabetes: a population-based study. *Diabetes Care*. 2010;**33**(12):2611–2616.
91. Chen X, Margolis KJ, Gershon MD, Schwartz GJ, Sze JY. Reduced serotonin reuptake transporter (SERT) function causes insulin resistance and hepatic steatosis independent of food intake. *PLoS One*. 2012;**7**(3):e32511.
92. Zha W, Ho HT, Hu T, Hebert MF, Wang J. Serotonin transporter deficiency drives estrogen-dependent obesity and glucose intolerance. *Sci Rep*. 2017;**7**(1): 1137.
93. Fink KB, Göthert M. 5-HT receptor regulation of neurotransmitter release. *Pharmacol Rev*. 2007; **59**(4):360–417.
94. Chau DT, Rada PV, Kim K, Kosloff RA, Hoebel BG. Fluoxetine alleviates behavioral depression while decreasing acetylcholine release in the nucleus accumbens shell (published correction appears in *Neuropsychopharmacology*. 2012 Sep;**37**(10):2346). *Neuropsychopharmacology*. 2011;**36**(8):1729–1737.
95. Bhagwagar Z, Wylezinska M, Taylor M, Jezzard P, Matthews PM, Cowen PJ. Increased brain GABA concentrations following acute administration of a selective serotonin reuptake inhibitor. *Am J Psychiatry*. 2004;**161**(2):368–370.
96. Zhou FM, Liang Y, Salas R, Zhang L, De Biasi M, Dani JA. Corelease of dopamine and serotonin from striatal dopamine terminals. *Neuron*. 2005;**46**(1): 65–74.
97. Hainer V, Kabrnova K, Aldhoon B, Kunesova M, Wagenknecht M. Serotonin and norepinephrine reuptake inhibition and eating behavior. *Ann N Y Acad Sci*. 2006;**1083**(1):252–269.
98. Serretti A, Mandelli L. Antidepressants and body weight: a comprehensive review and meta-analysis. *J Clin Psychiatry*. 2010;**71**(10):1259–1272.
99. Morrison SF, Madden CJ, Tupone D. Central neural regulation of brown adipose tissue thermogenesis and energy expenditure. *Cell Metab*. 2014;**19**(5): 741–756.
100. Madden CJ, Morrison SF. Serotonin potentiates sympathetic responses evoked by spinal NMDA. *J Physiol*. 2006;**577**(Pt 2):525–537.
101. Madden CJ, Morrison SF. Endogenous activation of spinal 5-hydroxytryptamine (5-HT) receptors contributes to the thermoregulatory activation of brown adipose tissue. *Am J Physiol Regul Integr Comp Physiol*. 2010;**298**(3):R776–R783.
102. McGlashon JM, Gorecki MC, Kozlowski AE, Thirnbeck CK, Markan KR, Leslie KL, Kotas ME, Potthoff MJ, Richerson GB, Gillum MP. Central serotonergic neurons activate and recruit thermogenic brown and beige fat and regulate glucose and lipid homeostasis. *Cell Metab*. 2015;**21**(5): 692–705.
103. Yadav VK, Oury F, Suda N, Liu ZW, Gao XB, Confavreux C, Klemenhagen KC, Tanaka KF, Gingrich JA, Guo XE, Tecott LH, Mann JJ, Hen R, Horvath TL, Karsenty G. A serotonin-dependent mechanism explains the leptin regulation of bone mass, appetite, and energy expenditure. *Cell*. 2009; **138**(5):976–989.
104. Gutknecht L, Araragi N, Merker S, Waider J, Sommerlandt FMJ, Mlinar B, Baccini G, Mayer U, Proft F, Hamon M, Schmitt AG, Corradetti R, Lanfumey L, Lesch KP. Impacts of brain serotonin deficiency following *Tph2* inactivation on development and raphe neuron serotonergic specification. *PLoS One*. 2012;**7**(8):e43157.
105. Calama E, García M, Jarque MJ, Morán A, Martín ML, San Román L. 5-Hydroxytryptamine-induced vasodilator responses in the hindquarters of the anaesthetized rat, involve β_2-adrenoceptors. *J Pharm Pharmacol*. 2003;**55**(10):1371–1378.
106. Dalton DW. The cardiovascular effects of centrally administered 5-hydroxytryptamine in the conscious normotensive and hypertensive rat. *J Auton Pharmacol*. 1986;**6**(1):67–75.
107. Shajib MS, Khan WI. The role of serotonin and its receptors in activation of immune responses and inflammation. *Acta Physiol (Oxf)*. 2015;**213**(3):561–574.
108. Hoffman JM, Tyler K, MacEachern SJ, Balemba OB, Johnson AC, Brooks EM, Zhao H, Swain GM, Moses PL, Galligan JJ, Sharkey KA, Greenwood-Van Meerveld B, Mawe GM. Activation of colonic mucosal 5-HT$_4$ receptors accelerates propulsive motility and inhibits visceral hypersensitivity. *Gastroenterology*. 2012;**142**(4):844–854.e4.
109. Liu MT, Kuan YH, Wang J, Hen R, Gershon MD. 5-HT$_4$ receptor-mediated neuroprotection and neurogenesis in the enteric nervous system of adult mice. *J Neurosci*. 2009;**29**(31):9683–9699.
110. Heredia DJ, Gershon MD, Koh SD, Corrigan RD, Okamoto T, Smith TK. Important role of mucosal serotonin in colonic propulsion and peristaltic reflexes: in vitro analyses in mice lacking tryptophan hydroxylase 1. *J Physiol*. 2013;**591**(23):5939–5957.
111. Spencer NJ, Nicholas SJ, Robinson L, Kyloh M, Flack N, Brookes SJ, Zagorodnyuk VP, Keating DJ. Mechanisms underlying distension-evoked peristalsis in guinea pig distal colon: is there a role for enterochromaffin cells? *Am J Physiol Gastrointest Liver Physiol*. 2011;**301**(3): G519–G527.
112. Keating DJ, Spencer NJ. Release of 5-hydroxytryptamine from the mucosa is not required for the generation or propagation of colonic migrating motor complexes. *Gastroenterology*. 2010;**138**(2): 659–670.e2.
113. Vincent AD, Wang XY, Parsons SP, Khan WI, Huizinga JD. Abnormal absorptive colonic motor activity in germ-free mice is rectified by butyrate, an effect possibly mediated by mucosal serotonin. *Am J Physiol Gastrointest Liver Physiol*. 2018;**315**(5): G896–G907.
114. Markham A. Telotristat ethyl: first global approval. *Drugs*. 2017;**77**(7):793–798.
115. Masab M, Saif MW. Telotristat ethyl: proof of principle and the first oral agent in the management of well-differentiated metastatic neuroendocrine tumor and carcinoid syndrome diarrhea.

Cancer Chemother Pharmacol. 2017;**80**(6):1055–1062.
116. Manocha M, Khan WI. Serotonin and GI disorders: an update on clinical and experimental studies. *Clin Transl Gastroenterol*. 2012;**3**(4):e13.
117. Bird JL, Wright EE, Feldman JM. Pancreatic islets: a tissue rich in serotonin. *Diabetes*. 1980;**29**(4):304–308.
118. Ekholm R, Ericson LE, Lundquist I. Monoamines in the pancreatic islets of the mouse. Subcellular localization of 5-hydroxytryptamine by electron microscopic autoradiography. *Diabetologia*. 1971;**7**(5):339–348.
119. Gylfe E. Association between 5-hydroxytryptamine release and insulin secretion. *J Endocrinol*. 1978;**78**(2):239–248.
120. Ohta Y, Kosaka Y, Kishimoto N, Wang J, Smith SB, Honig G, Kim H, Gasa RM, Neubauer N, Liou A, Tecott LH, Deneris ES, German MS. Convergence of the insulin and serotonin programs in the pancreatic β-cell. *Diabetes*. 2011;**60**(12):3208–3216.
121. Almaça J, Molina J, Menegaz D, Pronin AN, Tamayo A, Slepak V, Berggren PO, Caicedo A. Human beta cells produce and release serotonin to inhibit glucagon secretion from alpha cells. *Cell Reports*. 2016;**17**(12):3281–3291.
122. Bennet H, Mollet IG, Balhuizen A, Medina A, Nagorny C, Bagge A, Fadista J, Ottosson-Laakso E, Vikman P, Dekker-Nitert M, Eliasson L, Wierup N, Artner I, Fex M. Serotonin (5-HT) receptor 2b activation augments glucose-stimulated insulin secretion in human and mouse islets of Langerhans. *Diabetologia*. 2016;**59**(4):744–754.
123. Cataldo LR, Mizgier ML, Bravo Sagua R, Jaña F, Cárdenas C, Llanos P, Busso D, Olmos P, Galgani JE, Santos JL, Cortés VA. Prolonged activation of the Htr2b serotonin receptor impairs glucose stimulated insulin secretion and mitochondrial function in MIN6 cells. *PLoS One*. 2017;**12**(1):e0170213.
124. Feldman JM, Lebovitz HE. Serotonin inhibition of in vitro insulin release from golden hamster pancreas. *Endocrinology*. 1970;**86**(1):66–70.
125. Lundquist I, Ekholm R, Ericson LE. Monoamines in the pancreatic islets of the mouse. 5-Hydroxytryptamine as an intracellular modifier of insulin secretion, and the hypoglycaemic action of monoamine oxidase inhibitors. *Diabetologia*. 1971;**7**(6):414–422.
126. Quickel KE Jr, Feldman JM, Lebovitz HE. Inhibition of insulin secretion by serotonin and dopamine: species variation. *Endocrinology*. 1971;**89**(5):1295–1302.
127. Kim K, Oh CM, Ohara-Imaizumi M, Park S, Namkung J, Yadav VK, Tamarina NA, Roe MW, Philipson LH, Karsenty G, Nagamatsu S, German MS, Kim H. Functional role of serotonin in insulin secretion in a diet-induced insulin-resistant state. *Endocrinology*. 2015;**156**(2):444–452.
128. Kim H, Toyofuku Y, Lynn FC, Chak E, Uchida T, Mizukami H, Fujitani Y, Kawamori R, Miyatsuka T, Kosaka Y, Yang K, Honig G, van der Hart M, Kishimoto N, Wang J, Yagihashi S, Tecott LH, Watada H, German MS. Serotonin regulates pancreatic beta cell mass during pregnancy. *Nat Med*. 2010;**16**(7):804–808.
129. Stunes AK, Reseland JE, Hauso O, Kidd M, Tømmerås K, Waldum HL, Syversen U, Gustafsson BI. Adipocytes express a functional system for serotonin synthesis, reuptake and receptor activation. *Diabetes Obes Metab*. 2011;**13**(6):551–558.
130. Stock K, Westermann EO. Concentration of norepinephrine, serotonin, and histamine, and of amine-metabolizing enzymes in mammalian adipose tissue. *J Lipid Res*. 1963;**4**(3):297–304.
131. Kinoshita M, Ono K, Horie T, Nagao K, Nishi H, Kuwabara Y, Takanabe-Mori R, Hasegawa K, Kita T, Kimura T. Regulation of adipocyte differentiation by activation of serotonin (5-HT) receptors 5-HT2AR and 5-HT2CR and involvement of microRNA-448-mediated repression of KLF5. *Mol Endocrinol*. 2010;**24**(10):1978–1987.
132. Hansson B, Medina A, Fryklund C, Fex M, Stenkula KG. Serotonin (5-HT) and 5-HT2A receptor agonists suppress lipolysis in primary rat adipose cells. *Biochem Biophys Res Commun*. 2016;**474**(2):357–363.
133. Sumara G, Sumara O, Kim JK, Karsenty G. Gut-derived serotonin is a multifunctional determinant to fasting adaptation. *Cell Metab*. 2012;**16**(5):588–600.
134. Sidossis L, Kajimura S. Brown and beige fat in humans: thermogenic adipocytes that control energy and glucose homeostasis. *J Clin Invest*. 2015;**125**(2):478–486.
135. Cypess AM, Lehman S, Williams G, Tal I, Rodman D, Goldfine AB, Kuo FC, Palmer EL, Tseng YH, Doria A, Kolodny GM, Kahn CR. Identification and importance of brown adipose tissue in adult humans. *N Engl J Med*. 2009;**360**(15):1509–1517.
136. van Marken Lichtenbelt WD, Vanhommerig JW, Smulders NM, Drossaerts JM, Kemerink GJ, Bouvy ND, Schrauwen P, Teule GJ. Cold-activated brown adipose tissue in healthy men. *N Engl J Med*. 2009;**360**(15):1500–1508.
137. Virtanen KA, Lidell ME, Orava J, Heglind M, Westergren R, Niemi T, Taittonen M, Laine J, Savisto NJ, Enerbäck S, Nuutila P. Functional brown adipose tissue in healthy adults. *N Engl J Med*. 2009;**360**(15):1518–1525.
138. Ouellet V, Routhier-Labadie A, Bellemare W, Lakhal-Chaieb L, Turcotte E, Carpentier AC, Richard D. Outdoor temperature, age, sex, body mass index, and diabetic status determine the prevalence, mass, and glucose-uptake activity of ^{18}F-FDG-detected BAT in humans. *J Clin Endocrinol Metab*. 2011;**96**(1):192–199.
139. Ricquier D, Mory G, Nechad M, Combes-George M, Thibault J. Development and activation of brown fat in rats with pheochromocytoma PC 12 tumors. *Am J Physiol*. 1983;**245**(3):C172–C177.
140. Rozenblit-Susan S, Chapnik N, Froy O. Serotonin prevents differentiation into brown adipocytes and induces transdifferentiation into white adipocytes. *Int J Obes*. 2018;**42**(4):704–710.
141. Chouchani ET, Kazak L, Spiegelman BM. New advances in adaptive thermogenesis: UCP1 and beyond. *Cell Metab*. 2019;**29**(1):27–37.
142. Chang SH, Song NJ, Choi JH, Yun UJ, Park KW. Mechanisms underlying Ucp1 dependent and independent adipocyte thermogenesis. *Obes Rev*. 2019;**20**(2):241–251.
143. Sponton CH, Kajimura S. Multifaceted roles of beige fat in energy homeostasis beyond UCP1. *Endocrinology*. 2018;**159**(7):2545–2553.
144. Agudelo LZ, Ferreira DM, Cervenka I, Bryzgalova G, Dadvar S, Jannig PR, Pettersson-Klein AT, Lakshmikanth T, Sustarsic EG, Porsmyr-Palmertz M, Correia JC, Izadi M, Martínez-Redondo V, Ueland PM, Midttun Ø, Gerhart-Hines Z, Brodin P, Pereira T, Berggren PO, Ruas JL. Kynurenic acid and Gpr35 regulate adipose tissue energy homeostasis and inflammation. *Cell Metab*. 2018;**27**(2):378–392.e5.
145. Cantó C, Houtkooper RH, Pirinen E, Youn DY, Oosterveer MH, Cen Y, Fernandez-Marcos PJ, Yamamoto H, Andreux PA, Cettour-Rose P, Gademann K, Rinsch C, Schoonjans K, Sauve AA, Auwerx J. The NAD$^+$ precursor nicotinamide riboside enhances oxidative metabolism and protects against high-fat diet-induced obesity. *Cell Metab*. 2012;**15**(6):838–847.
146. Katsyuba E, Mottis A, Zietak M, De Franco F, van der Velpen V, Gariani K, Ryu D, Cialabrini L, Matilainen O, Liscio P, Giacchè N, Stokar-Regenscheit N, Legouis D, de Seigneux S, Ivanisevic J, Raffaelli N, Schoonjans K, Pellicciari R, Auwerx J. De novo NAD$^+$ synthesis enhances mitochondrial function and improves health. *Nature*. 2018;**563**(7731):354–359.
147. Osawa Y, Kanamori H, Seki E, Hoshi M, Ohtaki H, Yasuda Y, Ito H, Suetsugu A, Nagaki M, Moriwaki H, Saito K, Seishima M. L-Tryptophan-mediated enhancement of susceptibility to nonalcoholic fatty liver disease is dependent on the mammalian target of rapamycin. *J Biol Chem*. 2011;**286**(40):34800–34808.
148. Haub S, Ritze Y, Ladel I, Saum K, Hubert A, Spruss A, Trautwein C, Bischoff SC. Serotonin receptor type 3 antagonists improve obesity-associated fatty liver disease in mice. *J Pharmacol Exp Ther*. 2011;**339**(3):790–798.
149. Namkung J, Shong KE, Kim H, Oh CM, Park S, Kim H. Inhibition of serotonin synthesis induces negative hepatic lipid balance. *Diabetes Metab J*. 2018;**42**(3):233–243.
150. Choi W, Namkung J, Hwang I, Kim H, Lim A, Park HJ, Lee HW, Han KH, Park S, Jeong JS, Bang G, Kim YH, Yadav VK, Karsenty G, Ju YS, Choi C, Suh JM, Park JY, Park S, Kim H. Serotonin signals through a gut-liver axis to regulate hepatic steatosis (published correction appears in *Nat Commun*. 2019;**10**(1):158). *Nat Commun*. 2018;**9**(1):4824.
151. Tsuchida T, Friedman SL. Mechanisms of hepatic stellate cell activation. *Nat Rev Gastroenterol Hepatol*. 2017;**14**(7):397–411.
152. Ruddell RG, Oakley F, Hussain Z, Yeung I, Bryan-Lluka LJ, Ramm GA, Mann DA. A role for serotonin (5-HT) in hepatic stellate cell function and liver fibrosis. *Am J Pathol*. 2006;**169**(3):861–876.
153. Kim DC, Jun DW, Kwon YI, Lee KN, Lee HL, Lee OY, Yoon BC, Choi HS, Kim EK. 5-HT$_{2A}$ receptor antagonists inhibit hepatic stellate cell activation and facilitate apoptosis. *Liver Int*. 2013;**33**(4):535–543.
154. Ebrahimkhani MR, Oakley F, Murphy LB, Mann J, Moles A, Perugorria MJ, Ellis E, Lakey AF, Burt AD, Douglass A, Wright MC, White SA, Jaffré F, Maroteaux L, Mann DA. Stimulating healthy tissue regeneration by targeting the 5-HT$_2$B receptor in chronic liver disease. *Nat Med*. 2011;**17**(12):1668–1673.
155. Hajduch E, Rencurel F, Balendran A, Batty IH, Downes CP, Hundal HS. Serotonin (5-hydroxytryptamine), a novel regulator of glucose transport in rat skeletal muscle. *J Biol Chem*. 1999;**274**(19):13563–13568.
156. Coelho WS, Costa KC, Sola-Penna M. Serotonin stimulates mouse skeletal muscle 6-phosphofructo-1-kinase through tyrosine-phosphorylation of the enzyme altering its intracellular localization. *Mol Genet Metab*. 2007;**92**(4):364–370.
157. Schlittler M, Goiny M, Agudelo LZ, Venckunas T, Brazaitis M, Skurvydas A, Kamandulis S, Ruas JL, Erhardt S, Westerblad H, Andersson DC. Endurance exercise increases skeletal muscle kynurenine aminotransferases and plasma kynurenic acid in humans. *Am J Physiol Cell Physiol*. 2016;**310**(10):C836–C840.
158. Agudelo LZ, Femenía T, Orhan F, Porsmyr-Palmertz M, Goiny M, Martinez-Redondo V, Correia JC, Izadi M, Bhat M, Schuppe-Koistinen I, Pettersson AT, Ferreira DM, Krook A, Barres R, Zierath JR, Erhardt S, Lindskog M, Ruas JL. Skeletal muscle PGC-1α1 modulates kynurenine metabolism and mediates

resilience to stress-induced depression. *Cell*. 2014; **159**(1):33–45.
159. Nebigil CG, Choi DS, Dierich A, Hickel P, Le Meur M, Messaddeq N, Launay JM, Maroteaux L. Serotonin 2B receptor is required for heart development. *Proc Natl Acad Sci USA*. 2000;**97**(17):9508–9513.
160. Ayme-Dietrich E, Marzak H, Lawson R, Mokni W, Wendling O, Combe R, Becker J, El Fertak L, Champy MF, Matz R, Andriantsitohaina R, Doly S, Boutourlinsky K, Maroteaux L, Monassier L. Contribution of serotonin to cardiac remodeling associated with hypertensive diastolic ventricular dysfunction in rats. *J Hypertens*. 2015;**33**(11):2310–2321.
161. Qiu Y, Nguyen KD, Odegaard JI, Cui X, Tian X, Locksley RM, Palmiter RD, Chawla A. Eosinophils and type 2 cytokine signaling in macrophages orchestrate development of functional beige fat. *Cell*. 2014;**157**(6):1292–1308.
162. Rao RR, Long JZ, White JP, Svensson KJ, Lou J, Lokurkar I, Jedrychowski MP, Ruas JL, Wrann CD, Lo JC, Camera DM, Lachey J, Gygi S, Seehra J, Hawley JA, Spiegelman BM. Meteorin-like is a hormone that regulates immune-adipose interactions to increase beige fat thermogenesis. *Cell*. 2014;**157**(6):1279–1291.
163. Brestoff JR, Kim BS, Saenz SA, Stine RR, Monticelli LA, Sonnenberg GF, Thome JJ, Farber DL, Lutfy K, Seale P, Artis D. Group 2 innate lymphoid cells promote beiging of white adipose tissue and limit obesity. *Nature*. 2015;**519**(7542):242–246.
164. Lee MW, Odegaard JI, Mukundan L, Qiu Y, Molofsky AB, Nussbaum JC, Yun K, Locksley RM, Chawla A. Activated type 2 innate lymphoid cells regulate beige fat biogenesis. *Cell*. 2015;**160**(1-2):74–87.
165. Kalesnikoff J, Galli SJ. New developments in mast cell biology. *Nat Immunol*. 2008;**9**(11):1215–1223.
166. Enerbäck L. Serotonin in human mast cells. *Nature*. 1963;**197**(4867):610–611.
167. Theoharides TC, Bondy PK, Tsakalos ND, Askenase PW. Differential release of serotonin and histamine from mast cells. *Nature*. 1982;**297**(5863):229–231.
168. Kushnir-Sukhov NM, Brown JM, Wu Y, Kirshenbaum A, Metcalfe DD. Human mast cells are capable of serotonin synthesis and release. *J Allergy Clin Immunol*. 2007;**119**(2):498–499.
169. Nowak EC, de Vries VC, Wasiuk A, Ahonen C, Bennett KA, Le Mercier I, Ha D-G, Noelle RJ. Tryptophan hydroxylase-1 regulates immune tolerance and inflammation. *J Exp Med*. 2012;**209**(11):2127–2135.
170. Divoux A, Moutel S, Poitou C, Lacasa D, Veyrie N, Aissat A, Arock M, Guerre-Millo M, Clément K. Mast cells in human adipose tissue: link with morbid obesity, inflammatory status, and diabetes. *J Clin Endocrinol Metab*. 2012;**97**(9):E1677–E1685.
171. Liu J, Divoux A, Sun J, Zhang J, Clément K, Glickman JN, Sukhova GK, Wolters PJ, Du J, Gorgun CZ, Doria A, Libby P, Blumberg RS, Kahn BB, Hotamisligil GS, Shi GP. Genetic deficiency and pharmacological stabilization of mast cells reduce diet-induced obesity and diabetes in mice. *Nat Med*. 2009; **15**(8):940–945.
172. Bell CG, Walley AJ, Froguel P. The genetics of human obesity. *Nat Rev Genet*. 2005;**6**(3):221–234.
173. Walley AJ, Asher JE, Froguel P. The genetic contribution to non-syndromic human obesity. *Nat Rev Genet*. 2009;**10**(7):431–442.
174. Li P, Tiwari HK, Lin WY, Allison DB, Chung WK, Leibel RL, Yi N, Liu N. Genetic association analysis of 30 genes related to obesity in a European American population. *Int J Obes*. 2014;**38**(5):724–729.
175. McCarthy S, Mottagui-Tabar S, Mizuno Y, Sennblad B, Hoffstedt J, Arner P, Wahlestedt C, Andersson B. Complex *HTR2C* linkage disequilibrium and promoter associations with body mass index and serum leptin. *Hum Genet*. 2005;**117**(6):545–557.
176. Pooley EC, Fairburn CG, Cooper Z, Sodhi MS, Cowen PJ, Harrison PJ. A 5-HT_{2C} receptor promoter polymorphism (HTR2C – 759C/T) is associated with obesity in women, and with resistance to weight loss in heterozygotes. *Am J Med Genet B Neuropsychiatr Genet*. 2004;**126B**(1):124–127.
177. Opgen-Rhein C, Brandl EJ, Müller DJ, Neuhaus AH, Tiwari AK, Sander T, Dettling M. Association of *HTR2C*, but not *LEP* or *INSIG2*, genes with antipsychotic-induced weight gain in a German sample. *Pharmacogenomics*. 2010;**11**(6):773–780.
178. Chen C, Chen W, Chen C, Moyzis R, He Q, Lei X, Li J, Wang Y, Liu B, Xiu D, Zhu B, Dong Q. Genetic variations in the serotoninergic system contribute to body-mass index in Chinese adolescents. *PLoS One*. 2013;**8**(3):e58717.
179. Kwak SH, Park BL, Kim H, German MS, Go MJ, Jung HS, Koo BK, Cho YM, Choi SH, Cho YS, Shin HD, Jang HC, Park KS. Association of variations in *TPH1* and *HTR2B* with gestational weight gain and measures of obesity. *Obesity (Silver Spring)*. 2012; **20**(1):233–238.
180. Suviolahti E, Oksanen LJ, Öhman M, Cantor RM, Ridderstråle M, Tuomi T, Kaprio J, Rissanen A, Mustajoki P, Jousilahti P, Vartiainen E, Silander K, Kilpikari R, Salomaa V, Groop L, Kontula K, Peltonen L, Pajukanta P. The *SLC6A14* gene shows evidence of association with obesity. *J Clin Invest*. 2003;**112**(11): 1762–1772.
181. Durand E, Boutin P, Meyre D, Charles MA, Clement K, Dina C, Froguel P. Polymorphisms in the amino acid transporter solute carrier family 6 (neurotransmitter transporter) member 14 gene contribute to polygenic obesity in French Caucasians. *Diabetes*. 2004;**53**(9):2483–2486.
182. Corpeleijn E, Petersen L, Holst C, Saris WH, Astrup A, Langin D, MacDonald I, Martinez JA, Oppert JM, Polak J, Pedersen O, Froguel P, Arner P, Sørensen TI, Blaak EE. Obesity-related polymorphisms and their associations with the ability to regulate fat oxidation in obese Europeans: the NUGENOB study. *Obesity (Silver Spring)*. 2010;**18**(7):1369–1377.
183. Fuemmeler BF, Agurs-Collins TD, McClernon FJ, Kollins SH, Kail ME, Bergen AW, Ashley-Koch AE. Genes implicated in serotonergic and dopaminergic functioning predict BMI categories. *Obesity (Silver Spring)*. 2008;**16**(2):348–355.
184. Kim HJ, Kim JH, Noh S, Hur HJ, Sung MJ, Hwang JT, Park JH, Yang HJ, Kim MS, Kwon DY, Yoon SH. Metabolomic analysis of livers and serum from high-fat diet induced obese mice. *J Proteome Res*. 2011;**10**(2):722–731.
185. Young RL, Lumsden AL, Martin AM, Schober G, Pezos N, Thazhath SS, Isaacs NJ, Cvijanovic N, Sun EWL, Wu T, Rayner CK, Nguyen NQ, Fontgalland D, Rabbitt P, Hollington P, Sposato L, Due SL, Wattchow DA, Liou AP, Jackson VM, Keating DJ. Augmented capacity for peripheral serotonin release in human obesity. *Int J Obes*. 2018;**42**(11): 1880–1889.
186. Takahashi T, Yano M, Minami J, Haraguchi T, Koga N, Higashi K, Kobori S. Sarpogrelate hydrochloride, a serotonin2A receptor antagonist, reduces albuminuria in diabetic patients with early-stage diabetic nephropathy. *Diabetes Res Clin Pract*. 2002; **58**(2):123–129.
187. Kwon O, Yu JH, Jeong E, Yoo HJ, Kim MS. Meal-related oscillations in the serum serotonin levels in healthy young men. *Clin Endocrinol (Oxf)*. 2018; **88**(4):549–555.
188. Iqbal J, Hussain MM. Intestinal lipid absorption. *Am J Physiol Endocrinol Metab*. 2009;**296**(6):E1183–E1194.

Acknowledgments

The authors thank Natasha H. Thompson for the conceptual illustrations of Figures 2, 4, and 5.

Financial Support: This work was supported by Canadian Institutes of Health Research Grants 201709FDN-CEBA-116200 (to G.R.S.) and 144625-1 (to G.R.S. and W.I.K.). G.R.S. is supported by a Canada Research Chair and the J. Bruce Duncan Endowed Chair in Metabolic Diseases.

Correspondence and Reprint Requests: Gregory R. Steinberg, PhD, McMaster University, 1280 Main Street West, Hamilton, Ontario L8N 3Z5, Canada. E-mail. gsteinberg@mcmaster.ca.

Disclosure Summary: G.R.S. has received honoraria/consulting fees from Astra Zeneca, Boehringer, Eli-Lilly, Esperion Therapeutics, Novo Nordisk, Poxel, Pfizer, Merck, Rigel Therapeutics, and Terns Therapeutics. D.J.K. has received funding from Pfizer. G.R.S. has received research funding from Esperion Therapeutics. G.R.S., W.I.K., and A.E.G. hold a patent for inhibiting peripheral serotonin for the treatment of metabolic diseases, including obesity and NAFLD. The remaining authors have nothing to disclose.

Abbreviations

5-HIAA, 5-hydroxyindoleacetic acid; 5-HT, 5-hydroxytryptamine; 5-HTP, 5-hydroxytryptophan; AgRP, agouti-related peptide; ARC, arcuate nucleus; BAT, brown adipose tissue; BMI, body mass index; CNS, central nervous system; EC, enterochromaffin; ENS, enteric nervous system; HSC, hepatic stellate cell; HTR, 5-HT receptor; IDO, indoleamine 2,3-dioxygenase; MAO, monoamine oxidase; MC, mast cell; NAD, nicotinamide adenine dinucleotide; NAFLD, nonalcoholic fatty liver disease; NPY, neuropeptide Y; PGC1α, peroxisome proliferator–activated receptor γ coactivator 1-α; POMC, proopiomelanocortin; SERT, serotonin transporter; SSRI, selective serotonin reuptake inhibitor; TDO, tryptophan-2,3-dioxygenase; Tph, tryptophan hydroxylase; Ucp1, uncoupling protein 1; WAT, white adipose tissue.

1.5 MAIN OBJECTIVE

Assess the role of peripheral serotonin synthesis from various sources that are thought to be involved in lipid accretion such as adipose tissue and liver. Elucidating sources of peripheral serotonin synthesis that inhibit adipose tissue energy expenditure and promote hepatic lipid accretion will be pivotal to future targeted therapy for metabolic diseases such as obesity and NAFLD.

1.6 THESIS AIMS

Determine adipose tissue local sources by which serotonin exerts its inhibitory effects on thermogenic adipose tissue. Specifically, determine whether mast cells and adipocytes work in paracrine and autocrine manners, respectively to reduce energy expenditure attributed to thermogenic adipose tissue using tissue-specific genetic models of Tph1 ablation. We will also assess the role of circulating serotonin in whole body Tph1 knockout mice to determine if circulating serotonin is regulated by housing temperatures in mice to influence liver lipid accretion. Collectively, I aim to identify sources of serotonin that promotes lipid anabolism in adipose and liver.

CHAPTER TWO

GENETIC DELETION OF MAST CELL SEROTONIN SYNTHESIS PREVENTS THE DEVELOPMENT OF OBESITY AND INSULIN RESISTANCE

Published in *Nature Communications*. 2020. 11.
https://doi.org/10.1038/s41467-019-14080-7

Julian M. Yabut, Eric M. Desjardins, Eric J. Chan, Emily A. Day, Julie M. Leroux, Bo Wang, Elizabeth D. Crane, Wesley Wong, Katherine M. Morrison, Justin D. Crane, Waliul I. Khan & Gregory R. Steinberg

In this chapter, we identify that mast cells are a primary source of serotonin synthesis from Tph1. We subsequently identify that mast cells infiltrate white adipose tissue of obese mice when they are housed at thermoneutrality. To determine whether mast cell serotonin synthesis is important for suppressing white adipose tissue browning, we studied two genetic mouse models of mast cell-specific Tph1 deletion by: 1) inoculation of $Tph1^{-/-}$ versus $Tph1^{+/+}$ mast cells into mast cell-deficient $Kit^{w\text{-}sh/w\text{-}sh}$ mice and 2) mast cell-specific genetic deletion of Tph1 using Cpa3-Cre Tph1 flox gene deletion strategies. Inoculation of $Tph1^{+/+}$, but not $Tph1^{-/-}$ mast cells, induced obesity, insulin resistance and reduced WAT browning in $Kit^{w\text{-}sh/w\text{-}sh}$ mice. Similarly mast cell-specific Tph1 knockout mice were protected from developing HFD-induced obesity, insulin resistance and NAFLD. In both models reductions in obesity and insulin resistance were associated with increased energy expenditure and adipose tissue browning. These studies demonstrate that mast cell serotonin synthesis is an important inhibitor of beige adipose tissue development and is important for regulating obesity and insulin resistance in mice.

J.M.Y., E.M.D., K.M.M., J.D.C., W.I.K. and G.R.S. designed the experiments. J.M.Y., E.M.D., E.J.C., J.M.L., B.W., E.A.D., E.D.C., W.W. and J.D.C. conducted the experiments. J.M.Y. and G.R.S. wrote the paper. All authors offered edits to final manuscript.

J.M.Y. was involved in all experiments except the following: Fig. 1h (J.D.C.), Fig 2f-h (E.J.C.), Fig 3i (E.A.D.), Supplementary Fig 2a-b (J.D.C.), Supplementary Fig 2e-f (E.J.C.), Supplementary Fig 2g-h (E.D.C. & W.W.).

nature COMMUNICATIONS

ARTICLE

https://doi.org/10.1038/s41467-019-14080-7 OPEN

Genetic deletion of mast cell serotonin synthesis prevents the development of obesity and insulin resistance

Julian M. Yabut[1,2], Eric M. Desjardins[1,2], Eric J. Chan[1,3], Emily A. Day[1,2], Julie M. Leroux[1,2], Bo Wang[1,2], Elizabeth D. Crane[4], Wesley Wong[4], Katherine M. Morrison[1,5], Justin D. Crane[4], Waliul I. Khan[1,6,7] & Gregory R. Steinberg[1,2,3*]

Obesity is linked with insulin resistance and is characterized by excessive accumulation of adipose tissue due to chronic energy imbalance. Increasing thermogenic brown and beige adipose tissue futile cycling may be an important strategy to increase energy expenditure in obesity, however, brown adipose tissue metabolic activity is lower with obesity. Herein, we report that the exposure of mice to thermoneutrality promotes the infiltration of white adipose tissue with mast cells that are highly enriched with tryptophan hydroxylase 1 (Tph1), the rate limiting enzyme regulating peripheral serotonin synthesis. Engraftment of mast cell-deficient mice with Tph1$^{-/-}$ mast cells or selective mast cell deletion of Tph1 enhances uncoupling protein 1 (Ucp1) expression in white adipose tissue and protects mice from developing obesity and insulin resistance. These data suggest that therapies aimed at inhibiting mast cell Tph1 may represent a therapeutic approach for the treatment of obesity and type 2 diabetes.

[1] Centre for Metabolism, Obesity and Diabetes Research, McMaster University, 1280 Main St. W., Hamilton, ON, Canada L8N 3Z5. [2] Division of Endocrinology and Metabolism, Department of Medicine, McMaster University, 1280 Main St. W., Hamilton, ON, Canada L8N 3Z5. [3] Department of Biochemistry and Biomedical Sciences, McMaster University, 1280 Main St. W., Hamilton, ON, Canada L8N 3Z5. [4] Department of Biology, Northeastern University, Boston, MA 02115, USA. [5] Department of Pediatrics, McMaster University, 1280 Main St. W, Hamilton, ON, Canada L8N 3Z5. [6] Farncombe Family Digestive Health Research Institute, McMaster University, 1280 Main St. W., Hamilton, ON, Canada L8N 3Z5. [7] Department of Pathology and Molecular Medicine, McMaster University, 1280 Main St. W., Hamilton, ON, Canada L8N 3Z5. *email: gsteinberg@mcmaster.ca

Obesity is tightly linked with the development of non-alcoholic fatty liver disease (NAFLD), insulin resistance and cardiovascular disease and is characterized by an excessive accumulation of adipose tissue caused by an imbalance of energy intake and expenditure[1,2]. Brown adipose tissue (BAT) has a high capacity for fatty acid and glucose oxidation due to the presence of futile cycling mediated by mitochondrial uncoupling protein 1 (Ucp1)[3,4], which is activated by β-adrenergic stimuli in response to cold or nutrients[5]. Ucp1$^+$ beige/brite adipocytes are also interspersed within white adipose tissue (WAT) and can be recruited for non-shivering thermogenesis[3,4,6]. Since rodent beige/brite adipocytes have a molecular signature reminiscent of supraclavicular BAT in lean adult humans[7–9], studies aimed at understanding beige adipose tissue in rodents may have direct implications for human BAT. Human BAT can be stimulated by cold or β-adrenergic stimuli as measured by an increase in ^{18}F-labeled fluorodeoxyglucose (FDG) uptake measured with positron emission tomography/computerized tomography (PET/CT)[10,11]. However, the ability of cold to increase BAT metabolic activity is impaired in the obese compared to lean healthy controls, despite greater BAT volume[12]. In both rodents and humans, norepinephrine is a critical hormone required for the maintenance of adipose tissue thermogenic capacity;[3,4] however, the signals that inhibit this pathway during obesity remain incompletely understood[12].

A potentially important inhibitor of adipose tissue thermogenesis is serotonin[13,14]. Previous studies have indicated that genetic and chemical inhibition of the rate limiting enzyme regulating peripheral serotonin synthesis, tryptophan hydroxylase 1 (Tph1), enhances adipose tissue thermogenesis and protects mice against obesity and insulin resistance[13,14]. Circulating serotonin levels in the periphery are dependent on the expression of Tph1 within the gastrointestinal tract (for review see refs. [15,16]), yet surprisingly, the genetic deletion of Tph1 within the gastrointestinal tract does not result in a lean phenotype[17], which is in contrast to the anti-obesity phenotype of germline deletion[13,14]. While a previous study using Tph1 floxed mice crossed to mice expressing Ap2-Cre suggested adipocyte Tph1 was important for inhibiting adipose tissue thermogenesis[13], it is known that the Ap2-Cre is expressed in many different immune cells found within the stromal vascular fraction[18]. Thus, the primary Tph1 expressing cell type(s) that inhibit adipose tissue thermogenesis are currently unknown.

Here, we find that mice housed at thermoneutrality have elevations in mast cells, *Tph1* and serotonin in WAT that are associated with reductions in *Ucp1*. In mice fed a high-fat diet, genetic removal of Tph1 in mast cells from two distinct mouse models elevates basal metabolic rate, increases WAT *Ucp1* and protects mice from obesity, insulin resistance and fatty liver disease compared to relevant controls. These data establish a role for mast cells in regulating adipose tissue thermogenesis and suggest that the therapeutic targeting of mast cell Tph1 may be a future strategy for the treatment of obesity and related metabolic disorders including insulin resistance and NAFLD.

Results

Thermoneutrality increases WAT *Tph1* in HFD-fed mice. To delineate the potential role of Tph1 and peripheral serotonin for inhibiting adipose tissue thermogenesis and the primary cell type(s) that might be mediating this effect, we first conducted experiments in mice housed at thermoneutrality (TN; 29 °C); a condition known to dramatically reduce adipose tissue thermogenesis compared to housing mice at room temperature (RT; 22 °C)[19,20]. Mice housed at thermoneutrality had reductions in oxygen consumption (Supplementary Fig. 1a), energy expenditure (Supplementary Fig. 1b) and BAT activity (Supplementary Fig. 1c, d), effects which were independent of changes in body mass (Supplementary Fig. 1e) or fat mass (Supplementary Fig. 1f). As anticipated, thermoneutral housing reduced *Ucp1* expression in all adipose tissue depots (Fig. 1a). We subsequently examined *Tph1* expression and found that it was unchanged in BAT, but was significantly elevated in inguinal WAT (iWAT) and gonadal WAT (gWAT) (Fig. 1b).

Mast cell serotonin inhibits WAT browning in vitro. To identify cell types that may contribute to the increases in WAT *Tph1*, we first queried the BIOGPS gene atlas[21] for genes that were associated with *Tph1* expression and found 12 highly correlated genes (>0.95 R^2 value). Notably, seven of these genes were known to be highly enriched in mast cells (*Kit*, *FCER1a*, *Cpa3*, *Tpsg1*, *Cma1*, *Alox5*, and *Ms42a*) (Fig. 1c, Supplementary Table 1). However, this query did not identify genes associated with adipocytes as previously indicated[14], suggesting that mast cells may be the predominant cell type contributing to serotonin production in adipose tissue.

Mast cells are immune cells that reside within tissues to quickly respond to injury or other pro-inflammatory stimuli, secreting cytokines, proteases and bioamines to potentiate an inflammatory response[22]. Consistent with increases in WAT *Tph1* at thermoneutrality, we found increased expression of the mast cell marker tryptase β2 (*Tpsb2*), which was correlated with increased *Tph1* expression (Fig. 1d, e). Increased expression of both *Tpsb2* and *Tph1* at thermoneutrality was associated with elevated serotonin levels in both WAT depots (Fig. 1f), an effect independent of changes in whole blood serotonin (Supplementary Fig. 1g). These data indicate that thermoneutrality increases mast cells within WAT and this is associated with increases in Tph1 and serotonin.

To examine whether there might be a causal link between mast cells, *Tph1*, serotonin and reduced WAT *Ucp1* at thermoneutrality, we cultured mast cells in vitro and treated them with the Tph chemical inhibitor LP533401[23] followed by the calcium ionophore, A23187, to induce mast cell degranulation (Fig. 1g). As expected, A23187 treatment increased serotonin release (Fig. 1h), however, LP533401 pre-treatment dramatically reduced this effect (Fig. 1h). To examine whether this serotonin production from mast cells could directly inhibit *Ucp1* expression in WAT, we subsequently cultured iWAT stromal vascular cells and treated them with 1μM of serotonin starting at the beginning of differentiation (day 7) (Fig. 1i). Treatment of these cells with the pan-β-adrenergic agonist isoproterenol increased *Ucp1*, but this was mitigated by serotonin treatment (Fig. 1j). Collectively, these data suggest that at thermoneutrality, there are increases in the number of mast cells, Tph1 and serotonin which can inhibit isoproterenol-induced increases in *Ucp1* in WAT.

Mast cell Tph1 promotes obesity & insulin resistance. Previous studies have found that mast cells accumulate within obese WAT of both mice[24] and humans[25]. To examine whether mast cell serotonin contributes to obesity and insulin resistance, mice lacking functional mast cells (Kit$^{W\text{-}sh/W\text{-}sh}$) were injected with saline (Kit^{sham}) or in vitro-cultured bone marrow-derived mast cells (BMMCs) from Tph1$^{+/+}$ (Kit$^{Tph1+/+}$) or Tph1$^{-/-}$ (Kit$^{Tph-/-}$) mice and fed a HFD (Fig. 2a). Flow cytometry analysis (Supplementary Fig. 2a) using established markers of mast cell maturity (CD117$^+$/FcεR1$^+$) indicated that there were no differences in BMMC viability or purity between genotypes (Supplementary Fig. 2b) and, as expected, *Tph1* expression was dramatically reduced (~99.9%) in mast cells of Tph1$^{-/-}$ mice (Fig. 2b). Additionally, *Tph2* was nearly undetectable in both Tph1$^{+/+}$ or Tph1$^{-/-}$ mast cells (Fig. 2b) and the expression of

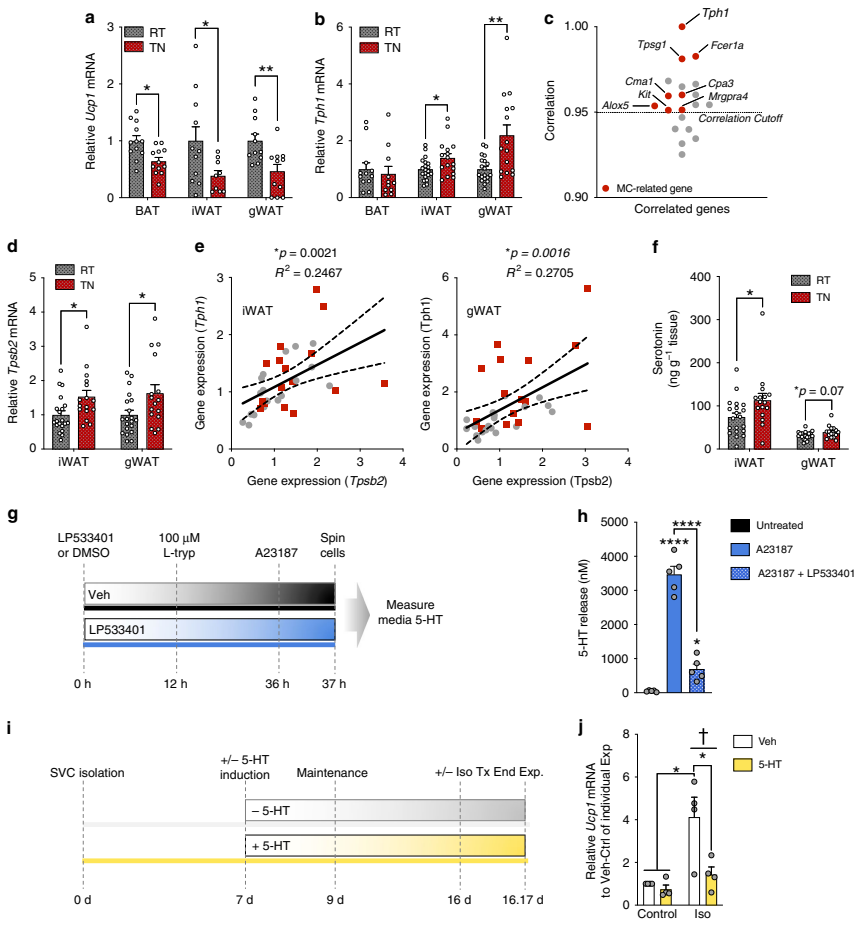

Fig. 1 Thermoneutrality reduces white adipose tissue *Ucp1* and increases *Tph1*, mast cells and serotonin in HFD-fed mice. a *Ucp1* expression in BAT ($n = 12$), iWAT ($n = 11$ RT, 9 TN) and gWAT ($n = 11$). **b** *Tph1* expression in BAT ($n = 12$ RT, 11 TN), iWAT ($n = 20$ RT, 16 TN) and gWAT ($n = 19$ RT, 15 TN). **c** BIOGPS *Tph1* Correlations highlighting mast cell-related genes with greater than 0.95 cutoff. **d** *Tpsb2* expression in WAT ($n = 20$ RT, 16 TN). **e** Correlation between *Tpsb2* and *Tph1* expression of RT (grey dots) and TN (red squares) housed mice in iWAT ($n = 36$) and gWAT ($n = 34$) Slopes were determined to be significantly ($^*p < 0.05$) non-zero by simple linear regression. **f** Serotonin (5-HT) in WAT ($n = 20$ RT, 16 TN) **g** Timeline of in vitro experiment. L-tryp, L-tryptophan. **h** Serotonin release stimulated with A23187 (2 µM) in vitro-cultured mast cells with or without 300 µM LP533401 ($n = 5$) as determined by One-way ANOVA and Tukey post hoc test. Significance ($^*p < 0.05$) compared to Untreated group, unless indicated otherwise. **i** Beige adipocyte progenitors were treated with vehicle (Veh) or 1 µM serotonin (5-HT) starting at the beginning of differentiation and terminated after a 4-hour exposure to 10 nM isoproterenol (Iso). **j** *Ucp1* expression in primary cultured beige adipocytes ($n = 4$). Significant effects ($^*p < 0.05$) and isoproterenol treatment effects ($^\dagger p < 0.05$) determined by two-way ANOVA with uncorrected Fisher's LSD post-test. RT-TN statistical significance assessed via Student's *t*-test. Significance denoted by $^*p < 0.05$, $^{**}p < 0.01$, $^{****}p < 0.0001$). Data are expressed as mean ± SEM.

the serotonin transporter did not differ between Tph1$^{+/+}$ or Tph1$^{-/-}$ mast cells (Supplementary Fig. 2c).

As others have shown[26,27], Kit^{sham} mice fed a HFD had attenuated weight gain and adiposity relative to controls, a phenotype that was reversed following the injection of mast cells from Tph1$^{+/+}$ (Kit$^{Tph1+/+}$) donors (Fig. 2c, d). However, this increase in weight gain and adiposity was not observed in mice injected with mast cells from Tph1$^{-/-}$ donors (Fig. 2c, d,

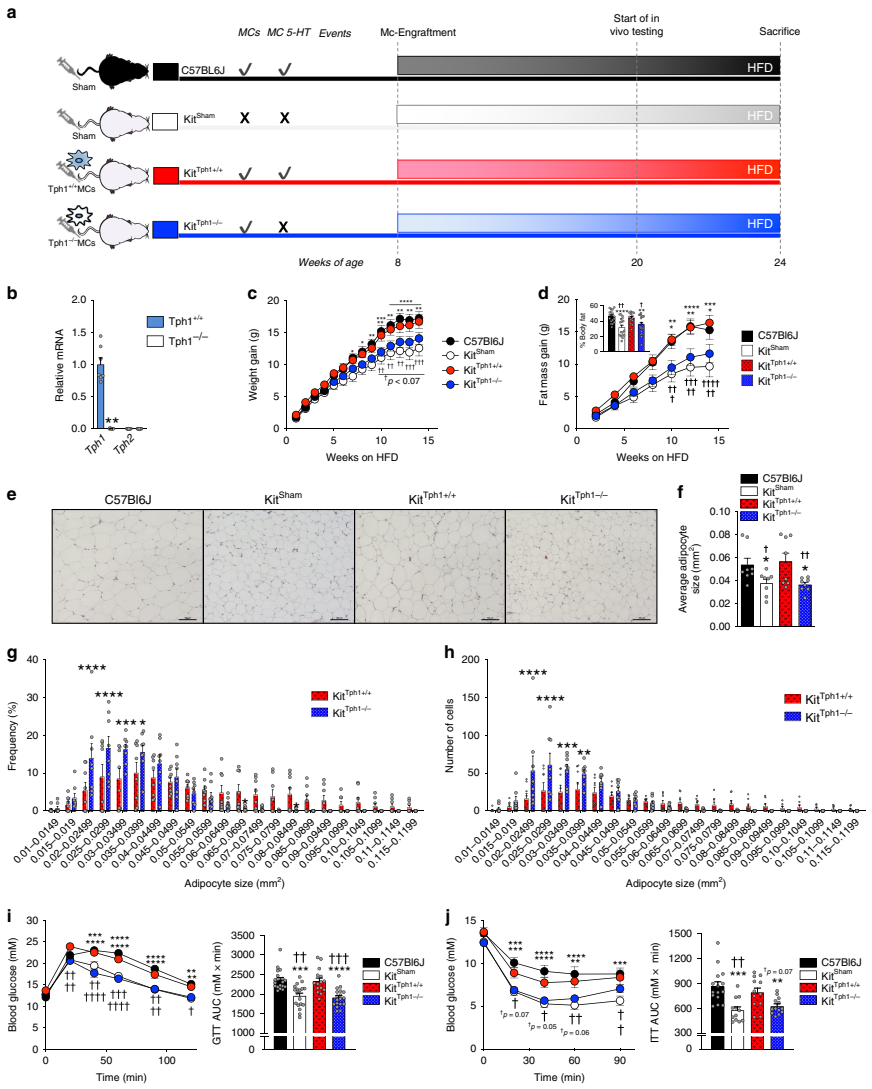

Supplementary Fig. 2d). Consistent with reduced adiposity, iWAT from Kit$^{Tph1-/-}$ mice had smaller adipocytes (Fig. 2e, f), that occurred with a higher frequency (Fig. 2g) and number (Fig. 2h) compared to Kit$^{Tph1+/+}$ mice, a finding similar to C57BL6J and Kit^{sham} controls (Supplementary Fig. 2e, f). Consistent with their reduced adiposity, Kit$^{Tph1-/-}$ mice had improved glucose tolerance (Fig. 2i) and insulin sensitivity (Fig. 2j) compared to controls. Importantly, these differences in metabolism between Kit$^{Tph1+/+}$ and Kit$^{Tph1-/-}$ mice were not due to differences in the number of mast cells within iWAT and gWAT, which were comparable between genotypes (Supplementary Fig. 2g, h).

Fig. 2 Mast cells are enriched in Tph1 and HFD-fed mice lacking mast cell serotonin are protected from obesity and insulin resistance. a HFD-fed C57BL6J (n = 19) and mast cell-deficient mice were engrafted with either sham, $Tph1^{+/+}$ or $Tph1^{-/-}$ mast cells beginning at 8 weeks of age for 12 weeks and in vivo tests following. The sample size indicated is for all figures unless otherwise stated. Significant effects of C57BL6J mice (*$p < 0.05$) and $Kit^{Tph1+/+}$ ($^{\dagger}p < 0.05$) between Kit^{Sham} and $Kit^{Tph1-/-}$ as determined by two-way RM ANOVA or one-way ANOVA with uncorrected Fisher's LSD post-test. **b** Relative expression of *Tph1* and *Tph2* from in vitro-cultured mast cells from $Tph1^{-/-}$ mice or wildtype littermates ($n = 5$) determined by Student's *t*-test. **c** Weight gain in grams over 14 weeks of HFD of C57BL6J ($n = 19$), Kit^{Sham} ($n = 17$), $Kit^{Tph+/+}$ ($n = 15$) and $Kit^{Tph-/-}$ ($n = 18$). **d** Fat mass gain in grams over 14 weeks and % Body fat at 12 weeks of HFD of C57BL6J ($n = 19$), Kit^{Sham} ($n = 17$), $Kit^{Tph+/+}$ ($n = 15$) and $Kit^{Tph-/-}$ ($n = 18$). **e** Representative H & E images of mast cell-engrafted $Kit^{W\text{-}sh/W\text{-}sh}$ mice iWAT, scale bars set at 100 μm. **f** Average adipocyte sizes of mast cell-engrafted $Kit^{W\text{-}sh/W\text{-}sh}$ mice iWAT ($n = 8$). **g** Frequency of adipocytes in iWAT of $Kit^{Tph+/+}$ and $Kit^{Tph-/-}$ mice ($n = 6$). Significance (*$p < 0.05$) determined by two-way ANOVA with uncorrected Fisher's LSD post-test. **h** Number of adipocytes in iWAT of $Kit^{Tph+/+}$ and $Kit^{Tph-/-}$ mice ($n = 6$). Significance (*$p < 0.05$) determined by two-way ANOVA with uncorrected Fisher's LSD post-test. **i** Glucose tolerance test (GTT), 1 g/kg glucose. **j** Insulin tolerance test (ITT), 0.7 U/kg insulin. ($n = 15$ C57BL6J, 12 Kit^{Sham}, 12 $Kit^{Tph+/+}$, and 13 $Kit^{Tph-/-}$). Significance denoted by *$p < 0.05$, **$p < 0.01$, ***$p < 0.001$, ****$p < 0.0001$). All data are expressed as mean ± SEM.

To further substantiate the observations that mast cell Tph1 promotes obesity and insulin resistance without the potential confounding metabolic effects of the $Kit^{W\text{-}sh/W\text{-}sh}$ mutation[28], we removed Tph1 in mast cells by crossing Tph1 floxed mice with mice expressing Cre recombinase linked to carboxypeptidase 3 promoter (Cpa3-Cre) to generate Tph1 mast cell null mice (Tph1 MCKO) (Fig. 3a) and confirmed deletion in intraperitoneal mast cells (Supplementary Fig. 2i). Tph1 MCKO mice were then fed a HFD starting at 8 weeks of age and similar to observations with $Kit^{Tph1-/-}$ mice, we found that Tph1 MCKO mice were also protected from HFD-induced weight gain (Fig. 3b, Supplementary Fig. 2j) due to reductions in adiposity (Fig. 3c, d). Tph1 MCKO mice were more glucose tolerant (Fig. 3e), insulin sensitive (Fig. 3f) and displayed a reduction in fasting blood glucose (Fig. 3g), liver weight (Fig. 3h) and liver lipids (Fig. 3i, j). These changes in metabolism were independent of alterations in free serotonin levels measured from platelet-poor plasma (Fig. 3k). These differences between genotypes were also independent of changes in markers of mast cells (*Tpsb2)* or other immune cell types such as basophils (*Basoph8*), M1 macrophages (*Nos*), eosinophils (*SiglecF*), M2 macrophages (*Arg1*) and ILC2s (*Gata3*) (Supplementary Fig. 2k). These data indicate that mice lacking Tph1 in mast cells are protected from obesity and insulin resistance independently of alterations in circulating serotonin.

Mast cell serotonin suppresses energy expenditure & WAT Ucp1. To examine the potential mechanisms contributing to reduced weight gain in the absence of mast cell Tph1, we assessed caloric intake and energy expenditure using indirect calorimetry. In the Kit model, food (Supplementary Fig. 3a) and water intake (Supplementary Fig. 3b) were comparable between genotypes. However, resting VO_2 (oxygen consumption during times of <30 beam breaks per 18-minute interval) (Fig. 4a) and 24 h VO_2 (Supplementary Fig. 3c, d) was elevated in both Kit^{sham} and $Kit^{Tph1-/-}$ mice compared to controls. This increase in VO_2 was present independent of differences in body mass (Supplementary Fig. 3e) and was not due to differences in physical activity levels, which were comparable between genotypes (Supplementary Fig. 3f). Similar to our studies in $Kit^{Tph1-/-}$ mice, Tph1 MCKO mice had no change in physical activity, food or water intake (Supplementary Fig. 3g–i), but did have increases in resting (Fig. 4b) and 24 h VO_2 (Supplementary Fig. 3j, k), however, this was measured at a time when there were differences in body mass (Supplementary Fig. 3l). Collectively, these data demonstrate that the deletion of Tph1 in mast cells increases resting energy expenditure.

To discern the tissues involved in enhanced energy expenditure in mice lacking mast cell Tph1, we first conducted assays focused on the potential role of BAT. Using an infrared thermography assay which directly detects Ucp1-mediated thermogenesis in BAT[29], we found no differences in interscapular surface temperatures between $Kit^{Tph1+/+}$ *and* $Kit^{Tph1-/-}$ mice following the injection of saline or CL-316,243 (Supplementary Fig. 4a). Consistent with this observation, Ucp1 mRNA (Supplementary Fig. 4b), Ucp1 protein expression (Supplementary Fig. 4c), BAT mass (Supplementary Fig. 4d) and morphology (Supplementary Fig. 4e) were comparable between $Kit^{Tph1+/+}$ *and* $Kit^{Tph1-/-}$ mice. Similarly, Tph1 MCKO mice also had no discernable difference from controls with respect to BAT mass and morphology (Supplementary Fig. 4f–h). These data indicate that mast cell serotonin is unlikely to elicit its beneficial effects on body mass and adiposity through modulation of BAT thermogenesis; a finding consistent with the observation that thermoneutrality does not alter *Tph1* expression in BAT (Fig. 1b).

In contrast to BAT, the iWAT of $Kit^{Tph1-/-}$ mice had reductions in *Tph1* expression and adipose tissue serotonin (Fig. 4c, d) and increased expression of *Ucp1* (Fig. 4e) compared to $Kit^{Tph1+/+}$ mice. Consistent with these observations, iWAT and gWAT from Tph1 MCKO mice tended and had significantly lower *Tph1* mRNA, respectively (Fig. 4f). These reductions in *Tph1* expression were associated with greater multilocular lipid droplet formation (Fig. 4g, top panel), greater Ucp1 protein (Fig. 4g, bottom panel) and mRNA (Fig. 4h) in iWAT and in gWAT (Fig. 4i, j). Similar findings with respect to the browning of iWAT has also recently been reported in mice fed a control chow diet[30].

Discussion

Mast cells accumulate in target tissues in response to allergic or inflammatory stimuli and secrete various signaling molecules such as cytokines, proteases and bioamines[22]. Previous studies have shown that mast cells accumulate within the WAT of both obese mice[24] and humans[25]. We now show that when mice are housed at thermoneutrality, a condition known to reduce *Ucp1* and adipose tissue thermogenesis[20], there is an increase in mast cells within WAT that occurs independent of changes in adiposity. This increase in mast cells is associated with increased WAT *Tph1* expression and serotonin. Using two distinct mouse models we subsequently demonstrate that genetic deletion of *Tph1* in mast cells reduces WAT serotonin and enhances WAT *Ucp1* and whole-body energy expenditure; an effect associated with a reduction in high-fat diet-induced obesity, insulin resistance and NAFLD. These data establish a critical role for mast cell serotonin synthesis in suppressing adipose tissue thermogenesis and suggest that therapeutic targeting of this pathway may exert beneficial metabolic effects in obesity.

In the current study, the increase in energy expenditure that we[13] and others[14] have observed with whole-body inhibition of Tph1 and subsequent reductions in circulating serotonin can be recapitulated by removing Tph1 in mast cells. These findings

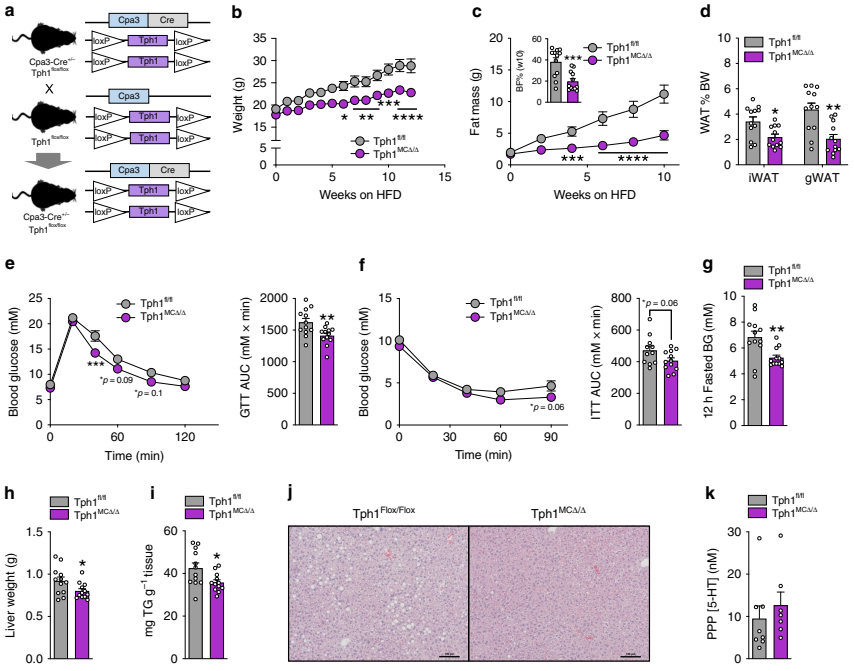

Fig. 3 Mast cell-specific Tph1 deletion protects HFD-fed mice from obesity and insulin resistance. a Breeding strategy to produce Carboxypeptidase-3 (Cpa3) Cre Tph1 double floxed mice. **b** Weight and **c** Fat mass over time ($n = 12$). **d** WAT mass % of body weight ($n = 12$). **e** Glucose tolerance test (GTT), 1.5 g/kg glucose ($n = 12$). **f** Insulin tolerance test (ITT), 1 U/kg insulin ($n = 12$). **g** Overnight 12 h fasted blood glucose (BG, $n = 12$). **h** Liver weight in grams ($n = 12$). **i** mg of Triglycerides (TG) per gram of liver tissue ($n = 12$). **j** Representative liver H & E images, scale bar 100 µm. **k** Serotonin concentration in platelet poor plasma (PPP) samples ($n = 8$ Tph1$^{fl/fl}$, 7 Tph1 MCKO). Statistical significance (*$p < 0.05$, **$p < 0.01$, ***$p < 0.001$, ****$p < 0.0001$) determined by two-way RM ANOVA with Bonferroni post-test or Student's *t*-test. All data are expressed as mean ± SEM.

seem paradoxical based on previous findings indicating that serotonin in the central nervous system increases BAT thermogenesis[31–34]. These opposing functions of central and peripheral serotonin are consistent with findings from other highly conserved regulators of energy balance such as the AMP-activated protein kinase where genetic reductions of hypothalamic AMPK increases energy expenditure[35], while reductions of AMPK in adipose tissue lower energy expenditure and iWAT browning[36]. A similar paradigm of opposing functions between central and adipose specific mTOR has also been observed[37–39]. Thus, there is a precedent by which central and peripheral pathways may exert opposing functions on energy expenditure. Collectively, these data support a model where Tph2 and central serotonin enhance energy expenditure in response to cold, but under thermoneutral conditions or with obesity, peripheral serotonin synthesis by mast cell Tph1 reduces thermogenic activation, thus lowering adipose tissue energy expenditure.

However, a fundamental question is why would mast cell serotonin production by Tph1 have evolved to suppress adipose tissue thermogenesis? Evolution inference has been shown to inform biological function[40]. Querying the Clustering by Inferred Models of Evolution (CLIME) portal (http://gene-clime.org/) for genes that are highly likely to have coevolved with Tph1 reveals, remarkably, only two hits: (1) the highly related orthologue Tph2 and (2) tyrosine hydroxylase, the primary enzyme regulating norepinephrine production and adipose tissue thermogenesis. As mast cells are the first responders to injury and primary cell type initiating anaphylaxis and inflammation[22], it is interesting to speculate that the suppression of adipose tissue thermogenesis by mast cell serotonin may have developed to reduce futile cycling so that substrate could be redirected towards other immune functions. Future studies investigating how mast cell serotonin reduces Ucp1, including the primary serotonin receptor and downstream signaling, and whether mast cell serotonin inhibits Ucp1-independent thermogenesis[41,42], will be important for further understanding the mechanisms linking mast cell Tph1 and adipose tissue thermogenesis.

Our findings also raise important questions about the role of mast cells in obesity and insulin resistance and the potential limitation of mouse models of mast cell deficiency to establish causality. Recent studies by Gutierrez and colleagues[28] indicated that previous findings linking mast cells with obesity-induced

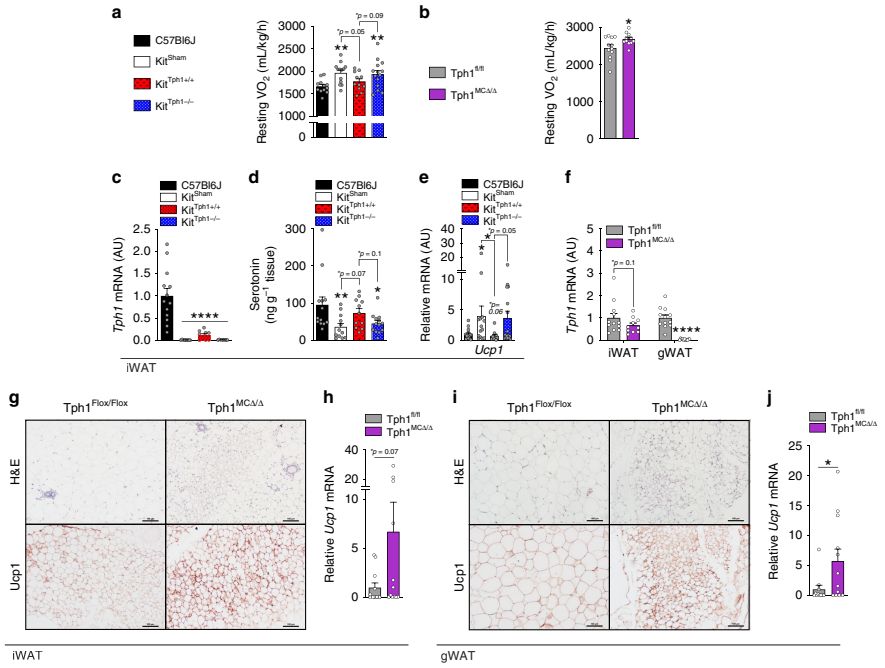

Fig. 4 Genetic removal of mast cell serotonin increases energy expenditure and causes adipose tissue browning. **a** Resting oxygen consumption of C57BL6J ($n = 12$), Kit^{Sham} ($n = 13$), $Kit^{Tph+/+}$ ($n = 11$) and $Kit^{Tph-/-}$ ($n = 14$). **b** Resting oxygen consumption of Tph1 MCKO mice ($n = 12$). **c** *Tph1* expression in iWAT of C57BL6J ($n = 13$), Kit^{Sham} ($n = 8$), $Kit^{Tph+/+}$ ($n = 9$) and $Kit^{Tph-/-}$ ($n = 8$). **d** Adipose tissue serotonin (5HT) of C57BL6J ($n = 13$), Kit^{Sham} ($n = 12$), $Kit^{Tph+/+}$ ($n = 11$) and $Kit^{Tph-/-}$ ($n = 13$). **e** *Ucp1* expression of C57BL6J ($n = 15$), Kit^{Sham} ($n = 14$), $Kit^{Tph+/+}$ ($n = 12$) and $Kit^{Tph-/-}$ ($n = 16$). **f** *Tph1* expression in WAT of Tph1 MCKO mice ($n = 12$). **g** Representative images of H & E and Ucp1 IHC-stained iWAT of Tph1 MCKO mice, Scale bar 100 µm. **h** *Ucp1* expression in iWAT from Tph1 MCKO mice ($n = 12$). **i** Representative images of H & E and Ucp1 IHC-stained gWAT of Tph1 MCKO model, Scale bar 100 µm. **j** *Ucp1* expression of gWAT from Tph1 MCKO model ($n = 12$). Statistical significant effects (*$p < 0.05$, **$p < 0.01$ and ****$p < 0.0001$) determined by one-way ANOVA with uncorrected Fisher's LSD post-test or Student's *t*-test where appropriate. All data are expressed as mean ± SEM.

insulin resistance[27] may have been due to effects intrinsic to the $Kit^{W\text{-}sh/W\text{-}sh}$ mutation rather than a direct result of mast cell reduction. These conclusions were based on the findings that: (1) the restoration of hematopoietic cells in $Kit^{W/Wv}$ mice, whether or not the hematopoietic cells could generate mast cells, led to weight gain when mice were fed a HFD and (2) mice containing an overexpressing Cre recombinase linked to Cpa3, which results in the death of mast cells, are not protected from HFD-induced obesity or insulin resistance. It should be noted that our studies differ in many ways from those of Gutierrez[28] or Liu and colleagues[27] as we did not directly test the role of mast cells per se in the regulation of obesity, but rather made comparisons between mast cells with or without Tph1 using two unique and completely distinct mouse models. First, we showed that reconstitution of $Kit^{W\text{-}sh/W\text{-}sh}$ mice with $Tph1^{+/+}$ mast cells increased weight gain and insulin resistance, while $Tph1^{-/-}$ mast cells did not. It is important to note this difference in weight gain between $Kit^{Tph1+/+}$ and $Kit^{Tph1-/-}$ mice was not due to differences in the number of mast cells within WAT, which were comparable upon reconstitution. Secondly and perhaps most importantly, given the potential confounding effects of the $Kit^{W\text{-}sh/W\text{-}sh}$ mutation on metabolism[28], we generated an entirely distinct mouse model in which Tph1 floxed mice were crossed to $Cpa3^{Cre/+}$ mice and observed similar results with respect to weight gain, adipose tissue *Ucp1*, energy expenditure and insulin sensitivity in mice lacking mast cell Tph1. And while it is known that Cpa3 is also expressed in basophils[43], it is important to note that mast cells have a much higher expression of Tph1 (>1000-fold) compared to basophils or other immune cells types such as macrophages making it unlikely that these cell types contributed to the phenotype[44]. Therefore, our findings, in two distinct mouse models as suggested[28,45] support the conclusions that mast cell Tph1 protects against obesity induced insulin resistance by enhancing adipose tissue *Ucp1* and whole body energy expenditure.

While these models are complementary, there are important differences in our results. The first and most evident is that the

protection from obesity-induced glucose intolerance and insulin resistance is more dramatic in the $Kit^{Tph1-/-}$ mice (Fig. 2) compared to the Tph1 MCKO mice (Fig. 3). This difference is most likely attributed to sex differences between models; since males were studied in the $Kit^{W\text{-}sh/W\text{-}sh}$ mast cell reconstitution experiments while female mice were studied in the Tph1 MCKO experiments. As female mice are lighter and more insulin sensitive than male mice at the same age and duration of high-fat diet feeding[46], this likely underlies the primary difference between the models. Other reasons for the more modest phenotype in the Tph1 MCKO mice is the time of testing which was after 8 weeks of high-fat diet compared to the 12 weeks for the $Kit^{Tph1-/-}$ mice. The longer duration of high-fat diet feeding in the $Kit^{Tph1-/-}$ mice was utilized to maximize mast cell engraftment as previously suggested[47]. Therefore, sex and duration of the high-fat diet before testing may explain the differences between models. However, we believe showing a similar phenotype in two different sexes, albeit to a lesser degree in the female mice, is an important strength of the study.

Another important consideration when interpreting our findings on energy expenditure are that serotonin is a potent regulator of vascular tone (reviewed here ref. [48]). The regulation of vasculature tone is extremely complex and depending on the tissues and serotonin receptors expressed, serotonin can induce either vasodilation or vasoconstriction to regulate heat loss and heat retention, respectively (reviewed here ref. [48]). Mice with germline deletions of Tph1 have altered blood pressure and vascular tone[49] and chemical inhibition of Tph1 can reduce hypoxia-induced pulmonary-arterial hypertension[50]. However, we have shown that in obese mice fed a HFD, similar to the current study, that treatment with the pan-Tph inhibitor, LP533401, does not affect heart rate or blood pressure, and that the effects of this compound on weight loss and insulin sensitivity are completely dependent on the expression of Ucp1[13]. These data suggest that in the context of high-fat diet-induced obesity it is unlikely that genetic deletion of Tph1 specifically in mast cells, which importantly had no effect on circulating serotonin, would elicit any effect on vasculature tone or heat loss. Lastly, while human mast cells synthesize serotonin via Tph1[51], it is important to highlight that there are relatively small amounts of serotonin secreted and stored in human mast cells in comparison to rodents. Future studies investigating the role of mast cell serotonin synthesis in humans and the potential impact this may have on vasculature tone are warranted.

In conclusion, our findings identify a role for mast cell serotonin for energy balance and suggest that inhibition of mast cell Tph1 may represent a promising strategy for the targeted treatment of obesity and insulin resistance. Future studies examining the importance of this pathway in humans with obesity and insulin resistance are warranted.

Methods

Animal housing and breeding. All animal experiments were performed in accordance with the McMaster Animal Care Committee guidelines and conducted under the Canadian guidelines for animal research (AUP: 16-12-41) and all study protocols received ethical approval. Tph1KO and WT littermates on C57BL6J background have been characterized previously that are bred in house[13,52]. Tph1 mast cell-specific knockout (Tph1 MCKO) mice were generated by crossing Tph1 floxed mice[53] with mice expressing Cre-Recombinase under the control of Carboxypeptidase-3 (Cpa3-cre)[43]. $Kit^{W\text{-}sh/W\text{-}sh}$ mice and Cpa3-cre (Stock No: 012861 & 026828, respectively) mice on a C57BL6J background were purchased from Jackson Laboratories and have been characterized previously[43,54].

Cell in vitro experiments. Male 6–16 week old $Tph1^{+/+}$ and $Tph1^{-/-}$ littermates were sacrificed and bone marrow from the tibia and femur were used to culture bone marrow-derived[47]. Briefly, mice were sacrificed by cervical dislocation and bone marrow was extracted from the femur and tibia by spinning the bones with severed ends. The resulting bone marrow was strained through a 10 µm strainer and topped up to 10 mL with DMEM media containing 10% FBS, 1% L-glutamine, 1% antibiotic (penicillin/streptomycin), 10 ng/mL recombinant mouse IL-3 (Peprotech, 213-13) and 50 µM β-mercaptoethanol. Media was changed every 3–4 days for 8–10 weeks with regular maturation checks with Kimura dye[55] within the first 6 weeks of culture. Maturation was confirmed by FACS using c-Kit (CD117) and FCeRI antibodies. For cell experiments, bone marrow-derived mast cells were counted and plated into 24-well plates (250,000 cells). For dose response and 5-HT release experiments, 1–1000 µM of LP533401 or DMSO vehicle were administered for 12 h and subsequently treated with 100 µM L-tryptophan for 24 h. A calcium ionophore that degranulates bone marrow-derived mast cells (A23187) was administered (2 µM) for 1 hour before cells were spun down (200 g) and media collected. For intraperitoneal lavage of mast cells, mice were sacrificed by cervical dislocation and 10 mL of PBS was injected into the intraperitoneal space of the mouse. The abdomen of the mouse was massaged and the contents drawn into a syringe, which was spun down at 2400 g for 10 min and used for RT-qPCR.

Animal experiments. Mice were maintained on a 12-h light and dark cycle (lights on at 0700) with food and water provided *ad libitum*. For experiments conducted in Fig. 1, male mice were housed at either room temperature (23 °C) or thermoneutrality (29 °C) and were fed a 60% HFD starting at 8 weeks of age for 10 weeks. All other experiments were performed in mice housed solely at room temperature. For bone marrow-derived mast cell reconstitution experiments (related to Figs. 2 and 4) male $Kit^{W\text{-}sh/W\text{-}sh}$ mice[47] at 9–10 weeks of age were separated into three different weight-matched groups and were injected with a total of 20 million mast cells from $Tph1^{+/+}$ ($Kit^{Tph1+/+}$) or $Tph1^{-/-}$ ($Kit^{Tph1-/-}$) mice at three different anatomical locations (10 million intravenously through tail vein, 5 million subcutaneously (dorsal interscapular area) and 5 million intraperitoneally). The third group of $Kit^{W\text{-}sh/W\text{-}sh}$ mice received an injection of equal volume saline at all three sites (Kit^{sham}). C57BL6J mice were also injected with equivalent amounts of saline at all aforementioned sites. After injections, mice were fed a 45% HFD (Cedarlane Canada; D12451) for 16 weeks (kept in animal facility for 24–25 weeks) with tissues collected after a 6-h fast and administration of 0.7 U/kg intraperitoneal insulin, 15 min prior to sacrifice by cervical dislocation. Female Tph1 MCKO mice (related to Figs. 3 and 4) were fed a HFD at 8 weeks of age for 12 weeks (kept in animal facility for 20 weeks) and sacrificed after a 6-h fast. Platelet poor plasma was extracted by pipetting 152 µL of whole blood into 8µL of 0.5 M EDTA, spun at 1500 g and top 20 µL of plasma removed. Liver, iWAT, gWAT and BAT from all mice were weighed and samples were kept at −80 °C.

Metabolic testing. Mice were weighed weekly and body composition analyzed biweekly using a Bruker minispec Whole Body Composition Analyzer. For Kit experiments mice were subjected to a 1 g/kg GTT and 0.7 U/kg ITT at 12 and 14 weeks post mast cell engraftment. For Tph1 MCKO experiments mice were subjected to 1.5 g/kg GTT and 0.75 U/kg ITT after 8 and 9 weeks of HFD. For both ITT and GTT experiments animals were fasted for 6 h starting at 0700 hours and basal blood glucose concentrations were measured using a glucometer (Aviva, Roche) at indicated time points. Measurements of metabolic parameters (respiratory exchange ratio, energy expenditure, activity, food and water intake) were assessed using a Comprehensive Laboratory Animal Monitoring System (CLAMS; Columbus Instruments) over a 48-h period.

Infrared imaging of Ucp1-mediated thermogenesis. Ucp1-mediated thermogenesis was assessed using an infrared imaging technique[29]. Briefly, mice are anesthetized with Avertin made with 25 g of 2,2,2-tribromoethanol (Sigma-Aldrich, #4, 840-2) in 15.5 mL tert-amyl alcohol to form a 80x stock solution and diluted to 20 mg/mL in saline. After 2 min post-Avertin injection, mice are injected intraperitoneally with either saline or CL-316,243 (0.0155 mg/kg, R&D Systems, Inc; Item # 1499/10). Average of oxygen consumption taken at 5 s intervals with an indirect calorimetry system (CLAMS, Columbus Instruments, Columbus, OH) from 19–20 min post Avertin injection and the top 10% interscapular dorsal temperature is determined by a thermal image taken 20 min post-Avertin by infrared camera (T650sc, emissivity of 0.98, FLiR Systems). Thermal images are analyzed using AMIDE-bin 1.0.5 software. Experiment is conducted on two different days (separated by 2–3 days between tests) on the same mice for saline and CL-316,243 injections.

Immunoblotting analysis. Tissues were placed in lysis buffer (20 mM Tris, 150 mM NaCl, 1 mM EDTA, 1 mM EGTA, 1% Triton-X, 2.5 mM sodium pyrophosphate, 0.5 mM DTT, 0.1% SDS, 1% Roche Protease Inhibitor, 0.5% sodium deoxycholate) and subsequently processed in a tissue homogenizer (Percellys). Samples were spun to extract supernatant and protein quantification was performed using the bicinchoninic acid (BCA) method (Pierce) as per manufacturer instructions. For UCP1, β-tubulin, β-actin protein analysis, BAT or iWAT lysates were diluted with 4× standard buffer (50% Sucrose, 7.5% SDS, 3.1% DTT) and loaded in Sodium dodecyl sulfate-polyacrylamide gel electrophoresis (SDS–PAGE) was performed using 10 or 12% gels. A Western Blotting apparatus (Bio-Rad) with electrophoresis buffer containing 12.5 mM Tris, 125 mM Glycine, 0.05% SDS. About 20 µg of sample was dispensed into wells along with Precision Plus Protein Dual Colour Standard (Bio-Rad). A wet transfer using a gel to membrane blotter

apparatus (BioRad) of PVDF membranes, 90 V for 90 min. Membranes were blocked with 5% skim milk in Tris-buffered saline (50 mM Tris–HCl, 150 mM NaCl) with Tween 20 (TBST) for 1 h. Subsequently, membranes were subject to primary antibody (1:1000 dilution) in TBST + 5% BSA overnight at 4 °C. Antibodies used were Anti-Mouse UCP1 (Alpha Diagnostics, 173435A4) and Anti-Mouse β-tubulin (Invitrogen, 322600). Membranes were rinsed in TBST and incubated in secondary antibody (1:10000 dilution in TBST + 5% BSA; Anti-mouse, 7076 S; Anti-rabbit, 7074 S) for 1 h. SuperSignal West Femto Maximum Sensitivity Substrate (Thermo Scientific) and a Fusion FX7 Chemiluminescence Visualizer (MBI) were used for detection. Densitometry analysis was performed using an ImageJ 3 analyzer.

Histological analysis. Tissues were immersed in 10% formalin, 90% PBS for 1 day and placed into 70% EtOH for paraffin embedding and H & E staining by the John Mayberry Histology facility at McMaster University. Adipocyte size assessment of H & E and immunohistochemistry for Ucp1 staining were done[56]. Briefly, H&E slides were taken at 10x magnification. A measurement of the farthest diameter for each adipocyte in the picture was used for data analysis using ImageJ. Images that filled the entire picture were used for this analysis. For Ucp1 staining, paraffin embedded slides are deparaffinized in xylenes. After 100% EtOH wash, endogenous peroxidase activity was blocked with hydrogen peroxide solution in 100% MeOH, followed by a 70% EtOH and dH_2O washes. Slides are placed in a pressure cooker at high temperature for 5 min in citrate buffer, cooled and washed in Tris buffer. Slides are blocked with 5% goat serum in Tris buffer. Primary antibody (Ucp1, 173435A4, Alpha Diagnostics) concentration of 1:200 was used followed by 1:500 of secondary antibody. Stepdavidin peroxidase (1:50, MJS BioLynx Inc.) is used followed by Nova red (MJS BioLynx Inc.) as per manufacturer's protocol. Images were captured with a light 90 Eclipse microscope (Nikon). For CD117 staining, tissues were sectioned at 4 microns on a microtome (Leica). After deparaffinization and re-hydration of the sections, we performed epitope retrieval using a pressure cooker (Cuisinart) and citrate buffer. We then used a mouse on mouse staining kit with an HRP-based Nova Red developing reagent (both Vector Labs). Blocking was performed with normal goat serum and secondary only control slides were included to confirm staining specificity. Slides were then cover slipped using Permount and later imaged using a Lifetech EVOS XL microscope.

RNA extraction. Tissue samples (50–100 mg) are homogenized in 1 mL of Trizol reagent (Life Technologies). Samples are spun for 10 min at 12,000 g in 4 °C, with supernatant drawn. In total 200 µL of chloroform is mixed and subsequently shaken for 15 s, followed by 2 min of room temperature incubation. Samples are spun and supernatant is collected. A 1:1 mixture of the sample to 70% EtOH was put into a RNA purifying column (RNEasy Kit; Qiagen) and followed manufacturer instructions. To reverse transcribe to cDNA, RNA (2 ng μL^{-1}) was placed in final concentrations of 0.5 mM dNTPs (Invitrogen) and 50 ng μL^{-1} random hexamers (Invitrogen). This solution was heated at 65 °C for 5 min and cooled to 4 °C. A mixture containing 50 units of SuperScript III (Invitrogen), 5× First-Strand Buffer (Invitrogen) and DTT (final concentration of 5 µM; Invitrogen) was added to the heated solution. The final mixture was held at room temperature (RT) for 5 min and subsequently, 50 °C for 1 h.

Real-Time quantitative PCR (RT-qPCR). Duplicate 25-ng cDNA samples were subjected to qPCR analysis using Rotor-Gene 6000 real-time rotary analyzer (Corbett Life Science; Concord NSW, Australia) with TaqMan Assay fluorogenic 5′nuclease chemistry (Invitrogen) as the fluorophore. Final concentrations for a 10-µL qPCR reaction with 25-ng of loaded cDNA include 0.25 U of AmpliTaq Gold DNA polymerase (Roche), 1.25 mM $MgCl_2$ (Roche), 100 µM dNTPs and 10× PCR buffer (Roche). Briefly, the samples are heated at 95 °C for 10 min. Samples are then subject to being heated at 95 °C for 10 s and then 58 °C for 45 s for a total of 45 cycles. Expression levels were normalized to that of peptidylprolyl isomerase A (PPIA) for tissues or Polr2A for cells mRNA using the delta–delta CT method ($2^{-\Delta\Delta CT}$). Gene expression data were gathered from various tissues. Arg 1 (Mm00475988_m1), Basph8 (Mm00484933_m1), Gata3 (Hs00231122_m1), Nos2 (Mm00440502_m1), Polr2a (Mm00839493_m1), Ppia (Mm02342430_g1), Siglecf (Mm00523987_m1), SERT (Mm00439391_m1), Tph1 spanning exons 2-3 (Mm01202614_m1), Tph1 probe spanning exon 4-5 (Mm00493794_m1), Tph2 (Mm00557715_m1), Tpsb2 (Mm01301240_g1), and Ucp1 (Mm01244861_m1) from Lifetechnologies were used.

Liver triglycerides quantification. Lipids were extracted from chipped liver (30–50 mg), homogenized in 1 mL of 2:1 chloroform: methanol, mixed overnight and subsequent isolation was carried out using an adapted Folch extraction protocol[57]. Briefly, samples are spun at 4500 g for 10 min at 4 °C, 200 µL of 0.9% NaCl is added and subsequently vortexed. Contents is spun again at the above conditions for 3 min. Clear bottom layer (400 µL) is drawn and resultant samples were freeze-dried and subsequently solubilized in 100% 2-propanol (200 µL). The Cayman Chemicals Triglyceride kit was used to assess triglyceride levels as directed by manufacturer instructions.

Serotonin quantification. Tissues were homogenized in 0.2 N perchloric acid in a tissue processing homogenizer (Percellys). The adipose tissue supernatant was extracted and mixed 1:1 in 1 M borate buffer (1 M boric acid, pH is brought up to 9.25 using concentrated NaOH). Platelet poor plasma is diluted 1:10. Tissues are undiluted. For mast cells, cells are spun down at 200 g for 5 min and media is extracted. Uninhibited and inhibited degranulated mast cell media are diluted 1:30 and 1:10, respectively. Serotonin concentrations are determined by an ELISA kit as per manufacturer's instructions (Serotonin EIA kit Beckman Coulter; IM1749). All aforementioned dilutions are done using the Dilution buffer provided by the Serotonin Kit.

Flow Cytometry Analysis. FCε-RI-PE (566608) and CD117-FITC (561680) antibodies (Becton Dickinson Canada Inc) were used (concentrations were optimized prior to experiment as per manufacturer recommendations) in combination with propidium iodide (Sigma-Aldrich) as a viability dye. Cultured mast cells were counted on a FACSCanto (BD Biosciences) and analyzed on FlowJo software 10.6.0 (FlowJo, LLC, Ashland, OR, USA). Briefly, 10^6 cells per sample were placed in FACS tubes and washed with FACS buffer (Phospho-buffered saline with 5 mg/mL Bovine serum albumin). Samples are spun at 500 g and liquid decanted. After 30 min incubation with appropriate antibody in FACS buffer, the samples are spun, decanted and resuspended in FACS buffer. The resuspended sample is filtered through nylon mesh before running samples into FACS machine. Cells were gated on lymphocytes, single cells, live/dead or FCε-RI vs. CD117. Acid-killed cell sample was used to set the gates for the live/dead stain and unstained sample was used to set the gates for FCε-RI vs. CD117.

Statistical analysis. Data were evaluated by two-tailed Student's *t*-test or one-way ANOVA where appropriate. A repeated measures ANOVA was used for body weights and composition plots, thermography, GTT and ITT data. Fisher-LSD was used to evaluate significance between selected groups. Significance was accepted at $p < 0.05$ and data were presented as mean ± SEM. All measurements were taken from distinct samples collected from individual mice.

Reporting summary. Further information on research design is available in the Nature Research Reporting Summary linked to this article.

Data availability

The BioGPS gene annotation portal using the "GeneAtlas MOE430, gcrma" dataset and 1419524_at Probeset (http://ds.biogps.org/?dataset=GSE10246&gene=21990) for the *Tph1* gene was used with a correlation cut-off of 0.95 used in Fig. 1c. Relevant data supporting the findings of this study are readily available within supplementary information files and source data. Source data can be found for Figs. 1a, b, d–f, h, j, 2b–d, f–j, 3b–k, 4a–f, h, j, Supplementary Fig. 1a–g, Supplementary Fig. 2a–k, Supplementary Fig. 3a–l, Supplementary Fig. 4a–d, f, h. Source data are provided as a Source Data File. All data contained in this study are available upon reasonable request from the corresponding author.

Received: 23 July 2019; Accepted: 16 December 2019;
Published online: 23 January 2020

References

1. Reilly, S. M. & Saltiel, A. R. Adapting to obesity with adipose tissue inflammation. *Nat. Rev. Endocrinol.* **13**, 633–643 (2017).
2. The GBD 2015 Obesity Collaborators, A. Health effects of overweight and obesity in 195 countries over 25 years. *N. Engl. J. Med.* **311**, 13–27 (2017).
3. Chouchani, E. T., Kazak, L. & Spiegelman, B. M. New advances in adaptive thermogenesis: ucp1 and beyond. *Cell Metab.* **29**, 27–37 (2018).
4. Kajimura, S., Spiegelman, B. M. & Seale, P. Review brown and beige fat: physiological roles beyond heat generation. *Cell Metab.* **22**, 546–559 (2015).
5. Kajimura, S. & Saito, M. A new era in brown adipose tissue biology: molecular control of brown fat development and energy homeostasis. *Annu. Rev. Physiol.* **76**, 225–249 (2014).
6. Shabalina, I. G. et al. UCP1 in Brite/Beige adipose tissue mitochondria is functionally thermogenic. *Cell Rep.* **5**, 1196–1203 (2013).
7. Sharp, L. Z. et al. Human BAT possesses molecular signatures that resemble beige/brite cells. *PLoS ONE* **7**, e49452 (2012).
8. Wu, J. et al. Beige adipocytes are a distinct type of thermogenic fat cell in mouse and human. *Cell* **150**, 366–376 (2012).
9. Jespersen, N. Z. et al. A classical brown adipose tissue mrna signature partly overlaps with brite in the supraclavicular region of adult humans. *Cell Metab.* **17**, 798–805 (2013).
10. Cypess, A. M. et al. Identification and importance of brown adipose tissue in adult humans. *N. Engl. J. Med.* **360**, 1509–1517 (2009).

11. van Marken Lichtenbelt, W. D. et al. Cold-activated brown adipose tissue in healthy men. *N. Engl. J. Med.* **360**, 1500–1508 (2009).
12. Leitner, B. P. et al. Mapping of human brown adipose tissue in lean and obese young men. *Proc. Natl Acad. Sci. USA* **114**, 8649–8654 (2017).
13. Crane, J. D. et al. Inhibiting peripheral serotonin synthesis reduces obesity and metabolic dysfunction by promoting brown adipose tissue thermogenesis. *Nat. Med.* **21**, 166–172 (2015).
14. Oh, C.-M. et al. Regulation of systemic energy homeostasis by serotonin in adipose tissues. *Nat. Commun.* **6**, 6794 (2015).
15. Mawe, G. M. & Hoffman, J. M. Serotonin signalling in the gut-functions, dysfunctions and therapeutic targets. *Nat. Rev. Gastroenterol. Hepatol.* **10**, 473–486 (2013).
16. Yabut, J. M. et al. Emerging roles for serotonin in regulating metabolism: new implications for an ancient molecule. *Endocr. Rev.* **40**, 1092–1107 (2019).
17. Sumara, G., Sumara, O., Kim, J. K. & Karsenty, G. Gut-derived serotonin is a multifunctional determinant to fasting adaptation. *Cell Metab.* **16**, 588–600 (2012).
18. Jeffery, E. et al. Characterization of Cre recombinase models for the study of adipose tissue. *Adipocyte* **3**, 206–211 (2014).
19. Feldmann, H. M., Golozoubova, V., Cannon, B. & Nedergaard, J. UCP1 ablation induces obesity and abolishes diet-induced thermogenesis in mice exempt from thermal stress by living at thermoneutrality. *Cell Metab.* **9**, 203–209 (2009).
20. Roh, H. C. et al. Warming induces significant reprogramming of beige, but not brown, adipocyte cellular identity. *Cell Metab.* **27**, 1121–1137.e5 (2018).
21. Wu, C. et al. BioGPS: An extensible and customizable portal for querying and organizing gene annotation resources. *Genome Biol.* **10**, (2009).
22. Kalesnikoff, J. & Galli, S. J. New developments in mast cell biology. *Nat. Immunol.* **9**, 1215–1223 (2008).
23. Liu, Q. et al. Discovery and characterization of novel tryptophan hydroxylase inhibitors that selectively inhibit serotonin synthesis in the gastrointestinal tract. *J. Pharmacol. Exp. Ther.* **325**, 47–55 (2008).
24. Hellman, B., Larsson, S. & Westman, S. Mast cell content and fatty acid metabolism in the epididymal fat pad of obese mice. *Acta Physiol. Scand.* **58**, 255–262 (1963).
25. Divoux, A. et al. Mast cells in human adipose tissue: link with morbid obesity, inflammatory status, and diabetes. *J. Clin. Endocrinol. Metab.* **97**, E1677–E1685 (2012).
26. Zhou, Y. et al. Leptin deficiency shifts mast cells toward anti-inflammatory actions and protects mice from obesity and diabetes by polarizing M2 macrophages. *Cell Metab.* **22**, 1–14 (2015).
27. Liu, J. et al. Genetic deficiency and pharmacological stabilization of mast cells reduce diet-induced obesity and diabetes in mice. *Nat. Med.* **15**, 940–945 (2009).
28. Gutierrez, D. A., Muralidhar, S., Feyerabend, T. B., Herzig, S. & Rodewald, H.-R. Hematopoietic kit deficiency, rather than lack of mast cells, protects mice from obesity and insulin resistance. *Cell Metab.* **21**, 678–691 (2015).
29. Crane, J. D., Mottillo, E. P., Farncombe, T. H., Morrison, K. M. & Steinberg, G. R. A standardized infrared imaging technique that specifically detects UCP1-mediated thermogenesis invivo. *Mol. Metab.* **3**, 490–494 (2014).
30. Zhang, X. et al. Functional inactivation of mast cells enhances subcutaneous adipose tissue browning in mice. *Cell Rep.* **28**, 792–803.e4 (2019).
31. Cano, G. et al. Anatomical substrates for the central control of sympathetic outflow to interscapular adipose tissue during cold exposure. *J. Comp. Neurol.* **460**, 303–326 (2003).
32. Madden, C. J. & Morrison, S. F. Serotonin potentiates sympathetic responses evoked by spinal NMDA. *J. Physiol.* **577**, 525–537 (2006).
33. Madden, C. J. & Morrison, S. F. Endogenous activation of spinal 5-hydroxytryptamine (5-HT) receptors contributes to the thermoregulatory activation of brown adipose tissue. *AJP Regul. Integr. Comp. Physiol.* **298**, R776–R783 (2010).
34. McGlashon, J. M. et al. Central serotonergic neurons activate and recruit thermogenic brown and beige fat and regulate glucose and lipid homeostasis. *Cell Metab.* **21**, 692–705 (2015).
35. López, M. Hypothalamic AMPK and energy balance. *Eur. J. Clin. Invest.* **48**, 1–10 (2018).
36. Mottillo, E. P. et al. Lack of adipocyte AMPK exacerbates insulin resistance and hepatic steatosis through brown and beige adipose tissue function. *Cell Metab.* **24**, 118–129 (2016).
37. Hu, F., Xu, Y. & Liu, F. Hypothalamic roles of mTOR complex I: integration of nutrient and hormone signals to regulate energy homeostasis. *Am. J. Physiol. - Endocrinol. Metab.* **310**, E994–E1002 (2016).
38. Polak, P. et al. Adipose-specific knockout of raptor results in lean mice with enhanced mitochondrial respiration. *Cell Metab.* **8**, 399–410 (2008).
39. Jung, S. M. et al. Non-canonical mTORC2 signaling regulates brown adipocyte lipid catabolism through SIRT6-FoxO1. *Mol. Cell* **75**, 807–822.e8 (2019).
40. Li, Y., Calvo, S. E., Gutman, R., Liu, J. S. & Mootha, V. K. Expansion of biological pathways based on evolutionary inference. *Cell* **158**, 213–225 (2014).
41. Ikeda, K. et al. UCP1-independent signaling involving SERCA2bmediated calcium cycling regulates beige fat thermogenesis and systemic glucose homeostasis. *Nat. Med.* **23**, 1454–1465 (2017).
42. Chen, Y. et al. Thermal stress induces glycolytic beige fat formation via a myogenic state. *Nature* **565**, 180–185 (2019).
43. Lilla, J. N. et al. Reduced mast cell and basophil numbers and function in Cpa3-Cre; Mcl-1 fl/fl mice. *Blood* **118**, 6930–6938 (2011).
44. Nowak, E. C. et al. Tryptophan hydroxylase-1 regulates immune tolerance and inflammation. *J. Exp. Med.* **209**, 2127–2135 (2012).
45. Reber, L. L., Marichal, T. & Galli, S. J. New models for analyzing mast cell functions in vivo. *Trends Immunol.* **33**, 613–625 (2012).
46. Pettersson, U. S., Waldén, T. B., Carlsson, P. O., Jansson, L. & Phillipson, M. Female mice are protected against high-fat diet induced metabolic syndrome and increase the regulatory T cell population in adipose tissue. *PLoS ONE* **7**, e46057 (2012).
47. Gaudenzio, N. et al. Analyzing the functions of mast cells in vivo using mast cell knock-in mice. *J. Vis. Exp.* **99**, 1–11 (2015).
48. Watts, S. W., Morrison, S. F., Davis, R. P. & Barman, S. M. Serotonin and blood pressure regulation. *Pharmacol. Rev.* **64**, 359–388 (2012).
49. Morecroft, I. et al. Effect of tryptophan hydroxylase 1 deficiency on the development of hypoxia-induced pulmonary hypertension. *Hypertension* **49**, 232–236 (2007).
50. Kay, J. M., Keane, P. M. & Suyama, K. L. Pulmonary hypertension induced in rats by monocrotaline and chronic hypoxia is reduced by p-chlorophenylalanine. *Respiration* **47**, 48–56 (1985).
51. Kushnir-Sukhov, N. M., Brown, J. M., Wu, Y., Kirshenbaum, A. & Metcalfe, D. D. Human mast cells are capable of serotonin synthesis and release. *J. Allergy Clin. Immunol.* **119**, 498–499 (2007).
52. Côté, F. et al. Disruption of the nonneuronal tph1 gene demonstrates the importance of peripheral serotonin in cardiac function. *Proc. Natl Acad. Sci. USA* **100**, 13525–13530 (2003).
53. Yadav, V. K. et al. Lrp5 controls bone formation by inhibiting serotonin synthesis in the duodenum. *Cell* **135**, 825–837 (2008).
54. Grimbaldeston, M. A. et al. Mast cell-deficient W-sash c-kit mutant Kit W-sh/W-sh mice as a model for investigating mast cell biology in vivo. *Am. J. Pathol.* **167**, 835–848 (2005).
55. Kimura, I., Moritani, Y. & Tanizaki, Y. Basophils in bronchial asthma with reference to reagin-type allergy. *Clin. Exp. Allergy* **3**, 195–202 (1973).
56. Wang, B. et al. Maternal retinoids increase PDGFRα+ progenitor population and beige adipogenesis in progeny by stimulating vascular development. *EBioMedicine* **18**, 288–299 (2017).
57. Folch, J., Lees, M. & Stanley, G. H. S. A simple method for the isolation and purification of total lipides from animal tissues. *J. Biol. Chem.* **226**, 497–509 (1957).

Acknowledgements

We thank Drs. Thomas Hawke and Jonathan Bramson from McMaster University for the use of microscope and flow cytometry equipment, respectively. We thank Dr. Gerard Karsenty from Columbia University for the generous gift of the Tph1 double floxed mice. This work was supported by grants from the Canadian Institutes of Health Research (201709FDN-CEBA-116200 to GRS and 144625-1 to GRS and WIK) and Diabetes Canada (DI-5-17-5302-GS to GRS). E.M.D. is a recipient of the Vanier Canada Graduate Scholarship. G.R.S. is supported by a Canada Research Chair and the J Bruce Duncan Endowed Chair in Metabolic Diseases.

Author contributions

J.M.Y., E.M.D., K.M.M., J.D.C., W.I.K. and G.R.S. designed the experiments. J.M.Y., E.M.D., E.J.C., J.M.L., B.W., E.A.D., E.D.C., W.W., and J.D.C. conducted the experiments. J.M.Y. and G.R.S. wrote the paper. Diagrams and drawn pictures on Figs. 1–3 were created by J.M.Y. on PowerPoint Office 365 and Procreate v4.3.9 for Mac iOS iPad Pro, respectively. All authors offered edits to final manuscript.

Competing interests

J.M.Y., E.M.D., E.J.C., J.M.L., B.W., E.A.D., E.D.C., W.W., J.D.C., W.I.K. declare no competing interests. K.M.M. provides advisory services to Akcea Therapeutics Canada Inc. G.R.S. has received honoraria/consulting fees from Astra Zeneca, Boehringer, Eli-Lilly, Esperion Therapeutics, Novo Nordisk, Poxel, Pfizer, Merck, Rigel Therapeutics and Terns Therapeutics. G.R.S. has received research funding from Esperion Therapeutics. G.R.S. and W.I.K. hold a patent for inhibiting peripheral serotonin for the treatment of metabolic diseases including obesity.

Additional information

Supplementary information is available for this paper at https://doi.org/10.1038/s41467-019-14080-7.

Correspondence and requests for materials should be addressed to G.R.S.

Peer review information *Nature Communications* thanks the anonymous reviewers for their contribution to the peer review of this work. Peer reviewer reports are available.

Reprints and permission information is available at http://www.nature.com/reprints

Publisher's note Springer Nature remains neutral with regard to jurisdictional claims in published maps and institutional affiliations.

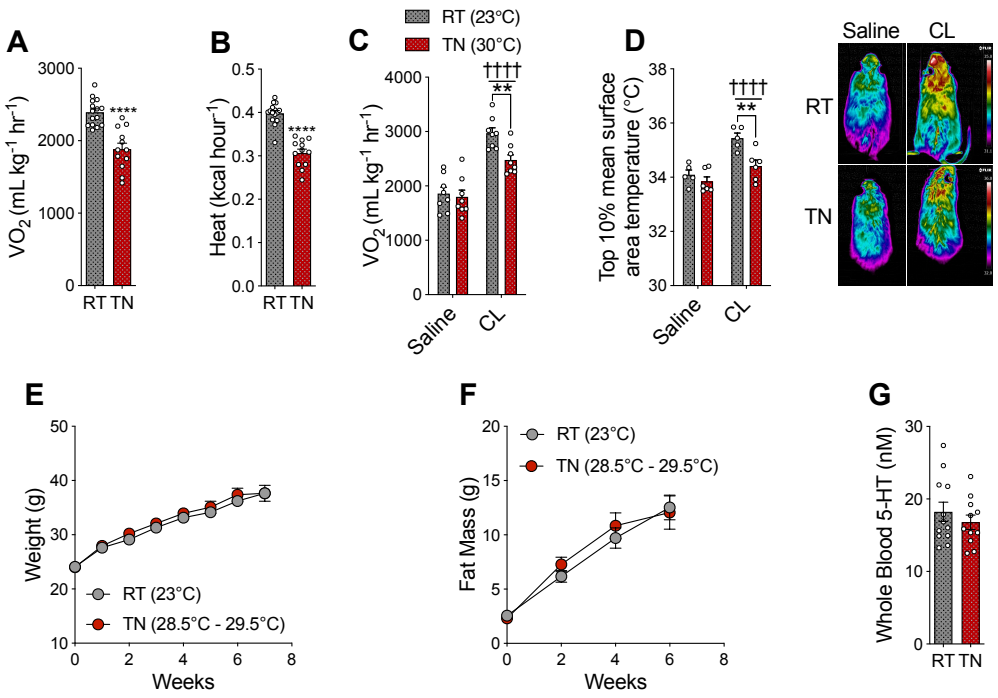

Supplementary Figure 1, Related to Figure 1: Thermoneutrality reduces BAT thermogenesis and whole body energy metabolism independent of changes in weight and circulating serotonin. (**A**) Oxygen consumption over 24h period and (**B**) Heat production over 24h period (n = 15 RT, 12 TN). (**C**) CL-induced oxygen consumption (n = 8). (**D**) CL-induced intrascapular temperature (n = 5 RT, 6 TN) with ††††p=0.0001 CL effect. (**E**) Weight gain (n = 23 RT, 11 TN) and (**F**) Fat mass (n = 12) in RT and TN housed mice over 7 weeks. (**G**) Whole blood serotonin (n = 12 RT, 11 TN) from sacrifice. Statistically significant effects (**p < 0.01, ****p < 0.0001) determined by Student's t test, two-way ANOVA with Bonferroni post-test where appropriate. All data are expressed as mean ± SEM.

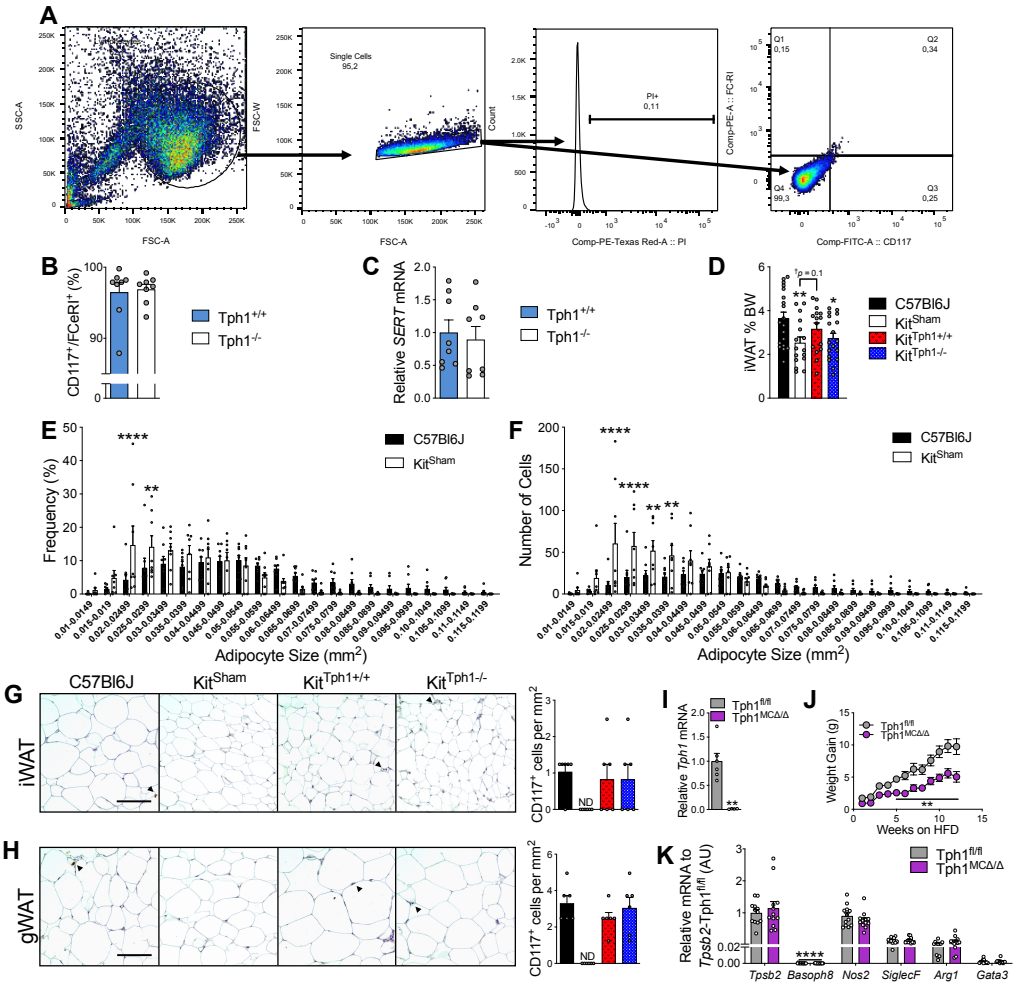

Supplementary Figure 2, Related to Figure 2 & 3: Characterization of in vitro-cultured mast cells and phenotyping of mice lacking mast cell serotonin synthesis. Gating strategy (**A**; detailed in Methods) of FACS analysis for mast cell purity ($CD117^+/Fc\varepsilon R1^+$) in $Tph1^{+/+}$ and $Tph1^{-/-}$ MCs (**B**) after 8 weeks of culture (n = 8). (**C**) Serotonin transporter (*SERT*) gene expression in $Tph1^{+/+}$ and $Tph1^{-/-}$ mast cells (n = 8). (**D**) % iWAT of body weight of C57BL6J (n = 19), Kit^{Sham} (n = 16), $Kit^{Tph+/+}$ (n = 15) and $Kit^{Tph-/-}$ (n = 18). (**E**) Frequency and (**F**) number of adipocyte sizes of C57BL6J and Kit^{sham} mice iWAT (n = 8). Representative (**G**) iWAT and (**H**) gWAT IHC images of mast cells using a $CD117^+$ antibody with respective quantification (n = 6). (**I**) *Tph1* expression in intraperitoneal lavage fluid (n = 6 $Tph1^{fl/fl}$, 4 $Tph1^{MC\Delta/\Delta}$). (**J**) Weight gain over 12 weeks (n = 12). (**K**) Gene expression of different immune cell markers implicated in influencing iWAT of $Tph1^{fl/fl}$ and $Tph1^{MC\Delta/\Delta}$ mice (n = 12). Statistically significant effects (*$p < 0.05$, **$p < 0.01$, ****$p < 0.0001$) determined by Student's t test, two-way ANOVA or two-way RM ANOVA with Bonferroni post-test where appropriate. All data are expressed as mean ± SEM.

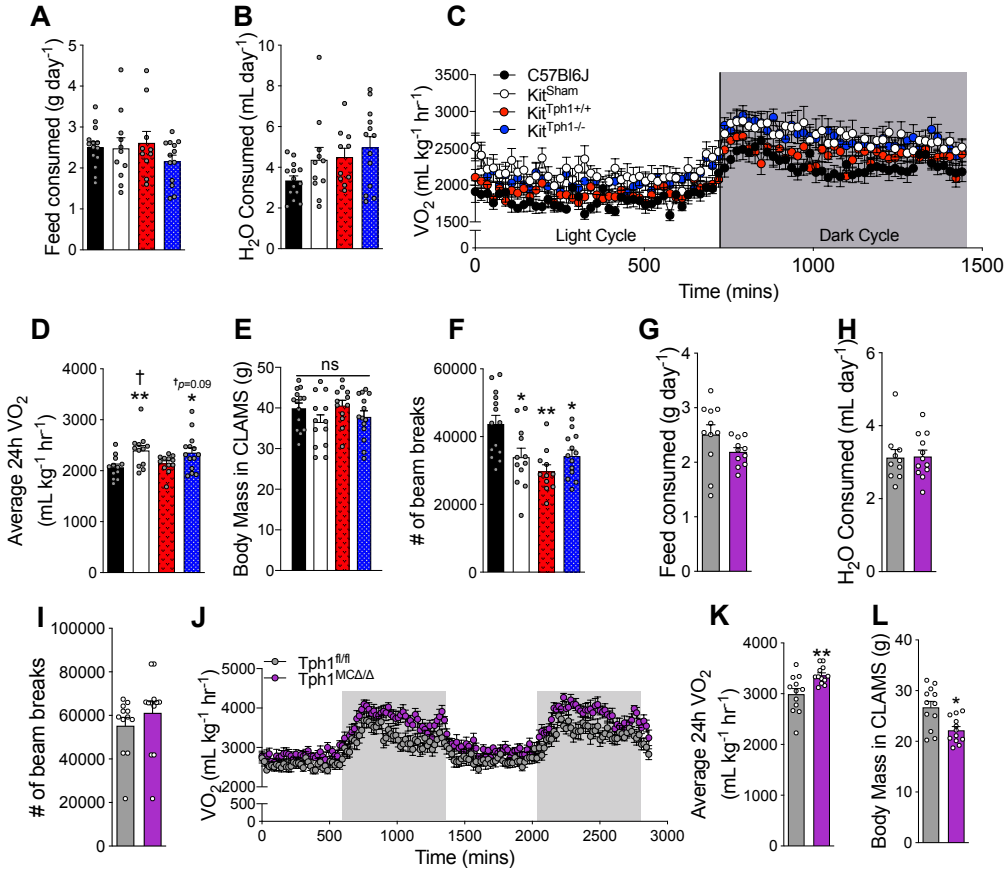

Supplementary Figure 3, Related to Figure 4: Energy balance of mouse models lacking mast cell serotonin. (**A**) Feed consumed in grams per day, (**B**) Water consumed per day, (**C**) Oxygen consumption over 24-hour period, (**D**) Average oxygen consumption over 24-hour period (**E**) Body mass of mice in CLAMS and (**F**) Activity levels as measured by beam breaks in metabolic cages over a 24-hour period of C57BL6J (n = 14), Kit^{Sham} (n = 11), $Kit^{Tph+/+}$ (n = 10) and $Kit^{Tph-/-}$ (n = 13). Statistically significant effects (*$p < 0.05$, **$p < 0.01$) of C57BL6J (*) and $Kit^{Tph1+/+}$ (†) between Kit^{Sham} and $Kit^{Tph1-/-}$ determined by one-way ANOVA with uncorrected Fisher's LSD post-test. (**G**) Feed consumed in grams per day (n = 11), (**H**) water consumed per day (n = 10 $Tph1^{fl/fl}$, 12 $Tph1^{MC\Delta/\Delta}$), (**I**) activity levels as measured by beam breaks in metabolic cages over a 24-hour period, (**J**) oxygen consumption over 48-hour period, (**K**) average oxygen consumption over 24-hour period and (**L**) body mass in clams of $Tph1^{fl/fl}$ and $Tph1^{MC\Delta/\Delta}$ mice (n = 12). Statistically significant effects (*$p < 0.05$, **$p < 0.01$) determined by Student's t test. All data are expressed as mean ± SEM.

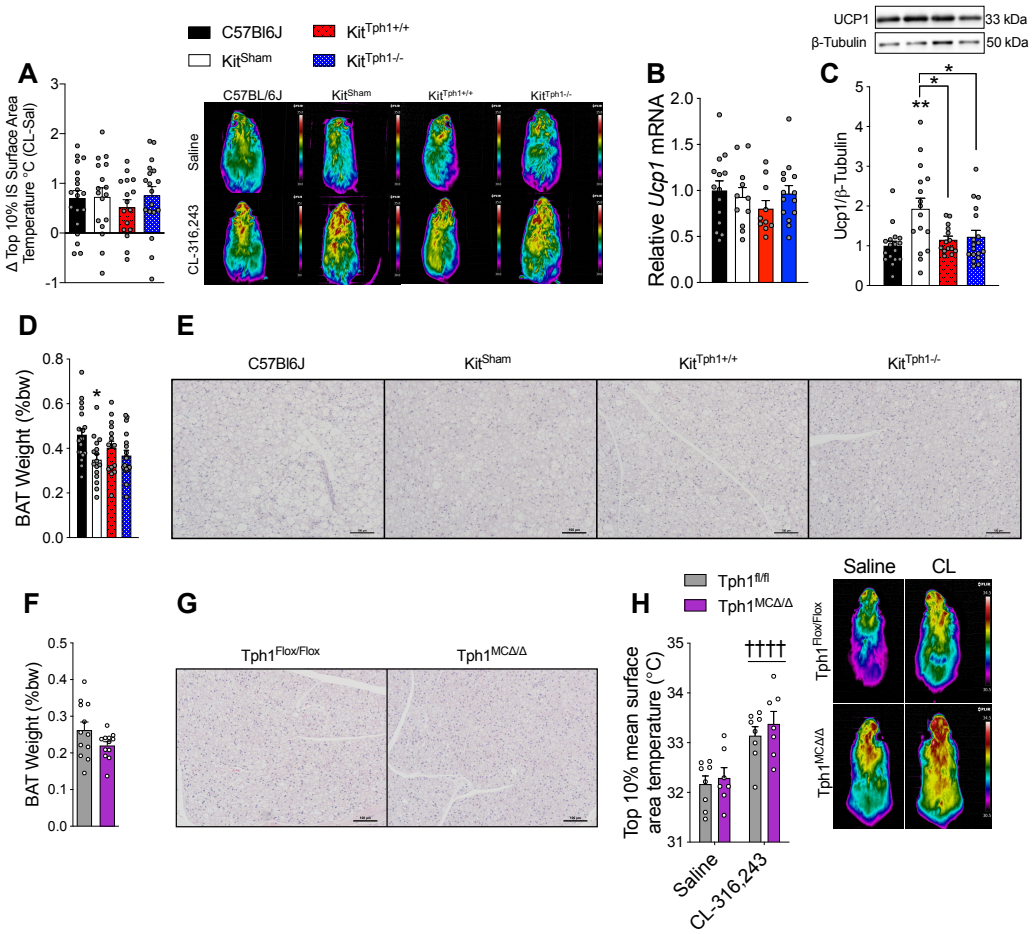

Supplementary Figure 4, Related Figure 4: Mice lacking mast cell serotonin exhibit little to no changes in BAT thermogenesis. (**A**) Delta top 10% intrascapular (IS) temperature between CL-316,243 and saline treatments with representative images in C57BL6J (n = 19), Kit^{Sham} (n = 17), $Kit^{Tph+/+}$ (n = 16) and $Kit^{Tph-/-}$ (n = 18). (**B**) *Ucp1* expression in C57BL6J (n = 14), Kit^{Sham} (n = 11), $Kit^{Tph+/+}$ (n = 10) and $Kit^{Tph-/-}$ (n = 14). (**C**) Ucp1 protein from in C57BL6J (n = 17), Kit^{Sham} (n = 18), $Kit^{Tph+/+}$ (n = 16) and $Kit^{Tph-/-}$ (n = 18). (**D**) BAT tissue weight in milligrams per gram of body weight and (**E**) Representative BAT H & E images with scale bars set at 100µm of C57BL6J (n = 19), Kit^{Sham} (n = 16), $Kit^{Tph+/+}$ (n = 15) and $Kit^{Tph-/-}$ (n = 18). Statistically significant effects (*$p < 0.05$, **$p < 0.01$) determined by one way ANOVA with uncorrected Fisher's LSD post-test. (**F**) BAT tissue weight in % body weight, (**G**) Representative BAT H & E, scale bars set to 100µm (n = 12), (**H**) Top 10% mean intrascapular surface area temperature with saline and CL-316,243 treatments (n = 8 $Tph1^{fl/fl}$, 7 $Tph1^{MCΔ/Δ}$) with representative thermal images of $Tph1^{fl/fl}$ and $Tph1^{MCΔ/Δ}$ mice. Statistically significant effects (††††$p < 0.0001$) determined by two-way ANOVA with Bonferroni post-test. All data are expressed as mean ± SEM.

SUPPLEMENTARY TABLE

Table 1: Correlations between Tph1 and mast cell-related genes (bolded) generated from BioGPS gene annotation database.

Correlation	ID	Gene Symbol	Reporter
1	21990	Tph1	1419524_at
0.9827	**14125**	**Fcer1a**	**1421775_at**
0.9812	**26945**	**Tpsg1**	**1449564_at**
0.9683	16189	Il4	1449864_at
0.9664	19270	Ptprg	1434360_s_at
0.9649	17423	Ndst2	1417931_at
0.9602	74603	Cd200r3	1453813_at
0.9601	**12873**	**Cpa3**	**1448730_at**
0.9595	**17228**	**Cma1**	**1449456_a_at**
0.9543	17082	Il1rl1	1425145_at
0.9543	14126	Ms4a2	1421475_at
0.9537	**11689**	**Alox5**	**1441962_at**
0.9513	**235854**	**Mrgpra4**	**1451926_at**
0.9512	**16590**	**Kit**	**1452511_a_at**
0.9469	225192	Hrh4	1426099_at
0.9402	14723	Gp1ba	1422316_at
0.9399	67874	Rprm	142252_at
0.9345	214084	Slc18a2	1437079_at
0.9316	27384	Akr1c13	14119672_at
0.9252	73910	Arhgap18	146952_at

CHAPTER THREE

REDUCTIONS IN ADIPOCYTE EXPRESSED TPH1 DO NOT ATTENUATE ADIPOSE TISSUE THERMOGENESIS

Prepared for Publication, 2020

Julian M. Yabut, Eric J. Chan, Eric M. Desjardins, Waliul I. Khan & Gregory R. Steinberg

The studies outlined in chapter three examined the role of adipocyte-specific deletion of Tph1. We find that adipocyte-specific Tph1 knockout mice display reduced Tph1 expression in adipocytes, but in contrast to prior findings, these mice have similar HFD-induced weight gain, insulin sensitivity, energy expenditure, BAT thermogenesis and WAT browning compared to controls. This study demonstrates that adipocyte-specific deletion of Tph1 has little effect on various metabolic parameters, further supporting the role of mast cell-derived serotonin as a critical source of serotonin reducing beige adipose tissue activity. In conjunction with the findings of chapter two, future therapies should be focused on inhibiting serotonin synthesis in mast cells rather than adipocytes.

JMY, WIK and GRS designed the study and experiments. JMY, EJC and EMD conducted the experiments. JMY and GRS wrote the paper. All authors offered edits to final manuscript.

JMY conducted all experiments and data analysis.

Reductions in adipocyte expressed tph1 do not attenuate adipose tissue thermogenesis

Julian M. Yabut[1,2], Eric J. Chan[1,3], Eric M. Desjardins[1,2], Waliul I. Khan[1,4,5], Gregory R. Steinberg[1,2,3†]

[1]Centre for Metabolism, Obesity and Diabetes Research,

[2]Division of Endocrinology and Metabolism, Department of Medicine,

[3]Department of Biochemistry and Biomedical Sciences,

[4]Farncombe Family Digestive Health Research Institute,

[5]Department of Pathology and Molecular Medicine, McMaster University, 1280 Main St. W., Hamilton, Ontario, Canada L8N 3Z5

[†]Corresponding Author, gsteinberg@mcmaster.ca

ABSTRACT

Reductions in brown and beige adipose tissue thermogenesis have been linked to the development of obesity and insulin resistance. Studies in mice have shown that serotonin synthesis by the enzyme tryptophan hydroxylase 1 (Tph1) inhibits brown and beige adipose tissue thermogenesis and promotes obesity and insulin resistance. Subsequent studies in mice in which Tph1 was genetically removed using the Ap2-Cre promoter, suggested serotonin synthesis in adipocytes may be important for suppressing adipose tissue thermogenesis. However, it is now recognized that Ap2 is expressed in adipose tissue as well as the CNS and immune cells such as macrophages, therefore the exact tissue(s) inhibiting adipose tissue thermogenesis is unknown. In order to directly examine the role of adipocyte Tph1, we created an inducible adipocyte-specific Tph1 null mouse ($Tph1^{iAd\Delta/\Delta}$) that reduced Tph1 in fractionated adipocytes. We find that $Tph1^{iAd\Delta/\Delta}$ mice had no change in Tph1 expression or serotonin content within inguinal or gonadal white adipose tissue (iWAT and gWAT) or brown adipose tissue (BAT). Consistent with similar Tph1 expression and serotonin content in adipose tissue depots there was no change in high-fat diet-induced weight gain, blood glucose, insulin sensitivity, energy expenditure, adipose tissue thermogenesis or markers of white adipose tissue browning. These data suggest that adipocyte Tph1derived serotonin synthesis is not important for inhibiting thermogenic adipose tissue or for promoting obesity and insulin resistance in mice fed a HFD. Future studies are required to identify the primary Tph1 expressing cell type(s) that inhibit BAT thermogenesis.

INTRODUCTION

Obesity is characterized by the accumulation of adipose tissue and is a global health problem that is associated with negative health consequences such as type 2 diabetes and cardiovascular disease (The GBD 2015 Obesity Collaborators, 2017). Excessive adipose tissue accumulation is due to chronic energy intake in comparison to expenditure. Therapies focused on increasing energy expenditure are promising avenues to mitigate the rise of obesity and its associated comorbidities. One potential mechanism to enhance energy expenditure in obesity involves increasing the metabolic activity of brown adipose tissue (BAT), which is reduced in obese humans for reasons that are not fully understood (Chouchani et al., 2019; Leitner et al., 2017; Ong et al., 2018).

Serotonin is a bioamine that is primarily produced outside of the central nervous system by the enzyme tryptophan hydroxylase 1 (Tph1). Studies in mice with germline deletion of Tph1 leads to reductions in serotonin and enhanced brown and beige adipose tissue-dependent thermogenesis (Crane et al., 2015; Oh et al., 2015) protecting mice from developing high-fat diet (HFD) induced obesity and insulin resistance(for review see (Yabut et al., 2019). Tph1 is highly expressed in the enterochromaffin cells of the gut and accounts for greater than 90% of whole-body serotonin synthesis (Sumara et al., 2012) (for review see (Yabut et al., 2019)). However, the gut cannot be the sole source of serotonin that improves the metabolic profile of HFD-fed Tph1 germline knockout (KO) mice, since gut-specific Tph1KO mice are not resistant to diet-induced obesity (Sumara et al., 2012). In support of

an alternative source of serotonin production that inhibits BAT thermogenesis, a HFD increases Tph1 expression in BAT and the genetic reduction of Tph1 in adipose tissue using Ap2-Cre leads to a lean and insulin sensitive phenotype similar to germline Tph1 null mice (Oh et al., 2015). However, it is now known that in addition to adipocytes, Ap2-Cre is expressed in the CNS as well as many immune cells that reside within adipose tissue (e.g. macrophages) (Jeffery et al., 2014), suggesting that adipocyte Tph1 may not be the primary inhibitor of BAT thermogenesis.

Therefore, to directly examine the role of adipose tissue Tph1 in regulating adipose tissue thermogenesis in obesity, we generated mice lacking Tph1 specifically in adipocytes by crossing Tph1 floxed mice to mice expressing an inducible adiponectin-Cre promoter. In contrast to previous observations using Ap2-Cre null mice, we find that energy expenditure, adipose tissue thermogenesis and serotonin content are similar between genotypes, suggesting that reducing adipocyte expressed Tph1 does not increase adipose tissue thermogenesis or protect mice from diet-induced obesity and insulin resistance.

METHODS

Animal Experiments

Animal experiments were completed in accordance within the Canadian and McMaster Animal Care Committee guidelines for animal research (AUP: 16-12-41). Tph1 adipocyte-specific knockout mice were generated by crossing Tph1 double floxed mice (Yadav et al., 2008) with tamoxifen-sensitive Cre Recombinase under the control of the adiponectin promoter (Mottillo et al., 2014). Mice were fed a 45% kcal from fat diet and water *ad libitum* in a room temperature (23°C) controlled facility on a 12 hour light and dark cycle starting at 0700. At 6-8 weeks of age, Cre was activated by administering tamoxifen (Cayman Chemical, MI, USA; 100mg/kg) solubilized in sterile-filtered (22 μM filter) sunflower oil for 5 consecutive days via oral gavage (Mottillo et al., 2014). After 3 weeks post-gavage of tamoxifen, mice were sacrificed to confirm deletion or placed on a HFD (D12451, Research Diets, New Brunswick, NJ). At sacrifice, platelet poor plasma (PPP) was isolated by pipetting 8μL of 0.5M EDTA into 152μL whole blood, spun at 1500g for 10 minutes and the top 25 μL removed. Liver, BAT, iWAT and gWAT were removed from all mice, weighed and stored at -80°C.

Metabolic Testing

Bimonthly body composition and weekly body weights were assessed using a Bruker minipsec Whole Body Composition Analyzer. At week 6 and 7 of HFD feeding, glucose and insulin tolerance tests were performed, respectively. Mice

were fasted during the day for 6 hours starting at 0700 and administered glucose (1g/kg) or insulin (1U/kg) with blood glucose concentrations determined using a glucometer (Aviva, Roche) at indicated time points. An overnight (1900 – 0700) fast was done on week 8 after start of HFD feeding and blood glucose concentrations were collected. On week 9, the Comprehensive Laboratory Animal Monitoring System (CLAMS; Columbus Instruments) were used to assess various metabolic and energy balance parameters (i.e. respiratory exchange ratio, energy expenditure, food and water intake) measured over a 48 hour period and averaged over the two days. On week 10, Ucp1-mediated thermogenesis was assessed using infrared imaging as described (Crane et al., 2014). Briefly, mice were anesthetized with an intraperitoneal injection of Avertin and on separate days, injected with saline or the β_3-adrenergic receptor agonist, CL-316,243 (0.0155 mg/kg, R&D Systems, Inc; Item #1499/10) to activate BAT. Oxygen consumption was recorded between 19-20 minutes post-Avertin injection and a thermal picture of the dorsal side of the mouse was taken 20 minutes post-Avertin with an infrared camera (T650sc, EMISSIVITY OF 0.98, FLiR Systems). The top 10% interscapular temperature was determined from the thermal images using AMIDE-bin 1.0.5 software.

Adipocyte Isolation

Inguinal WAT was excised from mice treated with tamoxifen 8-9 weeks prior, ensuring reductions in Tph1 were present at week 6 *in vivo* testing. Mice were

sacrificed and two iWAT pads per mouse were digested in HKRB + 4% BSA with 2 mg/mL collagenase Type II (C1764; Sigma, Canada) for 1 hour in 37°C. Resultant mixture was strained through a 100 μm strainer, solution topped up to 10mL with KHRB + 1% BSA in a 15mL tube and spun at 500rpm. Adipocyte fractions were drawn from the top of the spun samples and snap frozen at -80°C

Histological Analysis

Tissues were placed in 10% formalin in PBS for 24 hours and then placed into 70% EtOH. Paraffin embedding and Hemotoxylin and Eosin Staining was performed by the John Mayberry Histology facility at McMaster University. Slides of adipose tissues and liver were taken at 10x magnification using a light 90 Eclipse microscope (Nikon).

RNA Extraction & Real-Time quantitative PCR (RT-qPCR)

Tissues or adipocyte fractions were homogenized in 1mL Trizol (Life Technologies) and spun at 12000g for 10 minutes at 4°C. Supernatant was drawn and chloroform extraction was done. Samples are re-spun, supernatant collected and mixed 1:1 with 70% EtOH. This mixture was purified using the RNA purifying columns (RNEasy Kit, Qiagen), following manufacturer instructions. cDNA was generated by incubating purified RNA (2 ng μL^{-1}) in final concentrations of 0.5 mM dNTPs (Invitrogen) and 50 ng μL^{-1} random hexamers (Invitrogen). This mixture was heated at 65°C for 5 minutes and subsequently cooled to 4°C. SuperScript III

(50 units; Invitrogen), 5x First-Strand Buffer (Invitrogen) and DTT (final concentration of 5μM; Invitrogen) were added to the heated solution and then heated at 50°C for 1 hour. cDNA samples (duplicate, 25ng) were subjected to qPCR analysis using the Rotor-Gene 6000 real-time rotary analyzer (Corbett Life Science; Concord NSW, Australia) with TaqMan Assay Fluorogenic 5' nuclease chemistry (Invitrogen). The 10μL qPCR reaction was completed using AmpliTaq Gold DNA polymerase (Roche) as per manufacturer's instructions. Primers used include Cidea (Mm00432554_m1), Pdk4 (Mm01166879_m1), Ppia (Mm02342430_g1), Tph1 (Mm01202614_m1) and Ucp1 (Mm01244861_m1).

Liver and Serum Triglyceride and Fatty Acid Quantification

Lipids were analyzed from a sample of liver homogenized in 1 mL of 2:1 chloroform:methanol followed by mixing overnight using an adapted Folch extraction Protocol (Folch et al., 1957). Briefly, samples were spun (4500g) for 10 minutes at 4°C and 0.9% NaCl is added to the supernatant, vortexed for 20s. This mixture was spun again for 3 minutes and the clear bottom layer was drawn, placed into a new Eppendorf and freeze-dried. The resultant liquid was solubilized in 100% 2-propanol 200μL. Cayman Chemicals Triglyceride kit was used to assess the triglyceride levels of liver and serum, as per manufacturer's instructions. Non-esterified fatty acid (NEFA) concentrations were determined using a WAKO Diagnostics NEFA Reagent as per manufacturer's instructions.

Serotonin Quantification

Fat tissues were homogenized in perchloric acid (0.2N) in a homogenizer (Percellys). The supernatant was extracted and mixed with 1M borate buffer 1:1 (1M boric acid, pH was brought up to 9.25 using NaOH). Platelet poor plasma was diluted 1:10 in dilution buffer from ELISA kit (Serotonin EIA, kit Beckman Coulter, IM1749) and performed as per manufacturer instructions. Tissue homogenates are not diluted before use for ELISA kit.

Statistical Analysis

Two-tailed Student's t-test, two-way ANOVA with or without repeated measures were used where appropriate. Significance was determined if $p < 0.05$ and all data are presented as ± SEM. All sample sizes were taken from distinct samples collected from individual mice.

RESULTS

Mice with reductions in adipocyte Tph1 display no changes in adipose tissue *Tph1* expression or serotonin

A HFD has been shown to increase Tph1 expression in adipose tissue (Oh et al., 2015) therefore all experiments were conducted in mice fed a HFD. To determine the role of adipocyte Tph1, we crossed Tph1 floxed mice to mice expressing adiponectin Cre recombinase under the control of estrogen receptor T2 ($CreER^{T2}$) transgene. Cre-negative ($Tph1^{fl/fl}$) and Cre-positive ($Tph1^{iAd\Delta/\Delta}$) littermates were then treated with tamoxifen starting at 6 weeks of age for 2 weeks before starting a HFD at 8 weeks of age (Figure 1A). As anticipated adipocytes isolated from the inguinal WAT of $Tph1^{iAd\Delta/\Delta}$ mice had significantly lower expression of *Tph1* compared to $Tph1^{fl/fl}$ controls (Figure 1B). However, despite reductions in adipocyte Tph1, there was no reduction of *Tph1* (Figure 1C) in inguinal white adipose tissue (iWAT), gonadal white adipose tissue (gWAT) or brown adipose tissue (BAT) of $Tph1^{iAd\Delta/\Delta}$. Consistent with similar *Tph1* expression between genotypes, there was also no change in adipose tissue serotonin (Figure 1D) or changes in circulating platelet poor plasma (PPP) serotonin (Figure 1E). These data suggest that the primary source of serotonin in adipose tissue depots is not the adipocyte.

Mice with reductions in adipocyte Tph1 display no difference in hepatic insulin resistance

Consistent with similar Tph1 expression and serotonin in adipose tissue depots, $Tph1^{iAd\Delta/\Delta}$ mice had comparable body weight (Figure 2A), fat mass (Figure 2B) and lean mass (Figure 2C) compared to $Tph1^{fl/fl}$ controls on a HFD. Serum triglycerides were also not altered (Figure 2D). $Tph1^{iAd\Delta/\Delta}$ mice were modestly glucose intolerant compared to $Tph1^{fl/fl}$ controls (Figure 2E) but there was no change in insulin sensitivity (Figure 2F) or fasting blood glucose (Figure 2G) between genotypes. Consistent with similar insulin sensitivity, liver weight (Figure 2H), morphology (Figure 2I) and triglyceride content (Figure 2J) were not different between groups.

Mice with reductions in adipocyte Tph1 have no differences in energy expenditure or adipose tissue thermogenesis

Consistent with similar adiposity between genotypes there no changes in oxygen consumption (Figure 3A), heat production (Figure 3B), activity levels (Figure 3C) or food (Figure 3D) or water (Figure 3E) intake. There were also no differences in the respiratory quotient (VCO_2/VO_2, Figure 3F). Consistent with similar energy expenditure under ambient conditions, the injection of mice with the β_3-adrenergic receptor agonist CL-316,243, led to a similar increase in VO_2 (Figure 3G), interscapular temperature (Figure 3H) and serum free fatty acids (Figure 3I) between genotypes suggesting adipose tissue thermogenic capacity was not altered. Consistent with this idea iWAT, gWAT and BAT weights (Figure 4A-C) and morphology (Figure 4D-F) were similar between genotypes. There were also no

changes in markers of adipose tissue thermogenesis (*Ucp1, Cidea, Pdk4,* Figure 4G-I). Collectively, these data indicate that adipocyte Tph1 does not influence adipose thermogenesis.

DISCUSSION

Brown and beige adipose tissues are responsible for a small, yet potentially appreciable portion of resting energy expenditure (Leitner et al., 2017). The loss of thermogenic adipose tissue function is associated with obesity in humans (Leitner et al., 2017), suggesting restoration of its activity may be important. Reductions in peripheral serotonin due to germline deletions in Tph1 increases adipose tissue thermogenesis and subsequent studies using mice expressing Ap2-Cre suggested this may be mediated through Tph1 expression in adipocytes (Oh et al., 2015). However, we now show, using an inducible model of adipocyte Tph1 reduction, that the adipocyte is not the primary source of serotonin that reduces thermogenic adipose energy expenditure and promotes obesity and insulin resistance. These data suggest that previous observations indicating that genetic deletion of Tph1 using Ap2-Cre mice may have been due to cell types other than adipose tissue.

In the current study, we utilized Tph1 floxed mice generated by Yadav and colleagues (Yadav et al., 2008) that were also used by (Oh et al., 2015) but we did not observe the same metabolic improvements that were detected when these mice were crossed to mice expressing Ap2-Cre (Oh et al., 2015). However, it should be noted that our study differed in many ways. The first and most obvious difference was that we utilized mice expressing Cre-recombinase under the control of adiponectin, which in contrast to Ap2 is not expressed in immune cells or the CNS (Jeffery et al., 2014). Secondly, we utilized an inducible promoter in which Cre recombinase activity is activated via tamoxifen administration, achieving an

adipose-specific mouse model at a period after sexual maturity, thus avoiding potential confounding effects of serotonin deletion on adipocyte differentiation (Kinoshita et al., 2010).

Our study has several potential limitations. Since tamoxifen treatment in mice is known to induce browning (Hesselbarth et al., 2015; Zhao et al., 2020), early hepatic insulin resistance (Klöting et al., 2020) and adipogenesis (Ye et al., 2015), these factors may confound our results, however it should be noted that tamoxifen was delivered to all mice, making this less likely. Only male mice were used within this study and further studies examining the role of Tph1 in female adipocytes are warranted. A full ablation of *Tph1* in adipocytes was not achieved after tamoxifen administration, thus the lack of phenotype may have been due to residual expression. Lastly, the ubiquitous ablation of *Tph1* expression in all adipose tissue (both white and brown depots) may have masked potential effects. For example previous studies have suggested that serotonin is important for regulating lipogenesis in WAT (Oh et al., 2015). Therefore, further genetic studies that ablate Tph1 in either brown adipocytes or white adipocytes are required to elucidate the role of Tph1 in each of these individual adipocyte types.

In conclusion, we report that in contrast to mice with whole-body (Crane et al., 2015) or mast cell-specific (Yabut et al., 2020) deletions of Tph1, reductions in adipocyte Tph1 does not alter the thermogenic capacity of adipose tissue or improve metabolic homeostasis. Future studies examining the primary source of serotonin synthesis that inhibits BAT thermogenesis are required.

FIGURES

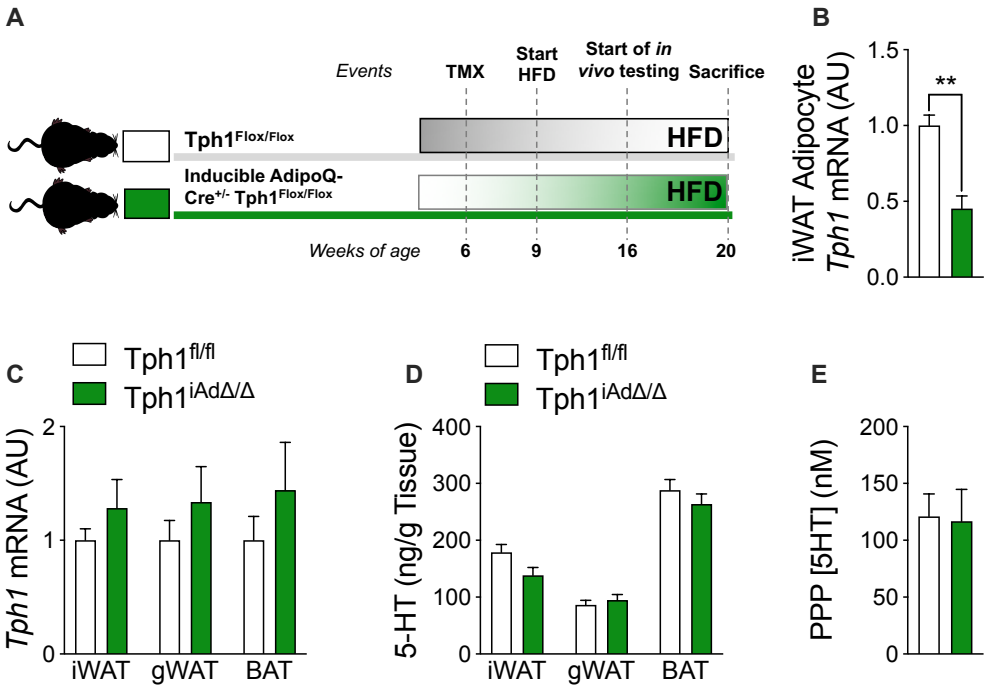

Figure 1 Reductions in adipocyte Tph1 does not change adipose tissue *Tph1* or serotonin levels. (A) *in vivo* schematic for tamoxifen gavage and HFD-feeding of $Tph1^{fl/fl}$ and $Tph1^{iAd\Delta/\Delta}$ mice. (B) Confirmation of *Tph1* deletion in inguinal WAT (iWAT) (n = 4-5). (C) *Tph1* expression (n = 6-9), and serotonin concentrations (n = 6-8) from iWAT, gWAT and BAT. (E) Platelet-poor plasma (PPP) serotonin concentration (n = 7-9). Significance denoted by $^{**}p < 0.01$. All data are expressed as mean ± SEM.

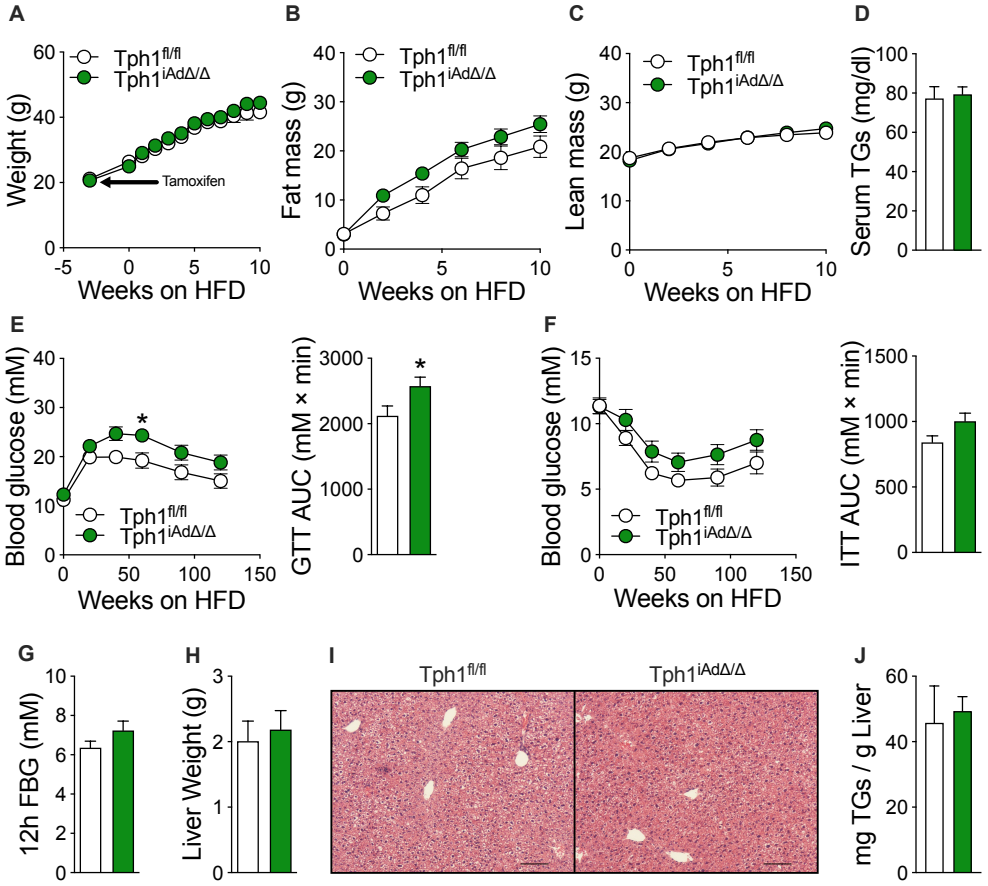

Figure 2 Reductions in adipocyte Tph1 induces modest glucose intolerance, but not hepatic insulin resistance. (A) Weight, (B) fat mass and (C) lean mass over 10 weeks of HFD feeding (n = 10-13). (D) Triglyceride (TG) concentration in serum (n = 7). (E) Glucose tolerance test (1g/kg) with area under the curve (n = 10-13), (F) Insulin tolerance test (1U/kg) with area under the curve (n = 10-13), (G) 12 hour overnight fasted blood glucose (n = 10-13), (H) liver weight at sacrifice (n = 10-13), (I) representative histology and (J) liver triglycerides (TG; n = 6-7) of HFD fed $Tph1^{fl/fl}$ and $Tph1^{iAd\Delta/\Delta}$ mice. Scale bar is equal to 100 μm. Significance denoted by $*p < 0.05$ and assessed via two-way ANOVA with repeated measures or Student's t-test. All data are expressed as mean ± SEM.

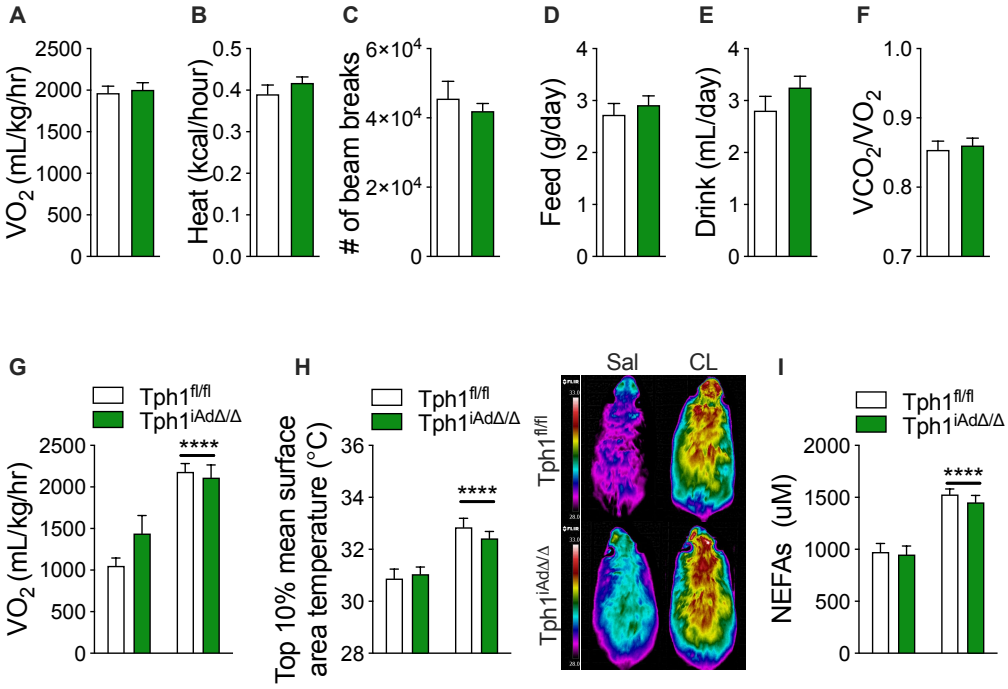

Figure 3 Reductions in adipocyte Tph1 has no effect on whole-body energy balance and BAT thermogenesis. (A) Oxygen consumption (VO_2), (B) heat emission, (C) activity, (D) food intake, (E) water intake and (F) substrate utilization of $Tph1^{fl/fl}$ and $Tph1^{iAd\Delta/\Delta}$ mice (n = 10-13). (G) Oxygen consumption, (H) top 10% mean intrascapular surface area temperature and (I) serum non-esterified fatty acid concentration with saline and CL-316,243 treatments with representative thermal images (n = 7-9). Scale bar is equal to 100 μm. Significance denoted by ****$p <$ 0.0001 and assessed via two-way ANOVA. All data are expressed as mean ± SEM.

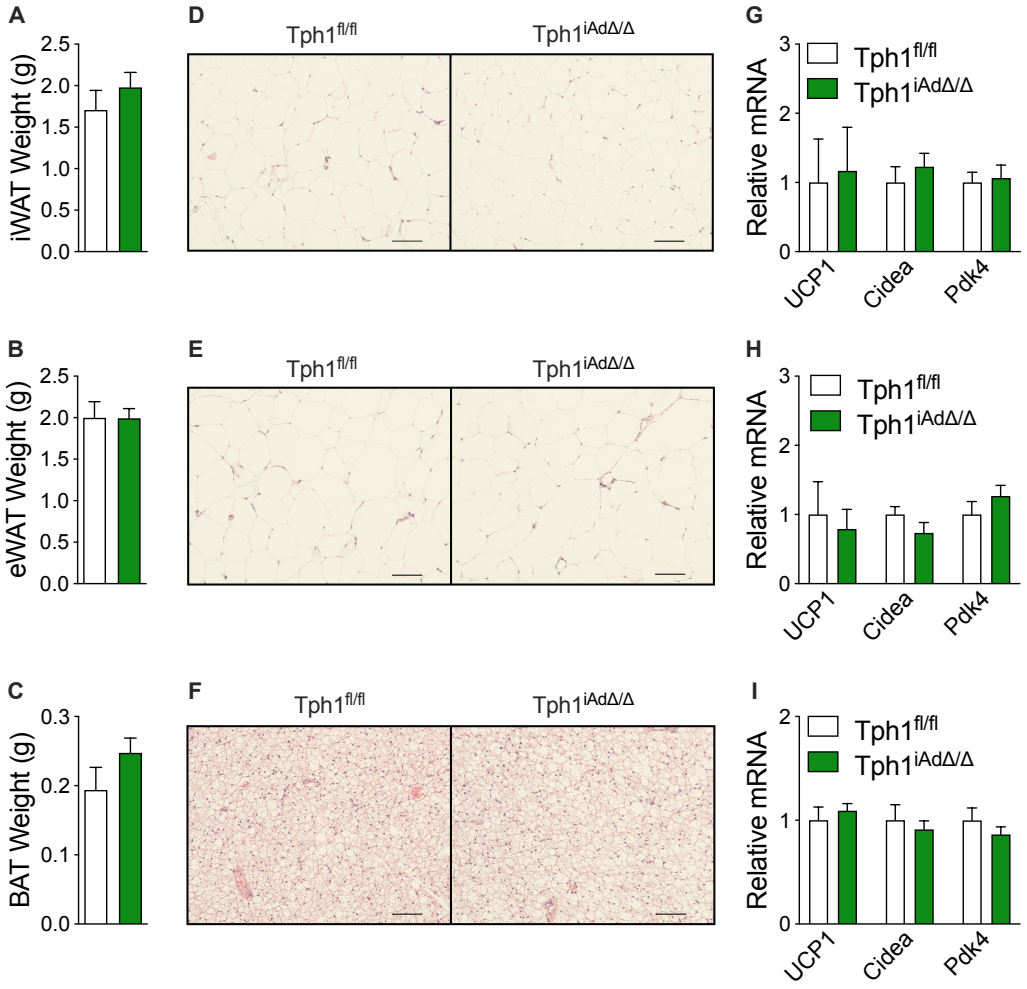

Figure 4 Reductions in adipocyte Tph1 display no changes in adipose tissue morphology or thermogenesis. Weights of (A) iWAT, (B) gWAT and (C) BAT from $Tph1^{fl/fl}$ and $Tph1^{iAd\Delta/\Delta}$ mice after sacrifice (n = 10-13). Representative histological images of (D) iWAT, (E) gWAT and (F) BAT, scale bar is equal to 100 µm (n = 10-13). Markers of adipose tissue thermogenesis in (G) iWAT (n = 7-9), (H) gWAT (n = 6-9) and (I) BAT (n = 7-9). All data are expressed as mean ± SEM.

ACKNOWLEDGEMENTS

We thank Dr. Thomas Hawke from McMaster University for the use of microscope. We thank Gerard Karsenty from Columbia University for the generous gift of the Tph1 double floxed mice. This work was supported by grants from the Canadian Institutes of Health Research (201709FDN-CEBA- 116200 to GRS and 144625-1 to GRS and WIK). EMD is a recipient of the Vanier Canada Graduate Scholarship. GRS is supported by a Canada Research Chair and the J Bruce Duncan Endowed Chair in Metabolic Diseases.

AUTHOR CONTRIBUTIONS

JMY, WIK and GRS designed the experiments. JMY, EJC and EMD, conducted the experiments. JMY and GRS wrote the paper. All authors offered edits to final manuscript.

COMPETING INTERESTS

JMY, EMD and EJC declare no competing interests. GRS has received honoraria or consulting fees from Astra Zeneca, Boehringer, Eli-Lilly, Esperion Therapeutics, Novo Nordisk, Poxel, Pfizer, Merck, Rigel Therapeutics and Terns Therapeutics. GRS has received research funding from Esperion and Espervita Therapeutics. GRS and WIK hold a patent for inhibiting peripheral serotonin for the treatment of metabolic diseases including obesity.

REFERENCES

Chouchani, E.T., Kazak, L., and Spiegelman, B.M. (2019). New Advances in Adaptive Thermogenesis: UCP1 and Beyond. Cell Metab. *29*, 27–37.

Crane, J.D., Mottillo, E.P., Farncombe, T.H., Morrison, K.M., and Steinberg, G.R. (2014). A standardized infrared imaging technique that specifically detects UCP1-mediated thermogenesis invivo. Mol. Metab. *3*, 490–494.

Crane, J.D., Palanivel, R., Mottillo, E.P., Bujak, A.L., Wang, H., Ford, R.J., Collins, A., Blümer, R.M., Fullerton, M.D., Yabut, J.M., et al. (2015). Inhibiting peripheral serotonin synthesis reduces obesity and metabolic dysfunction by promoting brown adipose tissue thermogenesis. Nat. Med. *21*, 166–172.

Folch, J., Lees, M., and Stanley, G.H.S. (1957). A simple method for the isolation and purification of total lipides from animal tissues. J. Biol. Chem. *226*, 497–509.

Hesselbarth, N., Pettinelli, C., Gericke, M., Berger, C., Kunath, A., Stumvoll, M., Blüher, M., and Klöting, N. (2015). Tamoxifen affects glucose and lipid metabolism parameters, causes browning of subcutaneous adipose tissue and transient body composition changes in C57BL/6NTac mice. Biochem. Biophys. Res. Commun. *464*, 724–729.

Jeffery, E., Berry, R., Church, C.D., Yu, S., Shook, B.A., Horsley, V., Rosen, E.D., and Rodeheffer, M.S. (2014). Characterization of Cre recombinase models for the study of adipose tissue. Adipocyte *3*, 206–211.

Kinoshita, M., Ono, K., Horie, T., Nagao, K., Nishi, H., Kuwabara, Y., Takanabe-Mori, R., Hasegawa, K., Kita, T., and Kimura, T. (2010). Regulation of Adipocyte Differentiation by Activation of Serotonin (5-HT) Receptors 5-HT 2A R and 5-HT 2C R and Involvement of MicroRNA-448-Mediated Repression of KLF5. Mol. Endocrinol. *24*, 1978–1987.

Klöting, N., Kern, M., Moruzzi, M., Stumvoll, M., and Blüher, M. (2020). Tamoxifen treatment causes early hepatic insulin resistance. Acta Diabetol. 10–13.

Leitner, B.P., Huang, S., Brychta, R.J., Duckworth, C.J., Baskin, A.S., McGehee, S., Tal, I., Dieckmann, W., Gupta, G., Kolodny, G.M., et al. (2017). Mapping of human brown adipose tissue in lean and obese young men. Proc. Natl. Acad. Sci. *114*, 8649–8654.

Mottillo, E.P., Balasubramanian, P., Lee, Y.-H., Weng, C., Kershaw, E.E., and Granneman, J.G. (2014). Coupling of lipolysis and de novo lipogenesis in brown, beige, and white adipose tissues during chronic β3-adrenergic receptor activation.

J. Lipid Res. *55*, 2276–2286.

Oh, C.-M., Namkung, J., Go, Y., Shong, K.E., Kim, K., Kim, H., Park, B.-Y., Lee, H.W., Jeon, Y.H., Song, J., et al. (2015). Regulation of systemic energy homeostasis by serotonin in adipose tissues. Nat. Commun. *6*, 6794.

Ong, F.J., Ahmed, B.A., Oreskovich, S.M., Blondin, D.P., Haq, T., Konyer, N.B., Noseworthy, M.D., Haman, F., Carpentier, A.C., Morrison, K.M., et al. (2018). Recent advances in the detection of brown adipose tissue in adult humans: A review. Clin. Sci. *132*, 1039–1054.

Sumara, G., Sumara, O., Kim, J.K., and Karsenty, G. (2012). Gut-derived serotonin is a multifunctional determinant to fasting adaptation. Cell Metab. *16*, 588–600.

The GBD 2015 Obesity Collaborators, A. (2017). Health Effects of Overweight and Obesity in 195 Countries over 25 Years. N. Engl. J. Med. *311*, 13–27.

Yabut, J.M., Crane, J.D., Green, A.E., Keating, D.J., Khan, W.I., and Steinberg, G.R. (2019). Emerging Roles for Serotonin in Regulating Metabolism: New Implications for an Ancient Molecule. Endocr. Rev. *40*, 1092–1107.

Yabut, J.M., Desjardins, E.M., Chan, E.J., Day, E.A., Leroux, J.M., Wang, B., Crane, E.D., Wong, W., Morrison, K.M., Crane, J.D., et al. (2020). Genetic deletion of mast cell serotonin synthesis prevents the development of obesity and insulin resistance. Nat. Commun. *11*, 1–11.

Yadav, V.K., Ryu, J.H., Suda, N., Tanaka, K.F., Gingrich, J.A., Schütz, G., Glorieux, F.H., Chiang, C.Y., Zajac, J.D., Insogna, K.L., et al. (2008). Lrp5 Controls Bone Formation by Inhibiting Serotonin Synthesis in the Duodenum. Cell *135*, 825–837.

Ye, R., Wang, Q.A., Tao, C., Vishvanath, L., Shao, M., McDonald, J.G., Gupta, R.K., and Scherer, P.E. (2015). Impact of tamoxifen on adipocyte lineage tracing: Inducer of adipogenesis and prolonged nuclear translocation of Cre recombinase. Mol. Metab. *4*, 771–778.

Zhao, L., Wang, B., Gomez, N.A., de Avila, J.M., Zhu, M.J., and Du, M. (2020). Even a low dose of tamoxifen profoundly induces adipose tissue browning in female mice. Int. J. Obes. *44*, 226–234.

CHAPTER FOUR

THERMONEUTRALITY PROMOTES NONALCOHOLIC FATTY LIVER DISEASE BY INCREASING CIRCULATING SEROTONIN

Prepared for Publication, 2020

Julian M. Yabut, Eric J. Chan, Eric M. Desjardins, Waliul I. Khan & Gregory R. Steinberg

The studies described in chapter four describe a new axis, identifying gut-derived serotonin as an important hormone linking thermoneutral housing to hepatic steatosis. In this manuscript, we find that obese mice housed at thermoneutrality have increased Tph1 expression in the gastrointestinal tract and this is associated with increased platelet poor plasma serotonin. Additionally, obese germline Tph1 knockout mice are not resistant to HFD-induced obesity and insulin resistance. This is associated with similar energy expenditure and no differences in BAT thermogenesis and WAT browning compared to wildtype controls. However, surprisingly, germline Tph1 knockout mice maintain modest insulin sensitivity and are protected from HFD-induced hepatic steatosis in thermoneutrality. Together, these findings suggest serotonin synthesis in the gastrointestinal tract increases at thermoneutrality and this is important for promoting hepatic steatosis; an effect that is independent of changes in energy expenditure and thermogenic adipose tissue activity. These findings suggest that gut-derived serotonin synthesis may be a potential target for treating NAFLD.

JMY, WIK and GRS designed the study and experiments. JMY, EJC and EMD conducted the experiments. JMY and GRS wrote the paper. All authors offered edits to final manuscript.

JMY conducted all experiments and data analysis.

Thermoneutrality promotes nonalcoholic fatty liver disease by increasing circulating serotonin

Julian M. Yabut[1,2], Eric J. Chan[1,3], Eric M. Desjardins[1,2], Waliul I. Khan[1,4,5], Gregory R. Steinberg[1,2,3†]

[1]Centre for Metabolism, Obesity and Diabetes Research,

[2]Division of Endocrinology and Metabolism, Department of Medicine,

[3]Department of Biochemistry and Biomedical Sciences,

[4]Farncombe Family Digestive Health Research Institute,

[5]Department of Pathology and Molecular Medicine, McMaster University, 1280 Main St. W., Hamilton, Ontario, Canada L8N 3Z5

ABSTRACT

The prevalence of non-alcoholic fatty liver disease (NAFLD) continues to grow in concert with obesity, but no pharmacotherapies exist to treat excessive hepatic lipid accumulation. A greater understanding of the molecular mechanisms that underly the progression and development of NAFLD is required to develop novel therapeutics that target hepatic steatosis. Housing mice at thermoneutrality (~30°C) accelerates the development of NAFLD independently of obesity or insulin resistance, but the mechanisms mediating this effect are incompletely understood. We and others have shown that deletion of tryptophan hydroxylase 1 (TPH1), the rate limiting enzyme that regulates peripheral serotonin synthesis, increases adipose tissue thermogenesis and prevents obesity, insulin resistance and NAFLD in mice housed at room temperature (~21°C); however, whether TPH1 is important at thermoneutrality is not known. Here, we show that thermoneutral housing increases TPH1 expression and platelet poor plasma serotonin compared to room temperature controls. Consistent with thermoneutrality blunting adipose tissue thermogenesis, whole body TPH1 knock out mice housed at thermoneutrality have no difference in high fat diet-induced weight gain, adiposity, energy expenditure, brown adipose tissue thermogenesis or white adipose tissue browning, but maintain modest improvements in insulin sensitivity compared to controls. Surprisingly, despite similar body mass, TPH1 knockout mice had reduced liver lipids and reductions in the mRNA of markers important for lipogenesis, fatty acid uptake, inflammation

and fibrosis. These data suggest that serotonin, plays a vital role in regulating liver lipid metabolism independently of adipose tissue thermogenesis.

INTRODUCTION

Non-alcoholic fatty liver disease (NAFLD) is an umbrella term for diseases involving excessive hepatic lipid accumulation and can develop into non-alcoholic steatohepatitis (NASH); an important cause of liver cirrhosis and hepatocellular carcinoma (Younossi et al., 2016). Obesity is a major risk factor for NAFLD and with the exception of weight loss, there are currently no approved therapies. Thus, a greater understanding of the mechanisms contributing to NAFLD are required to formulate new therapies to combat this prevalent disease.

Recent advances in NAFLD research has revealed environmental temperature is a critical factor that induces fatty liver in high fat diet (HFD)-fed mice (Giles et al., 2017). Mice are typically housed at temperatures suitable for human comfort (~22-23°C) and in turn, this results in a mild cold-induced stress that requires the recruitment of non-shivering thermogenesis. Brown adipose tissue (BAT) and beige adipocytes found in white adipose tissue (WAT) can generate heat in response to cold due to mitochondrial uncoupling protein 1 (Ucp1), which dissipates the proton gradient and produces heat (Chouchani and Kajimura, 2019) from lipids. However, adipose tissue thermogenesis is dramatically reduced when obese mice are placed in thermoneutrality, lowering whole-body energy expenditure and promoting ectopic lipid accumulation in metabolic tissues such as liver (Poekes et al., 2017). In addition to adipose tissue thermogenesis, the mechanisms by which thermoneutrality exacerbates HFD-induced NAFLD

development also involves alterations in the gut microbiome and increases in intestinal gut permeability and TLR4 signalling (Giles et al., 2017).

Serotonin is a monoamine hormone that regulates whole-body metabolism by inducing lipid anabolism in metabolic tissues such as adipose tissue and liver (Yabut et al., 2019). Although the liver does not synthesize serotonin itself, the gut synthesizes ~90% via tryptophan hydroxylase 1 (Tph1) and can be transported to the portal circulation to induce effects in peripheral tissues such as the liver. Recently, it was shown that gut-derived serotonin signals through the serotonin 2A receptor (HTR_{2A}) to increase hepatic steatosis (Choi et al., 2018). This data is consistent with lower hepatic lipids in high fat diet (HFD) fed $Tph1^{-/-}$ mice (Crane et al., 2015) and Tph inhibitor treated mice (Crane et al., 2015; Namkung et al., 2018). Importantly, the reduced lipid accumulation effects reported by Choi and colleagues (2019) with reductions in serotonin signaling are independent of energy expenditure from beige and brown adipose tissue (BAT), whose activity is reduced when exposed to serotonin (Crane et al., 2015; Oh et al., 2015; Rozenblit-Susan et al., 2018).

While thermoneutrality and serotonin are both factors that increase hepatic lipid accumulation in HFD-fed rodent models, it is unclear whether thermoneutrality affects gut-derived serotonin synthesis or thermogenic adipose tissue energy expenditure to increase hepatic steatosis. Here, we demonstrate that thermoneutrality increases gut Tph1 and subsequent serotonin levels to increase liver lipids and that these effects are independent of adipose tissue thermogenesis.

METHODS

Animal Housing and Breeding

All animal experiments were performed in accordance with the McMaster Animal Care Committee guidelines and conducted under the Canadian guidelines for animal research (AUP: 16-12-41). $Tph1^{-/-}$ and $Tph1^{+/+}$ littermates have been characterized previously. C57BL6J mice (Stock No: 000664) were purchased from Jackson Laboratories.

Metabolic Testing

Mice were weighed (once per week) and subject to body composition analysis (once every two weeks) in a Bruker minispec Whole Body Composition Analyzer. At 8 weeks HFD, $Tph1^{+/+}$ and $Tph1^{-/-}$ mice were subjected to a 2g/kg GTT and 0.75U/kg ITT 1 week after. Animals were fasted for 6 hours starting at 7am and basal blood glucose concentrations were measured using a glucometer (Aviva, Roche) at indicated time points. Measurements of metabolic parameters (respiratory exchange ratio, energy expenditure, activity, food and water intake) were assessed using a Comprehensive Laboratory Animal Monitoring System (CLAMS; Columbus Instruments) over a 48-hour period. For 12 hour fasting blood glucose values, mice were fasted from 7pm to 7am at which glucose values were taken via tail bleed.

Infrared Imaging of Ucp1-mediated Thermogenesis

An infrared imaging technique extensively described (Crane et al., 2014). Mice are anesthetized with Avertin and 2 minutes after are injected with either saline or CL-316,243 (on two separate days). Average oxygen consumption with an indirect calorimetry system (Columbus Instruments, Columbus, OH) from minutes 19-20 post-Avertin injection and the top 10% interscapular dorsal temperature is determined by a thermal image taken 20 minute post-Avertin (T650sc, emissivity of 0.98, FLiR Systems).

Animal experiments

All mice were housed in a temperature controlled facility (22-23°C for RT or 29-30°C for TN experiments) on a 12-hour light and dark cycle with food and water provided *ad libitum*. C57BL6/J and $Tph^{-/-}$ mice were fed 60% and 45% HFD, respectively, starting at 8 weeks of age and remained in room temperature or moved to thermoneutrality. After sacrifice via cervical dislocation, liver, iWAT, gWAT and BAT from all mice were weighed and other samples were kept at -80°C.

Whole blood and Platelet poor plasma collection

Whole blood serotonin samples were collected by mixing 30 μL of whole blood with 270 μL of 0.5M TCA/0.05M sodium ascorbate. This is followed by a 1500g spin for 10 minutes at 4°C and supernatant removed. TCA was extracted using water-saturated ethyl ether, anhydrous (5 parts ether, 1 part sample) with mixing and subsequent removal of top ether layer. TCA extraction is repeated twice

and remaining ether is boiled off at 70°C. Platelet poor plasma (PPP) was extracted by pipetting 152uL of fresh serum into 8uL of 0.5M EDTA, spun at 4000 rpm and top 20uL of plasma removed. All samples were frozen at -80°C.

Liver Triglycerides Quantification

Lipids were extracted from liver, homogenized in 1 mL of 2:1 chloroform:methanol and isolation carried out using an adapted Folch extraction. Resultant samples were freeze-dried and solubilized in 100% 2-propanol. The Caymen Chemicals Triglyceride kit was used to assess triglyceride levels as directed by manufacturer instructions.

Insulin and Serotonin ELISAs

Ultra Sensitive mouse Insulin ELISA Kit (Crystal Chem; 90080) was used to assess insulin levels of serum taken from sacrifice as per manufacturer instructions. Serotonin concentrations of whole blood and PPP were determined by a serotonin ELISA kit as per manufacturer instructions (Serotonin EIA kit Beckman Coulter; IM1749).

Histological Analysis

Tissues were immersed in 10% formalin, 90% PBS for 1 day and placed into 70% EtOH for paraffin embedding. Briefly, H&E slides were taken at 10x magnification. Images were captured with a light 90 Eclipse microscope (Nikon).

RNA Extraction

Tissue samples (50mg gWAT, iWAT, BAT) are homogenized in 1mL of Trizol reagent (Life Technologies). Samples are spun for 10 minutes at 12000g in 4°C, supernatant drawn. 200 µl of chloroform is mixed and subsequently shaken for 15s, followed by 2 minutes of room temperature incubation. Samples are spun and supernatant is collected. A 1:1 mixture of the sample to 70% EtOH was put into a RNA purifying column (RNEasy Kit; Qiagen) and followed manufacturer instructions. To reverse transcribe to cDNA, RNA (2 ng μL^{-1}) was placed in final concentrations of 0.5 mM dNTPs (Invitrogen) and 50 ng μL^{-1} random hexamers (Invitrogen). This solution was heated at 65 °C for 5 minutes and cooled to 4 °C. A mixture containing 50 units of SuperScript III (Invitrogen), 5x First-Strand Buffer (Invitrogen) and DTT (final concentration of 5 µM; Invitrogen) was added to the heated solution. The final mixture was held at room temperature (RT) for 5 minutes and subsequently, 50 °C for 1 hour.

Real-Time quantitative PCR (RT-qPCR)

Duplicate 25-ng cDNA samples were subjected to qPCR analysis using Rotor-Gene 6000 real-time rotary analyzer (Corbett Life Science; Concord NSW, Australia) with TaqMan Assay fluorogenic 5'nuclease chemistry (Invitrogen) as the flurophore. Final concentrations for a 10-µL qPCR reaction with 25-ng of loaded cDNA include 0.25 U of AmpliTaq Gold DNA polymerase (Roche), 1.25

mM $MgCl_2$ (Roche), 100 μM dNTPs and 10x PCR buffer (Roche). Briefly, the samples are heated at 95 °C for 10 minutes. Samples are then subject to being heated at 95 °C for 10 seconds and then 58 °C for 45 seconds for a total of 45 cycles. Expression levels were normalized to that of peptidylprolyl isomerase A (PPIA) for tissues or Polr2a for cells mRNA using the delta-delta CT method ($2^{-\Delta\Delta CT}$). Gene expression data were gathered from various tissues. Acaca (Mm01304257_m1), Acly (Mm01302282_m1), Acta2 (Mm00725412_s1), Ccl2 (Mm00441242_m1), Cd36 (Mm00432403_m1), Cd68 (Mm00839636_g1), Cidea (Mm00432554_m1), Col1a1 (Mm00801666_g1), Col4a1 (Mm01210125_m1), F480 (Adgre1; Mm00802529_m1), Fasn (Mm00662319_m1), Hadh (Mm00492535_m1), Mcp1 (Mm00441242_m1), Nos2 (Mm00440502_m1), Pdk4 (Mm01166879_m1), Pparg (Mm00440940_m1), Ppia (Mm02342430_g1), Srebp1 (Srebf; Mm00550338_m1), Tnf (Mm00443258_m1), Tph1 (Mm00493794_m1), Tph2 (Mm00557715_m1) and ucp1 (Mm01244861_m1) from Life technologies were used.

Immunoblotting Analysis

Tissues were placed in lysis buffer (20 mM Tris, 150 mM NaCl, 1mM EDTA, 1 mM EGTA, 1% Triton-X, 2.5 mM sodium pyrophosphate, 0.5 mM DTT, 0.1% SDS, 1% Roche Protease Inhibitor, 0.5% sodium deoxycholate) and subsequently processed in a tissue homogenizer (Percellys). Samples were spun to extract supernatant and protein quantification was performed using the bicinchonininc acid (BCA) method (Pierce) as per manufacturer instructions. For

UCP1 and β-tubulin protein analysis in BAT and for Tph1 and β-actin in colon, lysates were diluted with 4x standard buffer (50% Sucrose, 7.5% SDS, 3.1% DTT) and loaded in Sodium dodecyl sulfate-polyacrylamide gel electrophoresis (SDS-PAGE) was performed using 10% or 12% gels. A Western Blotting apparatus (Bio-Rad) with electrophoresis buffer containing 12.5 mM Tris, 125 mM Glycine, 0.05% SDS. About 20 ug of sample was dispensed into wells along with Precision Plus Protein Dual Colour Standard (Bio-Rad). A wet transfer using a gel to membrane blotter apparatus (BioRad) of PVDF membranes, 90V for 90 minutes. Membranes were blocked with 5% skim milk in Tris-buffered saline (50 mM Tris-HCl, 150 mM NaCl) with Tween 20 (TBST) for 1 hour. Subsequently, membranes were subject to primary antibody (1:1000 dilution) in TBST + 5% BSA overnight at 4°C. Unless otherwise stated, all antibodies were from Cell Signaling. Antibodies used were Anti-Mouse UCP1 (Alpha Diagnostics, 173435A4), anti-mouse β-tubulin (Invitrogen, 322600), Tph1 (NEB, 12339S) and β-actin (NEB, 5125S). Membranes were rinsed in TBST and incubated in secondary antibody (1:10000 dilution in TBST + 5% BSA; Anti-mouse, 7076S; Anti-rabbit, 7074S) for 1 hour. SuperSignal West Femto Maximum Sensitivity Substrate (Thermo Scientific) and a Fusion FX7 Chemiluminescence Visualizer (MBI) were used for detection. Densitometry analysis was performed using an ImageJ 3 analyzer.

Statistical Analysis

Data were evaluated by Student's t-test, one-way ANOVA where appropriate followed by a Tukey Multiple comparisons test. A repeated measures ANOVA was used for body weights and composition plots, GTT and ITT data. Significance was accepted at $p < 0.05$ and data were presented as mean ± SEM.

RESULTS

Tph1 and serotonin synthesis from the gut is altered by housing temperature

To investigate whether serotonin might contribute to increased liver lipid accumulation in mice house at TN, we assessed Tph1 levels in the colon and proximal small intestine of obese mice housed at room temperature (RT) or thermoneutrality (TN) (Figure 1A). *Tph1* mRNA (Figure 1B) and protein (Figure 1C) expression were increased in the colon of TN mice. There was no change in *Tph2* (Figure 1D). Similar observations in *Tph1* and *Tph2* expression were observed in proximal small intestine (SI) segments (Figure 1E-F). Importantly, these increases in Tph1 mirrored elevations in platelet poor plasma (PPP) serotonin (Figure 1G), the non-platelet bound fraction known to be available for import and signalling in peripheral tissues (Yabut et al., 2019).

Since Tph1 activity is increased with TN, we tested if Tph1 expression might be reduced with cold exposure. We found that housing HFD-fed mice at 4°C for 48 hours (Figure 1H) lowered Tph1 mRNA (Figure 1I) and protein levels (Figure 1J). The reduction in Tph1 was associated with a trend for lower PPP serotonin (Figure 1K). These data indicate that Tph1 expression in the gut is regulated by changes in housing temperature.

Thermoneutrality abolishes differences in weight gain and energy expenditure of obese Tph1 knockout mice

Tph1$^{-/-}$ mice housed at RT have profound reductions in peripheral serotonin synthesis from the gut and resulting circulating serotonin (Côté et al., 2003). In RT, mice lacking a germline deletion of Tph1 are resistant to HFD-induced obesity, insulin resistance and NAFLD compared to Tph1$^{+/+}$ controls due to elevated Ucp1-mediated BAT thermogenesis and WAT browning (Crane et al., 2015; Oh et al., 2015). To discern whether these metabolic improvements are dependent on thermogenic adipose tissue, we placed Tph1$^{-/-}$ mice and Tph1$^{+/+}$ littermates in TN, an environmental condition that is known to blunt BAT thermogenesis and WAT browning (Feldmann et al., 2009; Roh et al., 2018). Consistent with findings at RT, whole blood and PPP serotonin were reduced in Tph1$^{-/-}$ mice housed at TN (Figure 2A). However, in contrast to our previous findings (Crane et al., 2015), placing Tph1$^{-/-}$ mice at TN abolished protection from HFD-induced elevations in body weight (Figure 2B) and fat mass (Figure 2C) compared to Tph1$^{+/+}$ controls. Consistent with similar adiposity, energy expenditure (Figure 2D), heat emission (Figure 2E), substrate utilization (Figure 2F), activity levels (Figure 2G), food (Figure 2H) and water intake (Figure 2I) was comparable between Tph1$^{-/-}$ mice and Tph1$^{+/+}$ littermate controls. These data support previous conclusions that Tph1 primarily regulates body mass, adiposity and energy expenditure.

Tph1 knockout mice have similar BAT-dependent thermogenesis and energy expenditure in thermoneutrality

Since Tph1$^{-/-}$ mice housed in TN did not display protection from weight gain, we assessed whether TN blunts Ucp1-mediated thermogenesis of the BAT of Tph1$^{-/-}$ mice. Using an infrared thermography assay (Crane et al., 2014), we observed no changes in Ucp1-dependent oxygen consumption (Figure 3A) or interscapular surface temperatures (Figure 3B) in Tph1$^{-/-}$ mice compared to Tph1$^{+/+}$ littermates following the injection of saline and a β_3-adrenergic receptor agonist, CL-316,243. The fat pad weight (Figure 3C), morphology (Figure 3D), TG content (Figure 3E) and Ucp1 protein (Figure 3F) were also not different between Tph1$^{-/-}$ mice and Tph1$^{+/+}$ littermates. These data suggest that TN housing eliminates genotypic differences of Tph1$^{+/+}$ and Tph1$^{-/-}$ mice BAT thermogenesis.

Tph1 knockout mice display no differences in WAT browning in thermoneutrality

In addition to BAT thermogenesis, TN can blunt the browning program and energy expenditure of WAT (Roh et al., 2018) that is employed to protect mice from cold stress that is induced by RT housing (Giles et al., 2017). Since Tph1$^{-/-}$ mice and Tph1 inhibitor-treated mice display improved beige adipose tissue activity (Crane et al., 2015; Oh et al., 2015), we examined the subcutaneous inguinal (iWAT) and visceral gonadal WAT (gWAT) of Tph1$^{-/-}$ mice in TN. Tph1$^{-/-}$ mice and Tph1$^{+/+}$ littermates had comparable iWAT fat pad weight (Figure 4A), morphology (Figure 4B) and markers of browning (Figure 4C) compared to Tph1$^{+/+}$ TN housed mice. Similar findings were observed in gWAT (Figure 4D-F).

Furthermore, gWAT displayed similar levels of inflammatory markers (Figure 4G). Collectively, TN housing abolishes elevated BAT thermogenesis and WAT browning of Tph1$^{-/-}$ mice, suggesting protection from obesity is dependent on thermogenic adipose tissue increases in energy expenditure.

Tph1 knockout mice maintain modest improvements in glucose handling in thermoneutrality

HFD-fed Tph1$^{-/-}$ mice have superior glucose tolerance and insulin sensitivity compared to controls (Crane et al., 2015). Since these metabolic benefits were attributed to elevated BAT energy expenditure, we assessed the glucose tolerance and insulin sensitivity of HFD-fed Tph1$^{-/-}$ mice housed in TN. Despite similar body mass and adiposity and adipose tissue energy expenditure, when housed at TN, Tph1$^{-/-}$ mice maintained modest improvements in glucose tolerance (Figure 5A) and insulin sensitivity (Figure 5B). These data suggest that Tph1$^{-/-}$ mice have improved insulin sensitivity independent of changes in body mass or energy expenditure.

Tph1 knockout mice are protected from hepatic lipid accretion in thermoneutrality

Increases in liver lipids can contribute to insulin resistance (Samuel and Shulman, 2016). When we assessed the livers of TN Tph1$^{-/-}$ mice, they tended to have lower liver weights (Figure 5C) and histological examination demonstrated

less hepatic lipids (Figure 5D) and triglycerides (Figure 5E). To examine potential mechanisms mediating these effects we measured markers of lipogenesis, fatty acid uptake, fatty acid oxidation and found that they were reduced in $Tph1^{-/-}$ mice (Figure 5F). We then assessed markers of inflammation (Figure 5G) and fibrosis (Figure 5H) and found that they were also lower in $Tph1^{-/-}$ mice. Collectively, this data suggests that even in the absence of differences in body mass and adiposity, $Tph1^{-/-}$ mice housed in thermoneutral conditions are protected from HFD-induced NAFLD.

DISCUSSION

Serotonin is a hormonal signal that promotes anabolic processes (Yabut et al., 2019). In room temperature housing, obese Tph1$^{-/-}$ mice have increased thermogenic adipose tissue energy expenditure, protecting mice from obesity, insulin resistance and NAFLD (Crane et al., 2015; Oh et al., 2015). Placing mice at TN reduces adipocyte thermogenesis and promotes NAFLD (Roh et al., 2018). To examine whether thermogenic adipose tissue-dependent was required for lowering liver lipids, we placed Tph1$^{-/-}$ mice at TN and discovered that Tph1$^{-/-}$ mice maintained modest improvements in insulin sensitivity and lower liver lipids despite similar adiposity. These data suggest that improvements in NAFLD and insulin sensitivity previously described in Tph1$^{-/-}$ mice (Crane et al., 2015) is independent of increases in adipose tissue thermogenesis.

In our study, thermoneutrality was a sufficient stimulus to abolish the elevations in Ucp1-mediated thermogenesis in HFD-fed Tph1$^{-/-}$ mice (Crane et al., 2015). This is further supported by comparable levels of energy expenditure, markers of adipocyte thermogenesis and adipocyte cell size in Tph1$^{-/-}$ mice and wild type littermates. In contrast to our previous findings in room temperature where Tph1$^{-/-}$ mice are protected from obesity (Crane et al., 2015), our current findings are associated with no improvements in weight loss. These data suggest that the improvements in adipose thermogenesis due to germline Tph1 deletion in room temperature conditions is nullified by placing mice in thermoneutrality. Further,

these data uncouple the beneficial metabolic effects of thermogenic adipose tissue from improvements in hepatic steatosis in Tph1$^{-/-}$ mice.

In addition to effects on adipose tissue, recent studies have linked peripheral serotonin with liver lipid accumulation (Choi et al., 2018; Namkung et al., 2018). Genetic ablation of gut Tph1 — thereby reducing gut-derived serotonin synthesis — reduces lipid accumulation in the livers of HFD-fed mice independent of changes in BAT Ucp1 protein expression (Choi et al., 2018). Similarly, housing mice at TN eliminates genotypic differences in adipose tissue Ucp1 expression, which is elevated in Tph1$^{-/-}$ mice at room temperature (Crane et al., 2015). Despite no difference in Ucp1-mediated thermogenesis in thermoneutral-housed Tph1$^{-/-}$ mice, the reduction in liver lipids persisted when the mice were fed a HFD. This was a surprising result since the reduction in liver lipids in our previous study was attributed to increases in adipose tissue thermogenesis. The lack of hepatic steatosis in Tph1$^{-/-}$ mice may also explain the improvements in insulin sensitivity. These data suggest that serotonin is a key hormone that regulates temperature-dependent hepatic steatosis. Future experiments that employ gut-specific Tph1$^{-/-}$ mice under different temperature environments (i.e. cold, room temperature and thermoneutrality) are required to understand whether housing temperature induces gut-derived serotonin synthesis and drives hepatic steatosis.

Collectively, these data in combination with observations from other groups suggest that peripheral serotonin synthesis may act directly on the liver to promote lipid accumulation. We speculate that temperature-dependent changes in gut

serotonin synthesis may be the key hormone switch that induces hepatic steatosis in HFD challenged models. Further mouse models that utilize tissue-specific Tph1 ablation and serotonin receptor knockout mice will be important to elucidate the underlying mechanisms that promote hepatic insulin resistance and NAFLD.

FIGURES

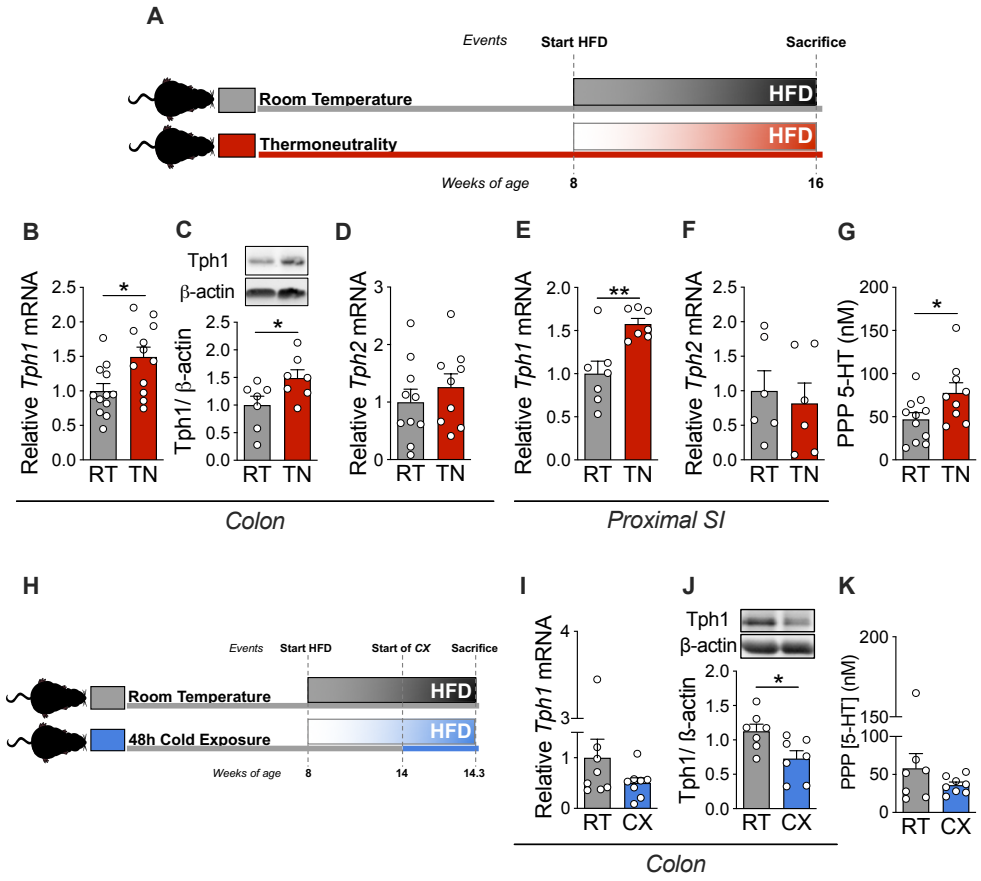

Figure 1 Temperature conditions positively correlates with Tph1 expression and serotonin in HFD-fed mice. (A) 8 week old mice were administered HFD and kept in room temperature (RT) or thermoneutrality (TN) for 8 weeks and sacrificed. (B) *Tph1* (n = 12) and (C) protein expression (n = 7) and (D) *Tph2* expression (9-10) in whole colon. (E) *Tph1* (n = 7) and (F) *Tph2* expression (n = 6) in proximal small intestine (SI). (G) Serotonin concentration in platelet-poor plasma (PPP; n = 9-11). (H) After 6 weeks of HFD feeding, mice either remained in RT or 48 hours of cold exposure (CX). (I) Tph1 gene (n = 8) and (J) protein expression (n = 7) in whole colon and platelet-poor plasma (PPP; n = 7-8) of RT or CX mice. Significance denoted by $*p < 0.05$, $**p < 0.01$ and assessed Student's t-test. All data are expressed as mean ± SEM.

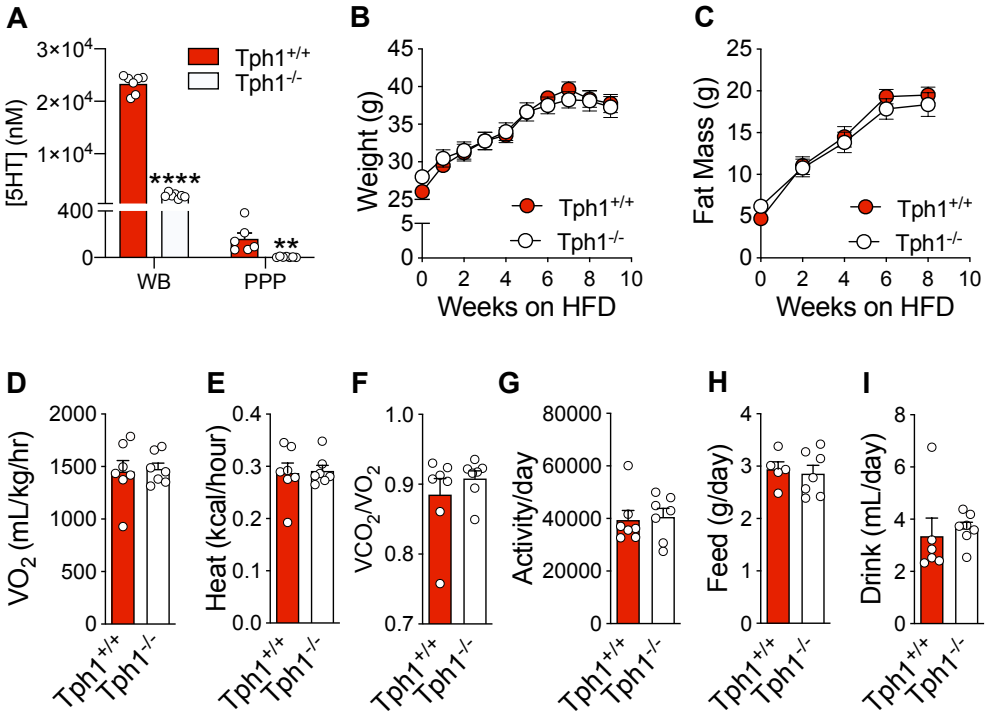

Figure 2 Thermoneutrality abolishes differences in weight gain, adiposity in obese Tph1 knockout mice. (A) Serotonin concentration of whole blood (WB) serum and platelet-poor plasma (n = 6-7; PPP). (B) Weight (n = 8) and (C) fat mass (n = 8) gained after 9 weeks of HFD feeding. (D) Oxygen consumption (n = 7), (E) heat emission (n = 7), (F) substrate utilization (n = 7), (G) activity (n = 7), (H) food (n = 5-7) and (I) drink intake (n = 6-7) after 8 weeks of high fat diet feeding. Significance denoted by $^{**}p < 0.01$, $^{****}p < 0.0001$ and assessed via Student's t-test. All data are expressed as mean ± SEM.

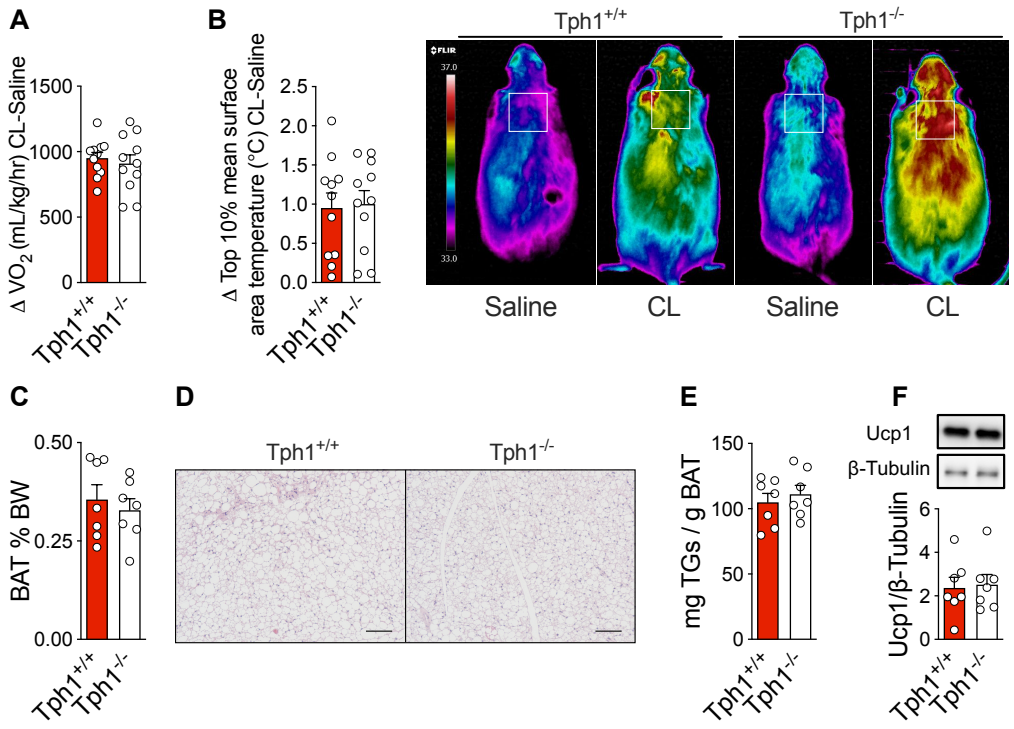

Figure 3 Tph1 knockout mice have similar BAT-dependent thermogenesis compared to controls in thermoneutral conditions. (A) Change in oxygen consumption (n = 11) and (B) top 10% mean surface area temperature (n = 11) with representative picture after two separate days of either saline or CL-316, 243 intra-mouse. (C) Weight (n = 7), (D) representative histology, (E) triglyceride (TG) content (n = 7) and (F) uncoupling protein 1 protein (n = 7) of brown adipose tissue (BAT). Scale bar is equal to 100 μm. All data are expressed as mean ± SEM.

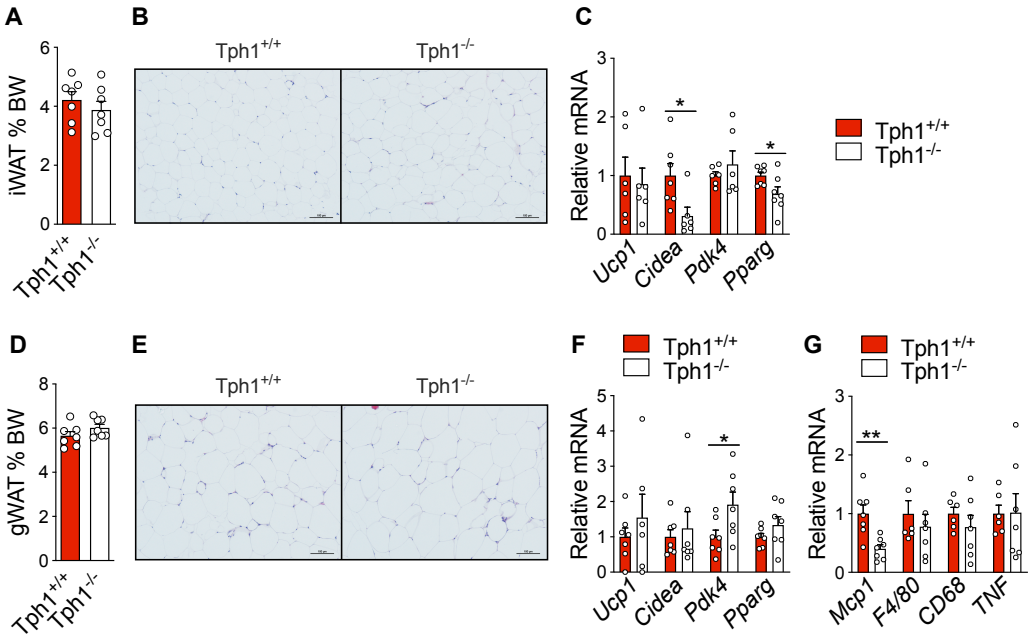

Fiure 4 Tph1 knockout mice have similar WAT browning compared to controls in thermoneutral conditions. (A) Weight (n = 7), (B) representative histology and (C) markers of browning (n = 6-7) in inguinal WAT (iWAT). (D) Weight (n = 7), (E) representative histology, (F) markers of browning (n = 6-7) and (G) inflammation (n = 6-7) in gonadal WAT (GWAT). Scale bar is equal to 100 µm. Significance denoted by *$p < 0.05$, **$p < 0.01$ and assessed Student's t-test. All data are expressed as mean ± SEM.

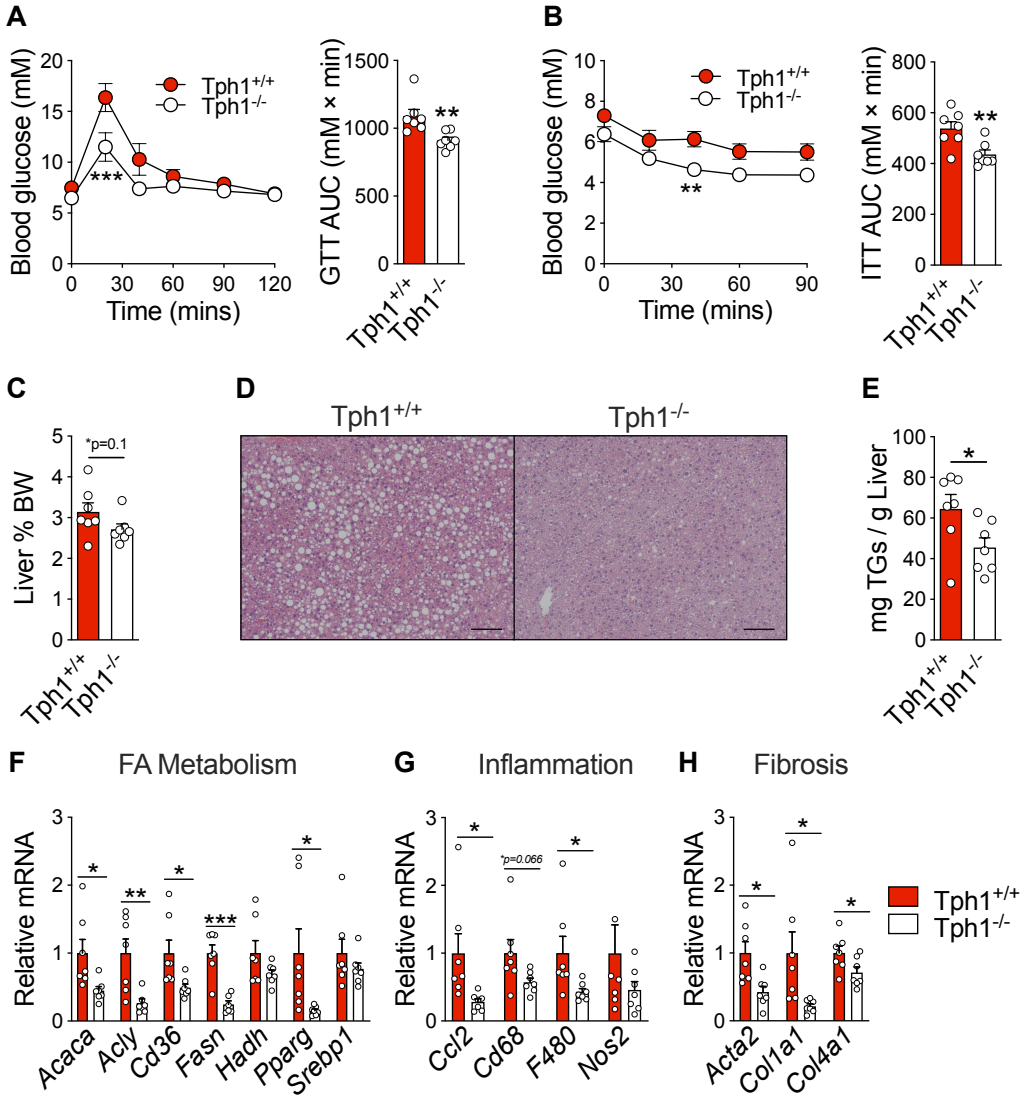

Figure 5 Tph1 knockout mice maintain insulin sensitivity, are protected from hepatic steatosis and display lower markers of NAFLD in thermoneutrality. (A) Glucose tolerance test (GTT; 2g/kg) and (B) insulin tolerance test (ITT; 0.75u/kg) (n = 7). (C) Weight (n = 7), (D) representative histology, (E) triglyceride (TG; n = 7), (F) fatty acid metabolism markers (n = 6-7), (G) inflammatory markers (n = 7), (H) fibrosis markers (n = 7). Scale bar is equal to 100 µm. Significance denoted by $*p < 0.05$, $**p < 0.01$, $***p < 0.001$ and assessed via Two-way ANOVA with repeated measures or Student's t-test were applicable. All data are expressed as mean ± SEM.

ACKNOWLEDGEMENTS

We thank Dr. Thomas Hawke from McMaster University for the use of microscope. This work was supported by grants from the Canadian Institutes of Health Research (201709FDN-CEBA- 116200 to GRS and 144625-1 to GRS and WIK). EMD is a recipient of the Vanier Canada Graduate Scholarship. GRS is supported by a Canada Research Chair and the J Bruce Duncan Endowed Chair in Metabolic Diseases.

AUTHOR CONTRIBUTIONS

JMY, WIK and GRS designed the experiments. JMY, EJC and EMD, conducted the experiments. JMY and GRS wrote the paper. All authors offered edits to final manuscript.

COMPETING INTERESTS

JMY, EMD and EJC declare no competing interests. GRS has received honoraria or consulting fees from Astra Zeneca, Boehringer, Eli-Lilly, Esperion Therapeutics, Novo Nordisk, Poxel, Pfizer, Merck, Rigel Therapeutics and Terns Therapeutics. GRS has received research funding from Esperion and Espervita Therapeutics. GRS and WIK hold a patent for inhibiting peripheral serotonin for the treatment of metabolic diseases including obesity.

REFERENCES

Choi, W., Namkung, J., Hwang, I., Kim, H., Lim, A., Park, H.J., Lee, H.W., Han, K.-H., Park, S., Jeong, J.-S., et al. (2018). Serotonin signals through a gut-liver axis to regulate hepatic steatosis. Nat. Commun. *9*, 1–9.

Chouchani, E.T., and Kajimura, S. (2019). Metabolic adaptation and maladaptation in adipose tissue. Nat. Metab. *1*, 189–200.

Côté, F., Thévenot, E., Fligny, C., Fromes, Y., Darmon, M., Ripoche, M.-A., Bayard, E., Hanoun, N., Saurini, F., Lechat, P., et al. (2003). Disruption of the nonneuronal tph1 gene demonstrates the importance of peripheral serotonin in cardiac function. Proc. Natl. Acad. Sci. U. S. A. *100*, 13525–13530.

Crane, J.D., Mottillo, E.P., Farncombe, T.H., Morrison, K.M., and Steinberg, G.R. (2014). A standardized infrared imaging technique that specifically detects UCP1-mediated thermogenesis invivo. Mol. Metab. *3*, 490–494.

Crane, J.D., Palanivel, R., Mottillo, E.P., Bujak, A.L., Wang, H., Ford, R.J., Collins, A., Blümer, R.M., Fullerton, M.D., Yabut, J.M., et al. (2015). Inhibiting peripheral serotonin synthesis reduces obesity and metabolic dysfunction by promoting brown adipose tissue thermogenesis. Nat. Med. *21*, 166–172.

Feldmann, H.M., Golozoubova, V., Cannon, B., and Nedergaard, J. (2009). UCP1 ablation induces obesity and abolishes diet-induced thermogenesis in mice exempt from thermal stress by living at thermoneutrality. Cell Metab. *9*, 203–209.

Giles, D.A., Moreno-Fernandez, M.E., Stankiewicz, T.E., Graspeuntner, S., Cappelletti, M., Wu, D., Mukherjee, R., Chan, C.C., Lawson, M.J., Klarquist, J., et al. (2017). Thermoneutral housing exacerbates nonalcoholic fatty liver disease in mice and allows for sex-independent disease modeling. Nat. Med. *23*, 829–838.

Namkung, J., Shong, K.E., Kim, H., Oh, C.M., Park, S., and Kim, H. (2018). Inhibition of serotonin synthesis induces negative hepatic lipid balance. Diabetes Metab. J. *42*, 233–243.

Oh, C.-M., Namkung, J., Go, Y., Shong, K.E., Kim, K., Kim, H., Park, B.-Y., Lee, H.W., Jeon, Y.H., Song, J., et al. (2015). Regulation of systemic energy homeostasis by serotonin in adipose tissues. Nat. Commun. *6*, 6794.

Poekes, L., Legry, V., Schakman, O., Detrembleur, C., Bol, A., Horsmans, Y., Farrell, G.C., and Leclercq, I.A. (2017). Defective adaptive thermogenesis contributes to metabolic syndrome and liver steatosis in obese mice. Clin. Sci. *131*, 285–296.

Roh, H.C., Tsai, L.T.Y., Shao, M., Tenen, D., Shen, Y., Kumari, M., Lyubetskaya, A., Jacobs, C., Dawes, B., Gupta, R.K., et al. (2018). Warming Induces Significant Reprogramming of Beige, but Not Brown, Adipocyte Cellular Identity. Cell Metab. *27*, 1121-1137.e5.

Rozenblit-Susan, S., Chapnik, N., and Froy, O. (2018). Serotonin prevents differentiation into brown adipocytes and induces transdifferentiation into white adipocytes. Int. J. Obes. *42*, 704–710.

Samuel, V.T., and Shulman, G.I. (2016). The pathogenesis of insulin resistance: Integrating signaling pathways and substrate flux. J. Clin. Invest. *126*, 12–22.

Yabut, J.M., Crane, J.D., Green, A.E., Keating, D.J., Khan, W.I., and Steinberg, G.R. (2019). Emerging Roles for Serotonin in Regulating Metabolism: New Implications for an Ancient Molecule. Endocr. Rev. *40*, 1092–1107.

Younossi, Z.M., Koenig, A.B., Abdelatif, D., Fazel, Y., Henry, L., and Wymer, M. (2016). Global epidemiology of nonalcoholic fatty liver disease—Meta-analytic assessment of prevalence, incidence, and outcomes. Hepatology *64*, 73–84.

CHAPTER FIVE

5. DISCUSSION

5.1 INSIGHTS INTO ENERGY BALANCE AND SEROTONIN

An organism thrives when energy intake and expenditure are balanced. Within times of energy surplus (i.e. daylight feeding or before hibernation), organisms store large amounts of calories to ensure enough energy has been accumulated to survive until the next feed. However, the advances in human technologies that prolong food preservation, eliminating the need for hunting and gathering, have influenced the energy balance equation to favour intake. Greater intake in tandem with sedentary lifestyles — thereby reducing energy expenditure —, has resulted in a disparity between the components of energy balance and has likely sparked the global emergence of non-communicable metabolic diseases such as obesity and type 2 diabetes.

Despite the resilience of metabolic tissues and their parenchymal constituents, modern day diets and lifestyles have overcome these cellular safeguards. Calorically-dense diets that consist of fats and sugars in excessive amounts has not only surmounted the energy-storing capabilities of the liver and adipose tissues, but uses our very own evolutionarily-conserved mechanisms to exacerbate the metabolic pathologies the human body attempts to protect us from. The human body did not evolve to defend against the excessive caloric intake and sedentary lifestyles often associated with Western societies. Current research is shifting to meet the need for therapies to combat obesity, type 2 diabetes and NAFLD. As outlined in my review of the literature (Yabut et al., 2019), I have

linked the neurotransmitter and peripheral hormone, serotonin to the aforementioned metabolic pathologies. In this dissertation, I attempt to identify sources of serotonin synthesis and validate whether they contribute to obesity, insulin resistance and hepatic steatosis.

Serotonin has been conserved for billions of years as a molecule that regulates multiple facets of cellular metabolism. Working in a similar way to insulin, serotonin mediates energy anabolism across many metabolic tissues. For example, serotonin suppresses brown and white adipocyte thermogenesis — a process largely reliant on lipids as a substrate — (Crane et al., 2015; Oh et al., 2015) and increases lipid accumulation into hepatocytes via activation of HTR_{2A} (Choi et al., 2018; Namkung et al., 2018). The effects of serotonin collectively promote lipid storage (Yabut et al., 2019). In the present studies, we aimed to identify key tissues and regulators of serotonin synthesis and the potential pathological importance in promoting obesity, insulin resistance and NAFLD.

5.2 MAST CELL AND ADIPOCYTE TPH1

5.2.1 MAST CELL TPH1 INHIBITS WHITE ADIPOSE BROWNING

Since serotonin can potently inhibit thermogenic adipose tissue function (Crane et al., 2015), we fed mice a HFD and placed mice them at thermoneutrality, which revealed that mast cells infiltrate white adipose tissue. It is well understood that immune cells play a large role in regulating adipose tissue and within the last decade, mast cells have emerged as an immune cell associated with obesity and

insulin resistance (Liu et al., 2009). Prior research (Enerbäck, 1963) demonstrated the capability of mast cells to synthesize and secrete serotonin, which has more recently been confirmed in both rodents and humans (Kushnir-Sukhov et al., 2007). Our data on the inhibitory action of mast cell serotonin on the browning of WAT offers an etiological explanation for a situation where upregulation of non-shivering adipocyte thermogenesis is not required (i.e. thermoneutrality) and a pathological condition known to reduce adipose tissue thermogenesis (i.e. obesity) can manifest.

Since enhancing thermogenic adipose tissue protects mice from obesity and insulin resistance, we wanted to test whether genetic deletion of mast cell Tph1 was critical for this effect. We subsequently created two models that reduced mast cell Tph1-derived serotonin by: 1) introducing *in vitro*-cultured Tph1$^{-/-}$ mast cells into mast cell deficient mice and through 2) mast cell-specific Cre deletion using Tph1 floxed mice. When fed a HFD, both our mouse models with mast cell-specific Tph1 deletion had similar metabolic phenotypes, characterized by protection from obesity, insulin resistance, smaller adipocytes and less liver lipids independent of changes in circulating serotonin levels. We attributed these metabolic benefits to increased energy expenditure (determined via indirect calorimetry), which was associated with increased white adipose tissue browning and Ucp1 expression. These changes in white adipose tissue Ucp1 were associated with reduced mast cell serotonin in the WAT of these mice. These changes in energy expenditure of mast cell-specific Tph1 knockout mice were independent of changes in activity and food or water consumed. We show, for the first time, that mast cell serotonin synthesis

via Tph1 promotes obesity and insulin resistance and is an interesting cellular target to increase energy expenditure for metabolic diseases that involve excessive caloric intake. Despite evidence for the role of mast cell serotonin to inhibit the induction of Ucp1 induction in white adipose tissue, we did not see any inhibitory effect of mast cell serotonin on BAT thermogenesis or UCP1 expression as we previously reported in mice with whole-body deletion of Tph1 (Crane et al., 2015). This may be due to the higher abundance of immune cell markers in WAT compared to BAT (Fitzgibbons et al., 2011), as mast cells and macrophages are well known to infiltrate WAT (Altintas et al., 2011).

5.2.2 ADIPOCYTE TPH1 DOES NOT CONTRIBUTE TO METABOLISM

Given our findings that mast cell serotonin synthesis did not alter BAT thermogenesis and prior research that indicated that BAT may be capable of synthesizing serotonin (Oh et al., 2015), we reassessed the role of adipocyte-derived serotonin by crossing inducible AdipoQ-Cre mice to Tph1 floxed mice and fed the progeny a HFD. To our surprise, and in contrast to the findings of others using Tph1 floxed mice crossed to mice expressing Ap2-Cre (Oh et al., 2015), inducible adipocyte-specific Tph1 knockout mice had comparable energy expenditure, BAT thermogenesis and WAT browning and were not protected from obesity and insulin resistance compared to Tph1 floxed controls. These findings using adipocyte-specific genetic Cre recombinase refutes the prior finding (Oh et al., 2015) that adipocytes work in an autocrine manner to reduce adipose thermogenesis. Further,

these data also provide further evidence that mast cells are likely the primary source of adipose tissue Tph1/serotonin synthesis that inhibits WAT thermogenesis. Interestingly, we also observed a moderate reduction in glycemic control in adipocyte-specific Tph1 knockouts, which is the opposite finding previously reported in HFD-fed Tph1-Ap2 Cre mice (Oh et al., 2015). However, it should be noted that a full knockdown of Tph1 was not achieved. Further studies employing a full deletion of Tph1, specifically in adipocytes, is warranted. Collectively, these studies establish mast cells — and exclude adipocytes — as the source of adipose tissue-local serotonin that inhibits WAT energy expenditure, promoting obesity and insulin resistance.

5.2.3 CONSIDERATIONS & FUTURE DIRECTIONS

In Chapter 2, we utilized innovative ($Kit^{W\text{-}sh/W\text{-}sh}$ model) and well accepted (Cpa3-Cre Tph1 floxed) models to delete Tph1 and serotonin synthesis in mast cells. In chapter 3 we were able to exclude the contribution of adipocyte-derived serotonin to mediating obesity and insulin resistance using a more specific and inducible adipocyte Cre recombinase. These studies establish mast cell serotonin synthesis as a primary signal to reduce adipose tissue thermogenesis in obesity. Given the immediate and initial role of mast cells in initiating the inflammatory response, our findings propose a potential etiological role of mast cell serotonin as a signal that can attenuate browning in rodents exposed to environmental conditions that do not require non-shivering thermogenesis to maintain core body temperature.

Protection from obesity and insulin resistance that is associated with elevated energy expenditure is inherently confounded by differing animal body weights, highlighting one potential limitation to our Tph1 mast cell knockout model. Metabolic alterations triggered by changes in body weight confounds the processes that initially caused the changes (Tschöp et al., 2012). In our study with genetic knockout mice with weight differences, it is unclear whether improvements are due to browning of WAT or the confounding variable of reduced body weight. More specifically, when Tph1 mast cell knockout mice were placed in metabolic cages, they had increased oxygen consumption and weighed less than $Tph1^{fl/fl}$ controls. It is unclear whether browning of WAT or less body weight resulted in increased oxygen consumption in Tph1 mast cell knockout mice. This paradoxical association is also a caveat in human research (Westerterp, 2017). Future research on Tph1 mast cell knockout energy expenditure should be completed at a time point when there is the absence of body weight difference, such as week 5 post-HFD, to verify WAT browning-dependent elevations in energy expenditure.

Additional experiments in mast cell and adipocyte-specific Tph1 knockout mice should be done at rodent thermoneutrality to elucidate whether Tph1 in these cell types requires non-shivering thermogenesis for beneficial metabolic effects. Thermoneutral housing temperatures removes the requirement for BAT thermogenesis and WAT browning in rodents (Roh et al., 2018), which are both associated with improvements in metabolism (Chouchani and Kajimura, 2019). Since mast cell infiltration is elevated in WAT of HFD-fed mice at thermoneutrality

compared to room temperature, it would be interesting to see the response in thermoneutral HFD-fed mast cell-specific Tph1 knockout mice. This experiment would show one of two results: these mice would still be resistant to diet-induced obesity since the elevated infiltration of mast cells in WAT would not have the necessary serotonin to blunt WAT browning, supporting the etiological role of mast cell serotonin to reduce non-shivering thermogenesis in thermoneutral conditions. The other alternative is these mice would demonstrate a similar phenotype to that of their double floxed littermates, implicating another compensatory mechanism that reduces WAT browning. Thermoneutral housing of mast cell-specific Tph1 knockout mice may yield important insights to understanding the positive metabolic effects associated with adipose thermogenesis.

A number of questions remain that were not addressed in our studies. These including the mechanism by which mast cell serotonin inhibits adipocyte thermogenesis. Firstly, a receptor type must be identified since HTRs have 7 isoforms followed by more subtypes per isoform (Yabut et al., 2019). Potential answers to this question can be generated by crossing the same inducible adipocyte-specific Cre mouse to novel HTR double floxed mice. Since HTR_{2A} has been implicated in lipogenesis (Oh et al., 2015), which is an opposing process to the oxidation of lipids associated with Ucp1-dependent thermogenesis (Chouchani and Kajimura, 2019), HTR_{2A} floxed mice should be crossed with adipocyte-specific Cre mice, potentially resulting in progeny with increased energy expenditure and WAT browning. Secondly, we did not assess what cellular pathways are employed post-

receptor. We have previously shown in brown adipocytes that serotonin reduces the cAMP-PKA cascade that ultimately reduces *Ucp1* expression (Crane et al., 2015). However, similar experiments were not completed in our study. And since HTRs that can trigger pathways that can potentially stimulate or influence white adipocyte Ucp1 expression, further experiments that achieve a greater understanding of the cellular biology and transcription factors induced by serotonin signaling are required. Thirdly, the source of serotonin that inhibits BAT thermogenesis is still unclear. However, the autocrine action of brown adipocyte thermogenesis cannot be overruled since one caveat of the findings in Chapter 3 is the ubiquitous deletion of Tph1 in both brown and white adipocytes. Infrared thermal camera experiments (Crane et al., 2014) that employ a brown adipocyte-specific Cre driver with Tph1 floxed mouse will be required to elucidate this. And lastly, one interesting angle that can also be explored in future experiments is the role of serotonin on Ucp1-independent thermogenesis. Glycolytic beige adipocytes (Chen et al., 2019), adipocyte creatine cycling (Kazak et al., 2017, 2019) and calcium cycling (Ikeda et al., 2017) are novel pathways that do not require Ucp1-dependent mitochondrial uncoupling, but contribute to whole-body energy expenditure. Future experiments focused on the role of serotonin to influence these Ucp1-independent pathways are warranted.

5.3 MAST CELLS AND TPH1 AS CLINICAL TARGETS

The association between mast cells and metabolic disease is clinically relevant. Epidemiological data suggest the positive association between asthma risk and obesity (Shore, 2008). Serum tryptase — a biomarker of mast cell activation — has been positively correlated to BMI (Fenger et al., 2012) and higher plasma IgE and protease levels were associated with impaired fasting glucose and glucose tolerance (Wang et al., 2013c). Consistent with these observations, Divoux and colleagues biopsied lean and obese nondiabetic humans and showed mast cells are activated in human adipose tissue (Divoux et al., 2012). Further, mast cell number increased in obese adipose tissue compared to lean and was positively associated with fasting glucose and HbA1c (Divoux et al., 2012). Individuals with metabolic syndrome are shown to have more mast cells and tryptase levels in subcutaneous adipose tissue (Gurung et al., 2019). Collectively, mast cells are associated with obesity and insulin resistance, reflecting similar findings to rodent studies (Liu et al., 2009).

Improvements in metabolism due to mast cell stabilization in humans also support the concept that therapies inhibiting mast cells may be effective for treating metabolic disease. For example, the treatment of people with obesity and type 2 diabetes with glimepiride and the mast cell stabilizer ketotifen versus glimepiride alone led to a reduction in BMI and fasting blood glucose (El-haggar et al., 2015). Similarly, treatment of obese individuals with type 2 diabetes with the mast cell stabilizer, Amlexanox for 12 weeks reduces body weight, HbA1c and insulin

resistance (Oral et al., 2017). Importantly, these changes were associated with an increase in thermogenic gene expression in subcutaneous WAT characterized by higher expression of *UCP1, ADBR3, PPARGC1A, PRDM16* and *IL4* (Oral et al., 2017). And while this effect was attributed to the inhibition of the inflammatory pathways involving IKKε and TBK1, it is interesting to speculate that these effects may have been instead due to the inhibition of the mast cell serotonin synthesis.

In addition to mast cell stabilization, Tph1 inhibition is currently FDA approved to treat carcinoid syndrome (Kulke et al., 2017), highlighting the feasibility of inhibiting serotonin synthesis in humans (Bader, 2020). The Tph inhibitor, Telotristat ethyl, has been shown to reduce jejunal serotonin by 95% independent on changes in brain serotonin levels (Margolis et al., 2014). Our findings in Chapter 2 used LP533401 — another peripherally-restricted Tph inhibitor — to inhibit activated rodent mast cell serotonin synthesis by ~80%. LP533401 was also administered via intraperitoneal injection to inhibit serotonin synthesis, resulting in a metabolic phenocopy to $Tph1^{-/-}$ mice fed HFD (Crane et al., 2015). Since mast cell stabilizers (ketotifen or amlexanox) and Tph1 inhibitors (telotristat ethyl) are currently FDA-approved, the ability to repurpose these therapeutics to treat obesity and insulin resistance may be possible. However, future studies in individuals with obesity and insulin resistance in conjunction with measures of energy expenditure and brown/beige adipose tissue, such as MRI or PET/CT (Ong et al., 2018), are required.

5.4 THE ROLE OF TPH1 IN HEPATIC STEATOSIS

5.4.1 CIRCULATING SEROTONIN REGULATES FATTY LIVER

In Chapter 2 and 3 we elucidated the role of mast cell serotonin to inhibit the browning of WAT. However, the source of serotonin blunting BAT thermogenesis was still unknown since neither adipocyte or mast cell Tph1 affected BAT. The gut produces ~90% of the total serotonin in the body (Yabut et al., 2019). Placing mice at thermoneutral conditions can reduce the need for Ucp1 in both BAT and subcutaneous WAT of mice (Feldmann et al., 2009; Roh et al., 2018). Therefore, we fed HFD to $Tph1^{-/-}$ mice and $Tph1^{+/+}$ littermates in thermoneutral conditions, removing the requirement for Ucp1-dependent thermogenesis and ultimately, the metabolic benefits of BAT non-shivering thermogenesis. Consistent with our hypothesis, placing $Tph1^{-/-}$ mice at thermoneutrality eliminated genotypic differences in adipose tissue UCP1 expression, energy expenditure and body mass/fat mass previously observed in $Tph1^{-/-}$ mice housed at room temperature (Crane et al., 2015), supporting a critical role for Tph1 in inhibiting brown and white adipose tissue thermogenesis.

Unlike humans, mice housed at room temperature need to rely on adipose tissue thermogenesis to maintain their body temperature. We found that in contrast to room temperature housing, when $Tph1^{-/-}$ mice were fed a HFD and housed at thermoneutrality, thereby negating the need for brown and white adipose tissue thermogenesis, there was no difference in body mass and adiposity compared to wildtype controls. However, $Tph1^{-/-}$ mice still had modest improvements in insulin

sensitivity compared to $Tph1^{+/+}$ controls. Considering the role of the liver in mediating insulin resistance in HFD-fed models and the recent discovery that the gut is involved in promoting hepatic steatosis (Choi et al., 2018), we assessed liver lipids and found that surprisingly, $Tph1^{-/-}$ mice had reduced liver lipids. Importantly, these reductions in liver lipids were associated with reduced markers of fatty acid synthesis, inflammation and fibrosis. These findings provided a key insight: reducing serotonin protects against NAFLD despite similar levels of weight gain, energy expenditure and BAT thermogenesis.

The data in Chapter 4 suggests a novel axis (i.e. thermoneutrality – gut serotonin – hepatic liver accumulation) that may explain how housing temperature regulates liver lipid levels. However, further studies are required to elucidate this relationship such as understanding what cell types are involved, the downstream mechanisms of these cell types and determining if thermoneutrality affects hepatic lipid accretion in mice with a gut-specific Tph1 deletion.

5.4.2 CONSIDERATIONS & FUTURE DIRECTIONS

Hepatic fat accumulation has been attributed to HTR_{2A} signalling in hepatocytes. However, hepatic stellate cells (HSC) are another resident cell in liver that are activated via HTR_{2A} to induce liver fibrosis (Tsuchida and Friedman, 2017). Inhibition of HTR_{2A} with the non-specific peripherally restricted antagonist sarpogrelate is associated with reductions in inflammation and fibrosis *in vitro* and *in vivo* (Kim et al., 2013). Thus, the beneficial liver phenotype of mice treated with

HTR_{2A} antagonists in the studies by Choi and colleagues may be partially attributed to reduction in HSC activation, which has profound impact on hepatocyte health and viability (Tsuchida and Friedman, 2017). Thus, future studies that utilize mice in which Cre expression is driven by lecithin-retinol acyltransferase (Lrat), an HSC-specific enzyme (Greenhalgh et al., 2015) and HTR_{2A} floxed mice are crossed and placed on a HFD at thermoneutrality will provide new evidence of serotonin's role in temperature-dependent liver lipid accumulation.

There are four main methods by which lipid can accumulate in the liver: 1. reduced lipid oxidation, 2. reduced lipid export 3. increased lipid uptake and 4. increased *de novo* synthesis. Markers of these pathways were reduced in $Tph1^{-/-}$ mice housed in thermoneutrality such as CD36 (lipid transport) and PPARγ (lipid synthesis). Since serotonin binding to HTR_{2A} increases intracellular Ca^{2+} and increases in Ca^{2+} are associated with activation of various isoforms of PKC that have been associated with steatosis such as PKCε (Samuel et al., 2004) and PKCδ (Bezy et al., 2011), examining the activity of these proteins should be considered. Thus, future *in vitro* experiments in hepatocytes from HTR_{2A} knockout mice or HTR_{2A} antagonist-treated hepatocytes are required.

As observed in Chapter 4, many fatty acid synthesis enzymes are significantly reduced in $Tph1^{-/-}$ mice housed in thermoneutrality. *In vitro* experiments in isolated primary hepatocytes from HTR_{2A} knockout mice or siRNA knockdown cells treated with H^3-labelled acetate can discern if this receptor mediates lipogenesis (Lally et al., 2019). Further, utilization of C^{13}-labelled

palmitate can discern if there are changes in long-chain fatty acid uptake and oxidation (Galic et al., 2011). If hepatic fatty acid metabolism is altered *in vitro*, *in vivo* models that use a liver specific Cre promoter, such as albumin Cre (Weisend et al., 2009), can be used in conjunction with HTR_{2A} floxed mice. Adeno-associated virus serotype 8 particles with Cre activity injected into HTR_{2A} floxed mice can also create a model with inducible deletion (Nakai et al., 2005). Placing these mice in thermoneutrality in conjunction with HFD feeding may elucidate and confirm mechanisms that can be further examined.

Lastly, we have discussed serotonin as a bioamine that may link thermoneutrality to hepatic fatty acid accumulation. Since we used Tph1 whole body knockout mice, the use of gut-specific Tph1 knockout mice (Choi et al., 2018; Sumara et al., 2012) will provide more evidence to support the role of gut-derived serotonin in temperature induced lipid accretion. Placing these mice at thermoneutrality should result in mice that are protected from HFD-induced hepatic accretion. Unlike our study in Chapter 4, room temperature, thermoneutral and cold-exposed gut-specific Tph1 knockout mice should be utilized to discern the dependence of hepatic lipid accretion on temperature. The proposed experiments will provide important mechanistic and in vivo insight of the role of serotonin in hepatic steatosis and can be exploited for future NAFLD therapies.

5.5 TPH1 AS A THERAPY FOR METABOLIC DISEASE

The clinical transferability of mast cell and gut serotonin synthesis is promising due to the presence of Tph1 in these cell types in humans (Kushnir-Sukhov et al., 2007; Van Lelyveld et al., 2007). However, metabolic improvements due to inhibition of these pathways has not yet been shown in any current clinical studies. In humans the number of mast cells in WAT increases with obesity and type 2 diabetes (Divoux et al., 2012; Wang et al., 2013c), but the low amount of serotonin synthesized by human, compared to rodent mast cells may not be clinically relevant (Kushnir-Sukhov et al., 2007). Specifically, rodent mast cells were shown to have ~110 ng of serotonin per million cells while human mast cells contain approximately a tenth of this (~ 12 ng of serotonin per million cells). However, this reduction in serotonin production in human mast cells may be offset by much greater mast cells numbers in obese human WAT, ~7 mast cells per mm^2, compared to ~1-2 mast cells per mm^2 in rodents (Liu et al., 2009). Thus, the amount of serotonin synthesized in whole adipose tissue depots in humans may still be clinically relevant, but future studies that utilize obese human white adipocytes treated with mast cell comparable concentrations of serotonin are warranted.

Highlighting the therapeutic potential of inhibiting Tph1, Telotristat ethyl has been approved for inhibiting the synthesis of tumour-derived serotonin synthesis in patients with carcinoid syndrome (Dillon and Chandrasekharan, 2018). And while telotristat ethyl is effective for reducing diarrhea, many patients experienced side effects with 1 in 4 individuals dropping out of the study due to

nausea and constipation (Strosberg et al., 2019). Interestingly, previous studies have found an association between carcinoid syndrome and liver fat (MacDonald, 1956; Roberts and Sjoerdsma, 1964).

5.6 SUMMARY & CONCLUSION

In this dissertation, we identified the source of serotonin that inhibits non-shivering thermogenesis within adipose tissue to be mast cells and not adipocytes. This was established by showing that genetic deletion of mast cells, but not adipocyte Tph1, increases the browning of WAT, protecting mice from HFD-induced obesity and insulin resistance. Further, we have described the role of serotonin in promoting hepatic steatosis by observing that Tph1 whole body knockout mice are protected from NAFLD despite similar levels of thermogenic adipose tissue function and HFD-induced weight gain. Since the ectopic accumulation of lipids has accelerated the global development of type 2 diabetes and NAFLD, the findings within this dissertation identifying mast cell Tph1 as a potential therapeutic target to improve energy expenditure by increasing futile cycling of white adipose tissue may be important. Our last set of findings supports the concept that serotonin promotes liver lipid storage independently of alterations in adipose tissue thermogenesis. Collectively, these data suggest that developing new ways to inhibit serotonin synthesis and signaling may help alleviate the global burden of obesity and related metabolic diseases.

REFERENCES

Aherne, W., and Hull, D. (1966). Brown adipose tissue and heat production in the newborn infant. J. Pathol. Bacteriol. *91*, 223–234.

Altintas, M.M., Azad, A., Nayer, B., Contreras, G., Zaias, J., Faul, C., Reiser, J., and Nayer, A. (2011). Mast cells, macrophages, and crown-like structures distinguish subcutaneous from visceral fat in mice. J. Lipid Res. *52*, 480–488.

Aron-Wisnewsky, J., Tordjman, J., Poitou, C., Darakhshan, F., Hugol, D., Basdevant, A., Aissat, A., Guerre-Millo, M., and Clément, K. (2009). Human adipose tissue macrophages: M1 and M2 cell surface markers in subcutaneous and omental depots and after weight loss. J. Clin. Endocrinol. Metab. *94*, 4619–4623.

Bader, M. (2020). Inhibition of serotonin synthesis: A novel therapeutic paradigm. Pharmacol. Ther. *205*, 107423.

Barbatelli, G., Murano, I., Madsen, L., Hao, Q., Jimenez, M., Kristiansen, K., Giacobino, J.P., De Matteis, R., and Cinti, S. (2010). The emergence of cold-induced brown adipocytes in mouse white fat depots is determined predominantly by white to brown adipocyte transdifferentiation. Am. J. Physiol. - Endocrinol. Metab. *298*, 1244–1253.

Bartelt, A., Bruns, O.T., Reimer, R., Hohenberg, H., Ittrich, H., Peldschus, K., Kaul, M.G., Tromsdorf, U.I., Weller, H., Waurisch, C., et al. (2011). Brown adipose tissue activity controls triglyceride clearance. Nat. Med. *17*, 200–205.

Bezy, O., Tran, T.T., Pihlajamäki, J., Suzuki, R., Emanuelli, B., Winnay, J., Mori, M.A., Haas, J., Biddinger, S.B., Leitges, M., et al. (2011). PKCδ regulates hepatic insulin sensitivity and hepatosteatosis in mice and humans. J. Clin. Invest. *121*, 2504–2517.

Biener, A., Cawley, J., and Meyerhoefer, C. (2018). The impact of obesity on medical care costs and labor market outcomes in the US. Clin. Chem. *64*, 108–117.

Brown, M.S., and Goldstein, J.L. (2008). Selective versus Total Insulin Resistance: A Pathogenic Paradox. Cell Metab. *7*, 95–96.

Cannon, B., and Nedergaard, J. (2004). Brown adipose tissue: function and physiological significance. Physiol. Rev. 277–359.

Carey, A.L., and Kingwell, B.A. (2013). Brown adipose tissue in humans: Therapeutic potential to combat obesity. Pharmacol. Ther. *140*, 26–33.

Chen, Y., Ikeda, K., Yoneshiro, T., Scaramozza, A., Tajima, K., Wang, Q., Kim, K., Shinoda, K., Sponton, C.H., Brown, Z., et al. (2019). Thermal stress induces glycolytic beige fat formation via a myogenic state. Nature *565*, 180–185.

Choi, W., Namkung, J., Hwang, I., Kim, H., Lim, A., Park, H.J., Lee, H.W., Han, K.-H., Park, S., Jeong, J.-S., et al. (2018). Serotonin signals through a gut-liver axis to regulate hepatic steatosis. Nat. Commun. *9*, 1–9.

Choo, H.J., Kim, J.H., Kwon, O.B., Lee, C.S., Mun, J.Y., Han, S.S., Yoon, Y.S., Yoon, G., Choi, K.M., and Ko, Y.G. (2006). Mitochondria are impaired in the adipocytes of type 2 diabetic mice. Diabetologia *49*, 784–791.

Chouchani, E.T., and Kajimura, S. (2019). Metabolic adaptation and maladaptation in adipose tissue. Nat. Metab. *1*, 189–200.

Chouchani, E.T., Kazak, L., and Spiegelman, B.M. (2019). New Advances in Adaptive Thermogenesis: UCP1 and Beyond. Cell Metab. *29*, 27–37.

Cohen, P., Levy, J.D., Zhang, Y., Frontini, A., Kolodin, D.P., Svensson, K.J., Lo, J.C., Zeng, X., Ye, L., Khandekar, M.J., et al. (2014). Ablation of PRDM16 and beige adipose causes metabolic dysfunction and a subcutaneous to visceral fat switch. Cell *156*, 304–316.

Crane, J.D., Mottillo, E.P., Farncombe, T.H., Morrison, K.M., and Steinberg, G.R. (2014). A standardized infrared imaging technique that specifically detects UCP1-mediated thermogenesis invivo. Mol. Metab. *3*, 490–494.

Crane, J.D., Palanivel, R., Mottillo, E.P., Bujak, A.L., Wang, H., Ford, R.J., Collins, A., Blümer, R.M., Fullerton, M.D., Yabut, J.M., et al. (2015). Inhibiting peripheral serotonin synthesis reduces obesity and metabolic dysfunction by promoting brown adipose tissue thermogenesis. Nat. Med. *21*, 166–172.

Cui, X., Nguyen, N.L.T., Zarebidaki, E., Cao, Q., Li, F., Zha, L., Bartness, T., Shi, H., and Xue, B. (2016). Thermoneutrality decreases thermogenic program and promotes adiposity in high-fat diet-fed mice. Physiol. Rep. *4*, 1–14.

Cypess, A.M., Lehman, S., Williams, G., Tal, I., Rodman, D., Goldfine, A.B., Kuo, F.C., Palmer, E.L., Tseng, Y.-H., Doria, A., et al. (2009). Identification and importance of brown adipose tissue in adult humans. N. Engl. J. Med. *360*, 1509–1517.

Dillon, J.S., and Chandrasekharan, C. (2018). Telotristat ethyl: A novel agent for the therapy of carcinoid syndrome diarrhea. Futur. Oncol. *14*, 1155–1164.

Divoux, A., Moutel, S., Poitou, C., Lacasa, D., Veyrie, N., Aissat, A., Arock, M., Guerre-Millo, M., and Clément, K. (2012). Mast Cells in Human Adipose Tissue: Link with Morbid Obesity, Inflammatory Status, and Diabetes. J. Clin. Endocrinol. Metab. *97*, E1677–E1685.

Doege, H., Grimm, D., Falcon, A., Tsang, B., Storm, T.A., Xu, H., Ortegon, A.M., Kazantzis, M., Kay, M.A., and Stahl, A. (2008). Silencing of hepatic fatty acid transporter protein 5 in vivo reverses diet-induced non-alcoholic fatty liver disease and improves hyperglycemia. J. Biol. Chem. *283*, 22186–22192.

El-haggar, S.M., Farrag, W.F., and Kotkata, F.A. (2015). Journal of Diabetes and Its Complications Effect of ketotifen in obese patients with type 2 diabetes mellitus. J. Diabetes Complications *29*, 427–432.

Enerbäck, L. (1963). Serotonin in Human Mast Cells. Nature *197*, 610–611.
Enerbäck, S., Jacobsson, A., Simpson, E.M., Guerra, C., Yamashita, H., Harper, M.E., and Kozak, L.P. (1997). Mice lacking mitochondrial uncoupling protein are cold-sensitive but not obese. Nature *387*, 90–94.

Feldmann, H.M., Golozoubova, V., Cannon, B., and Nedergaard, J. (2009). UCP1 ablation induces obesity and abolishes diet-induced thermogenesis in mice exempt from thermal stress by living at thermoneutrality. Cell Metab. *9*, 203–209.

Fenger, R. V., Linneberg, A., Vidal, C., Vizcaino, L., Husemoen, L.L., Aadahl, M., and Gonzalez-Quintela, A. (2012). Determinants of serum tryptase in a general population: The relationship of serum tryptase to obesity and asthma. Int. Arch. Allergy Immunol. *157*, 151–158.

Ferré, P., and Foufelle, F. (2010). Hepatic steatosis: A role for de novo lipogenesis and the transcription factor SREBP-1c. Diabetes, Obes. Metab. *12*, 83–92.

Fischer, K., Ruiz, H.H., Jhun, K., Finan, B., Oberlin, D.J., Van Der Heide, V., Kalinovich, A. V., Petrovic, N., Wolf, Y., Clemmensen, C., et al. (2017). Alternatively activated macrophages do not synthesize catecholamines or contribute to adipose tissue adaptive thermogenesis. Nat. Med. *23*, 623–630.

Fitzgibbons, T.P., Kogan, S., Aouadi, M., Hendricks, G.M., Straubhaar, J., and Czech, M.P. (2011). Similarity of mouse perivascular and brown adipose tissues and their resistance to diet-induced inflammation. Am. J. Physiol. - Hear. Circ. Physiol. *301*, 1425–1437.

Galic, S., Fullerton, M.D., Schertzer, J.D., Sikkema, S., Marcinko, K., Walkley, C.R., Izon, D., Honeyman, J., Chen, Z.P., Van Denderen, B.J., et al. (2011). Hematopoietic AMPK β1 reduces mouse adipose tissue macrophage inflammation

and insulin resistance in obesity. J. Clin. Invest. *121*, 4903–4915.

Gandotra, S., Le Dour, C., Bottomley, W., Cervera, P., Giral, P., Reznik, Y., Charpentier, G., Auclair, M., Delépine, M., Barroso, I., et al. (2011). Perilipin deficiency and autosomal dominant partial lipodystrophy. N. Engl. J. Med. *364*, 740–748.

Greenhalgh, S.N., Conroy, K.P., and Henderson, N.C. (2015). Cre-ativity in the liver: Transgenic approaches to targeting hepatic nonparenchymal cells. Hepatology *61*, 2091–2099.

Gregor, M.F., and Hotamisligil, G.S. (2011). Inflammatory Mechanisms in Obesity. Annu. Rev. Immunol. *29*, 415–445.

Guerra, C., Koza, R.A., Yamashita, H., Walsh, K., and Kozak, L.P. (1998). Emergence of brown adipocytes in white fat in mice is under genetic control effects on body weight and adiposity. J. Clin. Invest. *102*, 412–420.

Gurung, P., Moussa, K., Adams-Huet, B., Devaraj, S., and Jialal, I. (2019). Increased mast cell abundance in adipose tissue of metabolic syndrome: relevance to the proinflammatory state and increased adipose tissue fibrosis. Am. J. Physiol. Metab. *316*, E504–E509.

Harms, M.J., Ishibashi, J., Wang, W., Lim, H.W., Goyama, S., Sato, T., Kurokawa, M., Won, K.J., and Seale, P. (2014). Prdm16 is required for the maintenance of brown adipocyte identity and function in adult mice. Cell Metab. *19*, 593–604.

Hirai, S., Ohyane, C., Kim, Y.-I., Lin, S., Goto, T., Takahashi, N., Kim, C.-S., Kang, J., Yu, R., and Kawada, T. (2014). Involvement of mast cells in adipose tissue fibrosis. Am. J. Physiol. Endocrinol. Metab. *306*, E247-55.

Horton, J.D., Goldstein, J.L., and Brown, M.S. (2002). SREBPs: activators of the complete program of cholesterol and fatty acid synthesis in the liver. J. Clin. Invest. *109*, 1125–1131.

Ikeda, K., Kang, Q., Yoneshiro, T., Camporez, J.P., Maki, H., Homma, M., Shinoda, K., Chen, Y., Lu, X., Maretich, P., et al. (2017). UCP1-independent signaling involving SERCA2bmediated calcium cycling regulates beige fat thermogenesis and systemic glucose homeostasis. Nat. Med. *23*, 1454–1465.

Inagaki, T., Sakai, J., and Kajimura, S. (2016). Transcriptional and epigenetic control of brown and beige adipose cell fate and function. Nat. Rev. Mol. Cell Biol. *17*, 480–495.

de Jong, J.M.A., Sun, W., Pires, N.D., Frontini, A., Balaz, M., Jespersen, N.Z., Feizi, A., Petrovic, K., Fischer, A.W., Bokhari, M.H., et al. (2019). Human brown adipose tissue is phenocopied by classical brown adipose tissue in physiologically humanized mice. Nat. Metab. *1*, 830–843.

Kajimura, S. (2017). Adipose tissue in 2016: Advances in the understanding of adipose tissue biology. Nat. Rev. Endocrinol. *13*, 69–70.

Kajimura, S., Seale, P., Kubota, K., Lunsford, E., Frangioni, J. V., Gygi, S.P., and Spiegelman, B.M. (2009). Initiation of myoblast to brown fat switch by a PRDM16-C/EBP-β transcriptional complex. Nature *460*, 1154–1158.

Kazak, L., Chouchani, E.T., Lu, G.Z., Jedrychowski, M.P., Bare, C.J., Mina, A.I., Kumari, M., Zhang, S., Vuckovic, I., Laznik-Bogoslavski, D., et al. (2017). Genetic Depletion of Adipocyte Creatine Metabolism Inhibits Diet-Induced Thermogenesis and Drives Obesity. Cell Metab. *26*, 660-671.e3.

Kazak, L., Rahbani, J.F., Samborska, B., Lu, G.Z., Jedrychowski, M.P., Lajoie, M., Zhang, S., Ramsay, L.A., Dou, F.Y., Tenen, D., et al. (2019). Ablation of adipocyte creatine transport impairs thermogenesis and causes diet-induced obesity. Nat. Metab. *1*, 360–370.

Kim, D.C., Jun, D.W., Kwon, Y. Il, Lee, K.N., Lee, H.L., Lee, O.Y., Yoon, B.C., Choi, H.S., and Kim, E.K. (2013). 5-HT2Areceptor antagonists inhibit hepatic stellate cell activation and facilitate apoptosis. Liver Int. *33*, 535–543.

Kim, J.K., Zisman, A., Fillmore, J.J., Peroni, O.D., Kotani, K., Perret, P., Zong, H., Dong, J., Kahn, C.R., Kahn, B.B., et al. (2001). Glucose toxicity and the development of diabetes in mice with muscle-specific inactivation of glut4. J. Clin. Invest. *108*, 153–160.

Kulke, M.H., Hörsch, D., Caplin, M.E., Anthony, L.B., Bergsland, E., Öberg, K., Welin, S., Warner, R.R.P., Lombard-Bohas, C., Kunz, P.L., et al. (2017). Telotristat ethyl, a tryptophan hydroxylase inhibitor for the treatment of carcinoid syndrome. J. Clin. Oncol. *35*, 14–23.

Kushnir-Sukhov, N.M., Brown, J.M., Wu, Y., Kirshenbaum, A., and Metcalfe, D.D. (2007). Human mast cells are capable of serotonin synthesis and release. J. Allergy Clin. Immunol. *119*, 498–499.

Lally, J.S.V., Ghoshal, S., DePeralta, D.K., Moaven, O., Wei, L., Masia, R., Erstad, D.J., Fujiwara, N., Leong, V., Houde, V.P., et al. (2019). Inhibition of Acetyl-CoA Carboxylase by Phosphorylation or the Inhibitor ND-654 Suppresses Lipogenesis and Hepatocellular Carcinoma. Cell Metab. *29*, 174-182.e5.

Largis, E.E., Burns, M.G., Muenkel, H.A., Dolan, J.A., and Claus, T.H. (1994). Antidiabetic and antiobesity effects of a highly selective β3-adrenoceptor agonist (CL 316,243). Drug Dev. Res. *32*, 69–76.

Lee, M., Odegaard, J.I., Mukundan, L., Qiu, Y., Molofsky, A.B., Nussbaum, J.C., Yun, K., Locksley, R.M., and Chawla, A. (2014a). Activated Type 2 Innate Lymphoid Cells Regulate Beige Fat Biogenesis. Cell *160*, 74–87.

Lee, Y.-H., Mottillo, E.P., and Granneman, J.G. (2014b). Adipose tissue plasticity from WAT to BAT and in between. Biochim. Biophys. Acta *1842*, 358–369.

Lee, Y.H., Petkova, A.P., Mottillo, E.P., and Granneman, J.G. (2012). In vivo identification of bipotential adipocyte progenitors recruited by β3-adrenoceptor activation and high-fat feeding. Cell Metab. *15*, 480–491.

Van Lelyveld, N., Ter Linde, J., Schipper, M.E.I., and Samsom, M. (2007). Regional differences in expression of TPH-1, SERT, 5-HT3 and 5-HT4 receptors in the human stomach and duodenum. Neurogastroenterol. Motil. *19*, 342–348.

Li, Q., Blume, S.W., Huang, J.C., Hammer, M., and Ganz, M.L. (2015). Prevalence and healthcare costs of obesity-related comorbidities: Evidence from an electronic medical records system in the United States. J. Med. Econ. *18*, 1020–1028.

Liu, J., Divoux, A., Sun, J., Zhang, J., Clément, K., Glickman, J.N., Sukhova, G.K., Wolters, P.J., Du, J., Gorgun, C.Z., et al. (2009). Genetic deficiency and pharmacological stabilization of mast cells reduce diet-induced obesity and diabetes in mice. Nat. Med. *15*, 940–945.

Loh, R.K.C., Kingwell, B.A., and Carey, A.L. (2017). Human brown adipose tissue as a target for obesity management; beyond cold-induced thermogenesis. Obes. Rev. *18*, 1227–1242.

Loomba, R., Abraham, M., Unalp, A., Wilson, L., Lavine, J., Doo, E., and Bass, N.M. (2012). Association between diabetes, family history of diabetes, and risk of nonalcoholic steatohepatitis and fibrosis. Hepatology *56*, 943–951.

Lumeng, C.N., Bodzin, J.L., and Saltiel, A.R. (2007). Obesity induces a phenotypic switch in adipose tissue macrophage polarization. J. Clin. Invest. *117*, 175–184.

MacDonald, R.A. (1956). A study of 356 carcinoids of the gastrointestinal tract: Report of four new cases of the carcinoid syndrome. Am. J. Med. *21*, 867–878.

Man, K., Kutyavin, V.I., and Chawla, A. (2017). Tissue Immunometabolism: Development, Physiology, and Pathobiology. Cell Metab. *15*, 11–26.

Marchesini, G., Brizi, M., Morselli-Labate, A., Bianchi, G., Bugianesi, E., McCullough, A., Forlani, G., and Melchionda, N. (2007). Association of nonalcoholic fatty liver disease with serum adiponectin and insulin resistance. Am J Med *107*, 450–455.

Margolis, K.G., Stevanovic, K., Li, Z., Yang, Q.M., Oravecz, T., Zambrowicz, B., Jhaver, K.G., Diacou, A., and Gershon, M.D. (2014). Pharmacological reduction of mucosal but not neuronal serotonin opposes inflammation in mouse intestine. Gut *63*, 928–937.

van Marken Lichtenbelt, W.D., Vanhommerig, J.W., Smulders, N.M., Drossaerts, J.M.A.F.L., Kemerink, G.J., Bouvy, N.D., Schrauwen, P., and Teule, G.J.J. (2009). Cold-Activated Brown Adipose Tissue in Healthy Men. N. Engl. J. Med. *360*, 1500–1508.

Mayerson, A.B., Hundal, R.S., Dufour, S., Lebon, V., Befroy, D., Cline, G.W., Enocksson, S., Inzucchi, S.E., Shulman, G.I., and Petersen, K.F. (2002). The effects of rosiglitazone on insulin sensitivity, lipolysis, and hepatic and skeletal muscle triglyceride content in patients with type 2 diabetes. Diabetes *51*, 797–802.

Mottillo, E.P., Balasubramanian, P., Lee, Y.-H., Weng, C., Kershaw, E.E., and Granneman, J.G. (2014). Coupling of lipolysis and de novo lipogenesis in brown, beige, and white adipose tissues during chronic β3-adrenergic receptor activation. J. Lipid Res. *55*, 2276–2286.

Mraz, M., and Haluzik, M. (2014). The role of adipose tissue immune cells in obesity and low-grade inflammation. J. Endocrinol. *222*, 113–127.

Nakai, H., Fuess, S., Storm, T.A., Muramatsu, S. -i., Nara, Y., and Kay, M.A. (2005). Unrestricted Hepatocyte Transduction with Adeno-Associated Virus Serotype 8 Vectors in Mice. J. Virol. *79*, 214–224.

Namkung, J., Shong, K.E., Kim, H., Oh, C.M., Park, S., and Kim, H. (2018). Inhibition of serotonin synthesis induces negative hepatic lipid balance. Diabetes Metab. J. *42*, 233–243.

Nedergaard, J., and Cannon, B. (2010). The Changed Metabolic World with Human Brown Adipose Tissue: Therapeutic Visions. Cell Metab. *11*, 268–272.

Nguyen, K.D., Qiu, Y., Cui, X., Goh, Y.P.S., Mwangi, J., David, T., Mukundan, L., Brombacher, F., Locksley, R.M., and Chawla, A. (2011). Alternatively activated macrophages produce catecholamines to sustain adaptive thermogenesis. Nature *480*, 104–108.

Oh, C.-M., Namkung, J., Go, Y., Shong, K.E., Kim, K., Kim, H., Park, B.-Y., Lee, H.W., Jeon, Y.H., Song, J., et al. (2015). Regulation of systemic energy homeostasis by serotonin in adipose tissues. Nat. Commun. *6*, 6794.

Ohno, H., Shinoda, K., Spiegelman, B.M., and Kajimura, S. (2012). PPARγ agonists induce a white-to-brown fat conversion through stabilization of PRDM16 protein. Cell Metab. *15*, 395–404.

Ong, F.J., Ahmed, B.A., Oreskovich, S.M., Blondin, D.P., Haq, T., Konyer, N.B., Noseworthy, M.D., Haman, F., Carpentier, A.C., Morrison, K.M., et al. (2018). Recent advances in the detection of brown adipose tissue in adult humans: A review. Clin. Sci. *132*, 1039–1054.

Oral, E.A., Reilly, S.M., Gomez, A. V., Meral, R., Butz, L., Ajluni, N., Chenevert, T.L., Korytnaya, E., Neidert, A.H., Hench, R., et al. (2017). Inhibition of IKKε and TBK1 Improves Glucose Control in a Subset of Patients with Type 2 Diabetes. Cell Metab. *26*, 157-170.e7.

Perry, R.J., Samuel, V.T., Petersen, K.F., and Shulman, G.I. (2014). The role of hepatic lipids in hepatic insulin resistance and type 2 diabetes. Nature *510*, 84–91.

Perry, R.J., Camporez, J.P.G., Kursawe, R., Titchenell, P.M., Zhang, D., Perry, C.J., Jurczak, M.J., Abudukadier, A., Han, M.S., Zhang, X.M., et al. (2015). Hepatic acetyl CoA links adipose tissue inflammation to hepatic insulin resistance and type 2 diabetes. Cell *160*, 745–758.

Petersen, M.C., and Shulman, G.I. (2018). Mechanisms of insulin action and insulin resistance. Physiol. Rev. *98*, 2133–2223.

Pinkosky, S.L., Groot, P.H.E., Lalwani, N.D., and Steinberg, G.R. (2017). Targeting ATP-Citrate Lyase in Hyperlipidemia and Metabolic Disorders. Trends Mol. Med. *23*, 1047–1063.

Qiu, Y., Nguyen, K.D., Odegaard, J.I., Cui, X., Tian, X., Locksley, R.M., Palmiter, R.D., and Chawla, A. (2014). Eosinophils and Type 2 Cytokine Signaling in Macrophages Orchestrate Development of Functional Beige Fat. Cell *157*, 1292–1308.

Raddatz, K., Turner, N., Frangioudakis, G., Liao, B.M., Pedersen, D.J., Cantley, J., Wilks, D., Preston, E., Hegarty, B.D., Leitges, M., et al. (2011). Time-dependent effects of Prkce deletion on glucose homeostasis and hepatic lipid metabolism on dietary lipid oversupply in mice. Diabetologia *54*, 1447–1456.

Rajakumari, S., Wu, J., Ishibashi, J., Lim, H.W., Giang, A.H., Won, K.J., Reed, R.R., and Seale, P. (2013). EBF2 determines and maintains brown adipocyte identity. Cell Metab. *17*, 562–574.
Ravussin, E., and Galgani, J.E. (2011). The Implication of Brown Adipose Tissue for Humans. Annu. Rev. Nutr. *31*, 33–47.

Reusch, J.E.B., and Manson, J.A.E. (2017). Management of type 2 diabetes in 2017 getting to goal. JAMA - J. Am. Med. Assoc. *317*, 1015–1016.

Roberts, W.C., and Sjoerdsma, A. (1964). The cardiac disease associated with the carcinoid syndrome (carcinoid heart disease). Am. J. Med. *36*, 5–34.

Roh, H.C., Tsai, L.T.Y., Shao, M., Tenen, D., Shen, Y., Kumari, M., Lyubetskaya, A., Jacobs, C., Dawes, B., Gupta, R.K., et al. (2018). Warming Induces Significant Reprogramming of Beige, but Not Brown, Adipocyte Cellular Identity. Cell Metab. *27*, 1121-1137.e5.

Samuel, V.T., and Shulman, G.I. (2018). Nonalcoholic Fatty Liver Disease as a Nexus of Metabolic and Hepatic Diseases. Cell Metab. *27*, 22–41.

Samuel, V.T., Liu, Z.X., Qu, X., Elder, B.D., Bilz, S., Befroy, D., Romanelli, A.J., and Shulman, G.I. (2004). Mechanism of hepatic insulin resistance in non-alcoholic fatty liver disease. J. Biol. Chem. *279*, 32345–32353.

Samuel, V.T., Liu, Z.X., Wang, A., Beddow, S.A., Geisler, J.G., Kahn, M., Zhang, X.M., Monia, B.P., Bhanot, S., and Shulman, G.I. (2007). Inhibition of protein kinase Cε prevents hepatic insulin resistance in nonalcoholic fatty liver disease. J. Clin. Invest. *117*, 739–745.

Sanchez-Gurmaches, J., Tang, Y., Jespersen, N.Z., Wallace, M., Martinez Calejman, C., Gujja, S., Li, H., Edwards, Y.J.K., Wolfrum, C., Metallo, C.M., et al. (2018). Brown Fat AKT2 Is a Cold-Induced Kinase that Stimulates ChREBP-Mediated De Novo Lipogenesis to Optimize Fuel Storage and Thermogenesis. Cell Metab. *27*, 195-209.e6.

Seale, P., Kajimura, S., Yang, W., Chin, S., Rohas, L.M., Uldry, M., Tavernier, G., Langin, D., and Spiegelman, B.M. (2007). Transcriptional Control of Brown Fat Determination by PRDM16. Cell Metab. *6*, 38–54.

Seale, P., Bjork, B., Yang, W., Kajimura, S., Chin, S., Kuang, S., Scimè, A., Devarakonda, S., Conroe, H.M., Erdjument-Bromage, H., et al. (2008). PRDM16 controls a brown fat/skeletal muscle switch. Nature *454*, 961–967.

Seale, P., Conroe, H.M., Estall, J., Kajimura, S., Frontini, A., Ishibashi, J., Cohen,

P., Cinti, S., and Spiegelman, B.M. (2011). Prdm16 determines the thermogenic program of subcutaneous white adipose tissue in mice. J Clin Invest *121*, 96–105.

Seuring, T., Archangelidi, O., and Suhrcke, M. (2015). The Economic Costs of Type 2 Diabetes: A Global Systematic Review. Pharmacoeconomics *33*, 811–831.

Shabalina, I.G., Petrovic, N., deJong, J.M.A., Kalinovich, A. V., Cannon, B., and Nedergaard, J. (2013). UCP1 in Brite/Beige adipose tissue mitochondria is functionally thermogenic. Cell Rep. *5*, 1196–1203.

Sharp, L.Z., Shinoda, K., Ohno, H., Scheel, D.W., Tomoda, E., Ruiz, L., Hu, H., Wang, L., Pavlova, Z., Gilsanz, V., et al. (2012). Human BAT possesses molecular signatures that resemble beige/brite cells. PLoS One *7*, e49452.
Shore, S. (2008). Obesity and asthma. J. Investig. Allergol. Clin. Immunol. *121*, 1087–1093.

Shulman, G.I. (2014). Ectopic fat in insulin resistance, dyslipidemia, and cardiometabolic disease. N. Engl. J. Med. *371*, 1131–1141.

Stine, R.R., Shapira, S.N., Lim, H.W., Ishibashi, J., Harms, M., Won, K.J., and Seale, P. (2016). EBF2 promotes the recruitment of beige adipocytes in white adipose tissue. Mol. Metab. *5*, 57–65.

Strosberg, J., Joish, V.N., Giacalone, S., Perez-Olle, R., Fish-Steagall, A., Kapoor, K., Dharba, S., Lapuerta, P., and Benson, A.B. (2019). TELEPRO: Patient-Reported Carcinoid Syndrome Symptom Improvement Following Initiation of Telotristat Ethyl in the Real World. Oncologist *24*, 1446–1452.

Sumara, G., Sumara, O., Kim, J.K., and Karsenty, G. (2012). Gut-derived serotonin is a multifunctional determinant to fasting adaptation. Cell Metab. *16*, 588–600.

The GBD 2015 Obesity Collaborators, A. (2017). Health Effects of Overweight and Obesity in 195 Countries over 25 Years. N. Engl. J. Med. *311*, 13–27.
Tilg, H., Moschen, A.R., and Roden, M. (2017). NAFLD and diabetes mellitus. Nat. Rev. Gastroenterol. Hepatol. *14*, 32–42.

Tschöp, M.H., Speakman, J.R., Arch, J.R.S., Auwerx, J., Brüning, J.C., Chan, L., Eckel, R.H., Farese, R. V., Galgani, J.E., Hambly, C., et al. (2012). A guide to analysis of mouse energy metabolism. Nat. Methods *9*, 57–63.

Tsuchida, T., and Friedman, S.L. (2017). Mechanisms of hepatic stellate cell activation. Nat. Rev. Gastroenterol. Hepatol. *14*, 397–411.

Virtanen, K., Lidell, M., Orava, J., Heglind, M., Westergren, R., Niemi, T.,

Taittonen, M., Laine, J., Savisto, N., Enerbäck, S., et al. (2009). Functional Brown Adipose Tissue in Healthy Adults. N. Engl. J. Med. *360*, 1518–1525.

Wang, W., and Seale, P. (2016). Control of brown and beige fat development. Nat. Rev. Mol. Cell Biol. *17*, 691–702.

Wang, F., Mullican, S.E., DiSpirito, J.R., Peed, L.C., and Lazar, M.A. (2013a). Lipoatrophy and severe metabolic disturbance in mice with fat-specific deletion of PPARγ. Proc. Natl. Acad. Sci. U. S. A. *110*, 18656–18661.

Wang, H.Y., Ducommun, S., Quan, C., Xie, B., Li, M., Wasserman, D.H., Sakamoto, K., Mackintosh, C., and Chen, S. (2013b). AS160 deficiency causes whole-body insulin resistance via composite effects in multiple tissues. Biochem. J. *449*, 479–489.

Wang, W., Kissig, M., Rajakumari, S., Huang, L., Lim, H.-W., Won, K.-J., and Seale, P. (2014). Ebf2 is a selective marker of brown and beige adipogenic precursor cells. Proc. Natl. Acad. Sci. U. S. A. *111*, 14466–14471.

Wang, Z., Zhang, H., Shen, X.H., Jin, K.L., Ye, G.F., Qiu, W., Qian, L., Li, B., Zhang, Y.H., and Shi, G.P. (2013c). Immunoglobulin E and mast cell proteases are potential risk factors of impaired fasting glucose and impaired glucose tolerance in humans. Ann. Med. *45*, 220–229.

Ward, Z.J., Bleich, S.N., Cradock, A.L., Barrett, J.L., Giles, C.M., Flax, C., Long, M.W., and Gortmaker, S.L. (2019). Projected U.S. State-Level Prevalence of Adult Obesity and Severe Obesity. N. Engl. J. Med. *381*, 2440–2450.

Weisberg, S., McCann, D., Desai, M., Rosenbaum, M., Leibel, R.L., and Ferrante, A.W. (2003). Obesity is associated with macrophage accumulation in adipose tissue. J. Clin. Invest. *112*, 1796–1808.

Weisend, C.M., Kundert, J.A., Suvorova, E.S., Prigge, J.R., and Schmidt, E.E. (2009). Cre activity in fetal albCre mouse hepatocytes: Utility for developmental studies. Genesis *47*, 789–792.

Westerterp, K.R. (2017). Control of energy expenditure in humans. Eur. J. Clin. Nutr. *71*, 340–344.

Wilson, C.G., Tran, J.L., Erion, D.M., Vera, N.B., Febbraio, M., and Weiss, E.J. (2016). Hepatocyte-specific disruption of CD36 attenuates fatty liver and improves insulin sensitivity in HFD-fed mice. Endocrinology *157*, 570–585.

Xiao, Y.X., Lanza, I.R., Swain, J.M., Sarr, M.G., Nair, K.S., and Jensen, M.D.

(2014). Adipocyte mitochondrial function is reduced in human obesity independent of fat cell size. J. Clin. Endocrinol. Metab. *99*, 209–216.

Yabut, J.M., Crane, J.D., Green, A.E., Keating, D.J., Khan, W.I., and Steinberg, G.R. (2019). Emerging Roles for Serotonin in Regulating Metabolism: New Implications for an Ancient Molecule. Endocr. Rev. *40*, 1092–1107.

Younossi, Z.M., Koenig, A.B., Abdelatif, D., Fazel, Y., Henry, L., and Wymer, M. (2016). Global epidemiology of nonalcoholic fatty liver disease—Meta-analytic assessment of prevalence, incidence, and outcomes. Hepatology *64*, 73–84.

Zhou, Y., Yu, X., Chen, H., Sjöberg, S., Roux, J., Zhang, L., Ivoulsou, A.-H., Bensaid, F., Liu, C.-L., Liu, J., et al. (2015). Leptin Deficiency Shifts Mast Cells toward Anti- Inflammatory Actions and Protects Mice from Obesity and Diabetes by Polarizing M2 Macrophages Article Leptin Deficiency Shifts Mast Cells toward Anti-Inflammatory Actions and Protects Mice from Obesity and. Cell Metab. *22*, 1–14.